



CSIC



UNIVERSITAS
Miguel
Hernández



INSTITUTO DE NEUROCIENCIAS

Consejo Superior de Investigaciones Científicas
Universidad Miguel Hernández
Instituto de Neurociencias

Pharmacological modulation of the native and
recombinant thermosensitive ion channel
Transient Receptor Potential Melastatin 8

Presented by:

Jan-Albert Manenschijn

For the degree of Doctor in Neuroscience from the University Miguel
Hernández de Elche

Director: Dr. Félix Viana de la Iglesia

San Juan de Alicante, Spain
2014


A QUIEN CORRESPONDA,

Prof. Juan Lerma Gómez, Director del Instituto Neurociencias, centro mixto de la Universidad Miguel Hernández (UMH) y la Agencia Estatal Consejo Superior de Investigaciones Científicas (CSIC)

CERTIFICA,

Que la Tesis Doctoral “Pharmacological modulation of the native and recombinant thermosensitive ion channel Transient Receptor Potential Melastatin 8”, ha sido realizada por D. Jan-Albert Manenschijn, Licenciado, bajo la dirección del Dr. Félix Viana de la Iglesia, y da su conformidad para que se presente la tesis a la Comisión de Doctorado de la Universidad Miguel Hernández.

Para que así conste, y a los efectos oportunos, expide y firma el presente Certificado en San Juan de Alicante a 20 de mayo de 2014


Fdo. Juan Lerma
Director



A QUIEN CORRESPONDA,

Dr. Félix Viana de la Iglesia, Investigador Científico del Consejo Superior de Investigaciones Científicas, en el Instituto de Neurociencias de Alicante, centro mixto de la Universidad Miguel Hernández (UMH) y la Agencia Estatal Consejo Superior de Investigaciones Científicas (CSIC)

CERTIFICA,

Que D. Jan-Albert Manenschijn, Licenciado, ha realizado bajo su dirección el trabajo experimental que recoge en su Tesis Doctoral “Pharmacological modulation of the native and recombinant thermosensitive ion channel Transient Receptor Potential Melastatin 8”.

Que ha revisado los contenidos científicos y los aspectos formales del trabajo y da su conformidad para que se presente la tesis a la Comisión de Doctorado de la Universidad Miguel Hernández.

Para que así conste, y a los efectos oportunos, expide y firma el presente Certificado en San Juan de Alicante a 20 de mayo de 2014



Fdo. Félix Viana de la Iglesia

Index

Abbreviations

1. Introduction

1.1. Ion channels	4
1.2. The TRP ion channel superfamily	5
1.2.1. TRP nomenclature and filogenetic distribution	6
1.2.2. General TRP structure and permeability	8
1.2.3. Gating, expression and function: TRP channels as ideal polymodal sensors	10
1.2.4. TRP channels and disease.....	13
1.2.5. ThermoTRPs	13
1.2.6. Functional organization of peripheral thermotransduction	14
1.3. TRPM8	15
1.3.1. Identification, structure and permeability.....	15
1.3.2. TRPM8 gating.....	18
1.3.3. TRPM8 expression profile	21
1.3.4. TRPM8 pharmacology.....	22
1.3.5. Modulation of TRPM8.....	24
1.3.6. Physiological role of TRPM8	27
1.3.7. Molecular determinants of thermal thresholds and signal propagation.....	30
1.3.8. The role of TRPM8 in (an)algesia	32
1.3.9. TRPM8 and cancer.....	36
1.3.10. Therapeutic potential of pharmacological modulators of TRPM8	37

2. Objectives

2.1. General objectives.....	38
2.2. Specific objectives	38

3. Materials and methods

3.1. HEK293 cells	39
3.1.1. Transient transfection of TRPM8 mutants.....	40
3.2. CR#1 cells	41
3.3. CHO-A1 cells.....	42
3.4. Sensory neuron cultures.....	42
3.5. TRPM8 ^{EYFP} transgenic mice.....	43
3.6. Reagents	43
3.7. Intracellular calcium imaging	44
3.8. Temperature stimulation.....	46
3.9. Intra- and extracellular solutions	46

3.10. Electrophysiological recordings	49
3.10.1. Whole-cell voltage-clamp	50
3.10.2. Cell-attached voltage clamp in neurons	51
3.10.3. Whole-cell current clamp	51
3.10.4. Single channel cell-attached and excised inside-out patch.....	52
3.11. Data analysis	53
3.11.1. Analysis of voltage dependent activation of TRPM8	53
3.11.2. Single channel data analysis	54
3.11.3. Analysis of thermal threshold	54

4. Results

4.1. Studying the effects of 5-benzyloxytryptamine on heterologously and natively expressed TRPM8 channels	55
4.1.1. Effects of 5-BT on cold-evoked activity in heterologously and natively expressed TRPM8.....	56
4.1.2. 5-BT shifts the midpoint of voltage activation of TRPM8 to positive values.....	58
4.1.3. Effects of channel mutations on the ability of 5-BT to antagonize TRPM8 activation.....	61
4.2. Studying the effects of chloroform on heterologously and natively expressed TRPM8 channels	64
4.2.1. Effect of low concentrations of CLF on $[Ca^{2+}]_i$ in cold-sensitive neurons from mice DRG	66
4.2.2. Effect of CLF on $[Ca^{2+}]_i$ in HEK293 cells stably expressing TRPM8	67
4.2.3. Effect of CLF on $[Ca^{2+}]_i$ on cold-sensitive TRPM8-expressing neurons.....	69
4.2.4. Electrophysiological characterization of CLF elicited current through heterologously expressed TRPM8	71
4.2.5. Electrophysiology in TRPM8 neurons	74
4.2.6. Effect of CLF on several mutants of TRPM8.....	77
4.2.7. Effect of bilayer curvature altering agents on activation of TRPM8 by CLF.....	78
4.2.8. Effects of CLF on single channel currents in the cell-attached and inside-out configuration	86

5. Discussion

5.1. Inhibition of TRPM8 by 5-BT	92
5.2. Activation of TRPM8 by CLF	94

6. Conclusions

7. Bibliography

Abbreviations

6TM	: six-transmembrane
5-BT	: 5-benzyloxytryptamine
5-HT	: 5-hydroxytryptamine
ATP	: adenosine triphosphate
ARD	: ankyrin repeat domain
BAT	: brown adipose tissue
BCTC	: 4-(3-chloro-pyridin-2-yl)-piperazine-1-carboxylic acid (4-tert-butyl-phenyl)-amide
$[Ca^{2+}]_i$: intracellular calcium concentration
Caps	: capsaicin
CCI	: chronic constriction injury
CFA	: complete Freund's adjuvant
CGRP	: calcitonin gene-related peptide
CLF	: chloroform
CMR1	: cold-menthol receptor type 1
CPZ	: chlorpromazine
DAG	: diacyl glycerol
DMEM	: Dulbecco's Modified Eagle's Medium
DMSO	: dimethyl sulfoxide
DRG	: dorsal root ganglia
EC ₅₀	: half-maximal excitatory concentration
EGTA	: ethylene glycol tetraacetic acid
F ₃₄₀	: fluorescence emitted by Fura-2 excited at 340 nm
F ₃₈₀	: fluorescence emitted by Fura-2 excited at 380 nm
Fura 2-AM	: fura-2-acetoxymethyl ester
GDNF	: glial cell-line derived neurotrophic factor
GFP	: green fluorescent protein
GFR α 3	: GDNF family receptor α 3
G _{max}	: maximum conductance
HC30031	: 2-(1,3-Dimethyl-2,6-dioxo-1,2,3,6-tetrahydro-7H-purin-7-yl)-N-(4-isopropylphenyl)acetamide
HCN	: hyperpolarization-activated cyclic nucleotide-gated
HEK293	: Human Embryonic Kidney 293
HEPES	: 4-(2-hydroxyethyl)-1-piperazineethanesulfonic acid
HT	: high-threshold
I	: current
IB4	: isolectin B4
I=0	: current-clamp mode at which amplifier current is kept at 0 A
IC ₅₀	: half-maximal inhibitory concentration
iPLA ₂	: calcium-insensitive phospholipase A2
ipRGC's	: intrinsically photosensitive mammalian retinal ganglion cells
I-clamp	: current-clamp
I _h	: hyperpolarized-activated inward current (I _h)
I _{max}	: maximal current
IP ₃	: inositol 1,4,5-triphosphate
I-V	: current-voltage

LT : low-threshold
 MHR : TRPM homology region
 NET : neuroendocrine tumor cells
 NOMP-C : NO mechanoreceptor potential C
 PBMC : 1-phenylethyl-4-(benzyloxy)-3-methoxybenzyl(2-aminoethyl)carbamate
 P_{Ca} : permeability for calcium
 PI(4,5)P₂ : phosphatidylinositol 4,5-bisphosphate or PtdIns(4,5)P₂
 Pirt : phosphoinositide interacting regulator of TRP
 PKA : protein kinase A
 PKD : protein kidney disease
 PKC : protein kinase C
 PLC : phospholipase C
 P_{Na} : permeability for sodium
 polyP : inorganic polyphosphate
 P_{open} : open probability
 pRGC : photosensitive retinal ganglion cell
 SAC : stretch-activated channel
 SKF96356 : 1-β[3-(4-methoxyphenyl)propoxy]-4-methoxyphenethyl-1Himidazole hydrochloride
 siRNA : small interference RNA
 TTX_r : tetrodotoxin-resistant
 TTX_s : tetrodotoxin-sensitive
 TG : trigeminal ganglia
 TM : transmembrane domain
 TM5 : transmembrane domain segment 5
 TM6 : transmembrane domain segment 6
 TNP : trinitrophenol
 T_r : risetime
 TRP : transient receptor potential
 TRPA : transient receptor potential ankyrin
 TRPC : transient receptor potential canonical
 TRPP : transient receptor potential polycystic
 TRPM : transient receptor potential melastatin
 TRPML : transient receptor potential melastatin-like
 TRPN : transient receptor potential NOMPC
 TRPV : transient receptor potential vanilloid
 UCP1 : uncoupling protein 1
 V : voltage
 V-clamp : voltage-clamp
 V_m : membrane potential
 V_{rev} : reversal potential
 WAT : white adipose tissue
 Wt : wild-type

1. Introduction

Para su supervivencia, todos los organismos dependen de su capacidad para percibir, interpretar y reaccionar ante cambios en su medio ambiente. La percepción de la temperatura es un elemento importante en la fisiología de los animales, puesto que posibilita respuestas comportamentales apropiadas frente a cambios en la temperatura ambiental, y permite evitar el contacto prolongado con objetos a temperaturas dañinas. El sistema sensorial de los mamíferos es capaz de detectar variaciones sutiles en la temperatura a través de terminales nerviosas termosensibles que representan una fracción de todas las fibras sensoriales. Estas terminaciones nerviosas termosensibles expresan una serie de canales iónicos no selectivos de la familia TRP ("Transient Receptor Potential"), los cuales responden a un amplio rango de temperaturas, desde calor quemante hasta el frío helado. De entre estos canales TRP termosensitivos, TRPM8 ("Transient Receptor Potential Melastatin 8") es el principal sensor del frío y también se piensa que pueda estar implicado en el desarrollo del dolor al frío en condiciones patológicas. Además, su expresión elevada y su función están relacionadas con la transformación maligna en varios tipos de cáncer. Finalmente, hay evidencias emergentes que demuestran un papel del TRPM8 como agente analgésico en determinadas condiciones. Estos roles diversos confieren una perspectiva prometedora al desarrollo de moduladores de TRPM8, que podrían constituir una terapia atenuante importante para el tratamiento de diversas condiciones patológicas. El estudio de moduladores de TRPM8 es un campo emergente y ha permitido entender mejor las propiedades biofísicas de TRPM8 y su función, tanto en el organismo sano como en situaciones patológicas. Sin embargo, esto representa sólo "la punta del iceberg", la cual espero que esta tesis contribuya a destapar un poco más.

For survival, all organisms depend on their ability to perceive, interpret and react to changes in their environment. Temperature sensing is an important element in the functioning of organisms, allowing for appropriate behavioral responses to changes in environmental temperature and the avoidance of prolonged contact with harmfully hot or cold objects. The mammalian sensory system is able to detect subtle changes in temperature through thermosensitive nerve terminals of primary afferent sensory neurons, which represent a fraction of the total of sensory afferents. These thermosensitive nerve-endings express a subset of non-selective cationic ion channels of the Transient Receptor Potential (TRP) family, which respond to a range of different temperatures, spanning the whole range of the perceived temperature spectrum from burning hot to ice cold. Of these thermosensitive TRP channels, Transient Receptor Potential Melastatin 8 (TRPM8) is the principal cold sensor and is believed to be involved in the development of cold pain during pathological conditions. Furthermore, its expression and function is linked to several cancerous malignancies. Finally, evidence is emerging that activation of TRPM8 might confer an anesthetic effect in certain conditions. These diverse roles make for a promising therapeutical prospect for the development of TRPM8 channel modulators, in the hope that it can offer therapeutic relief from various pathological conditions. The study of TRPM8 modulators is an emerging field and has enhanced our understanding of the biophysical properties of TRPM8 and, as a tool, helped in elucidating the physiological role of TRPM8 in health and disease. However, this is only the tip of the proverbial iceberg, of which this thesis hopes to uncover a little more.

1.1. Ion channels

Each cell is enclosed by a membrane, consisting of a double layer of phospholipids, which holds the essential cellular components together and separates them from the external environment. Due to the tight packing of lipid molecules, the bilayer is hydrophobic in nature and acts as a barrier to the diffusion of small charged molecules and ions such as Na^+ , K^+ , Ca^{2+} or Cl^- . For a proper and controlled regulation of ion flow, cell membranes contain specialized transmembrane proteins such as ion transporters and ion channels. Ion channels allow for the passive diffusion of ions, determined by a favorable electrochemical gradient, set up and maintained by ATP-driven ionic transporters that actively pump ions across the membrane. When an ion channel opens, the ions rapidly diffuse through the channel pore, generating a flow of current and changing the membrane potential. Ion channels are found in the membranes of all cells, where they fulfill several essential functions. These include controlling the resting membrane potential, shaping electrical signals in excitable cells and gating the flow of messenger Ca^{2+} ions (Hille, 2001).

Regulated ion flow is the basis for excitation and electrical signaling in the nervous system. Opening an ion channel, changing the transmembrane potential accordingly, can facilitate the opening of neighboring ion channels that are able to sense a change in transmembrane potential. A cascade of voltage-gated ion channels can thus propagate an action potential along the nerve, serving as a signal in the nervous system. Eventually, the depolarizing electrical signal generates a nonelectrical response by opening voltage-gated Ca^{2+} -permeable channels. Ca^{2+} acts as an intracellular messenger, and the change in intracellular free Ca^{2+} generates a versatile response in the cell, depending on the diverse calcium signaling pathways and their effectors (e.g. kinases, other ion channels). In this fashion, electric signaling controls a host of diverse biological processes like the contraction of muscle fibers, neurotransmitters release, hormone secretion, gene expression, cellular division and sensory transduction.

Ion channels open and close their permeation pathway (i.e. pore) because of conformational changes of the channel protein, which is referred to as gating. Gating occurs by several mechanisms, such as the binding of a specific natural ligand or pharmacological compound, transmembrane voltage changes, mechanical

perturbation of the membrane, light or temperature changes. A further defining feature of ion channels is their pore, the ion conductive pathway, which is selectively permeable and so allows only the passage of a certain class of ions. Ion channels are classified by their gating mechanism, their ionic selectivity and by filogenetic criteria like the homology of their amino acid sequences (Berridge *et al.*, 2000; Hille, 2001).

1.2. The TRP ion channel superfamily

Transient Receptor Potential (TRP) ion channels are an important superfamily of ion channels and derive their name from the phenotype of a mutant *Drosophila melanogaster* fly, the *Trp*-mutant. Measurements of the receptor potential response in the fly eye to visual stimuli, known as the electroretinogram, revealed that *Trp*-mutant flies display a transient negative receptor potential that quickly returns to baseline under continuous illumination, unlike their wild type counterparts in which the negative receptor potential is sustained (Cosens and Manning, 1969). Later, the *Trp* gene was cloned and identified to code for a Ca^{2+} -permeable cation channel in the rhabdomeres of *Drosophila* photoreceptors (Montell and Rubin, 1989; Hardie and Minke, 1992). Since then, more than a hundred *Trp* genes were identified in various animal species. In humans, twenty-seven have been described (Montell, 2005).

TRP channels are non-selective cationic ionic channels, mediating the flow of Ca^{2+} and Na^{+} across the cell membrane. The opening of a TRP channel causes membrane depolarization, facilitating the generation of action potentials in excitable cells. In non-excitable cells, TRP channels can mediate a large fraction of Ca^{2+} entry upon stimulation.

The TRP superfamily has been found to display a greater diversity in gating mechanisms than any other group of ion channels, and it is this diversity that allow them to play critical roles in sensory physiology, which includes vision, hearing, olfaction, touch, thermo- and osmosensation, nociception, pheromone signaling and taste transduction (Nilius and Owsianik, 2011).

1.2.1. TRP nomenclature and filogenetic distribution

The diverse cation channels that together make up the TRP superfamily vary markedly in their ion selectivity and gating mechanisms. However, they share significant sequence homology and therefore are classified based upon their protein sequence similarity (Montell *et al.*, 2002). The TRP superfamily is subdivided into seven subfamilies of which three (TRPC, TRPV and TRPM) are closely related to the classical TRP channel, whilst four additional subfamilies (TRPA, TRPML, TRPP and TRPN) are more divergent (Figure 1). Dependent on the organism in which they are expressed, the number of different TRP channels range from 17 in *Drosophila melanogaster* and *Caenorhabditis elegans* to 28 in the mouse *Mus musculus* (Table 1).

Briefly, the TRPC ('Canonical') subfamily consists of 7 members and is closely related to the TRP originally described in *Drosophila* (Montell and Rubin, 1989; Hardie and Minke, 1992). It was the first TRP subfamily reported in mammals (Wes *et al.*, 1995). A homolog of the TRPC2 gene exists in humans, but is non-functional. The TRPM ('Melastatin') subfamily has 8 members and is named after its first identified member, TRPM1, which was previously called melastatin (Duncan *et al.*, 1998). By using the vanilloid compound capsaicin as a ligand, the first member of the TRPV ('Vanilloid') subfamily was discovered (Caterina *et al.*, 1997). The TRPV subfamily includes 6 members. The TRPA ('Ankyrin') subfamily consists of only one member in mammals, and its name refers to the numerous ankyrin repeats in its N-terminus. The TRPP ('Polycystin') subfamily contains 3 members that are also known as polycystic kidney disease (PKD) proteins. Mutations in TRPP1 and TRPP2 underlie the most common form of hereditary kidney disease (Wu *et al.*, 1998). The TRPML ('Mucolipin') subfamily encompasses 3 members, and mutations in TRPML1 are associated with mucopolipidosis type IV, a neurodegenerative lysosomal storage disorder (Sun *et al.*, 2000).

Finally, the TRPN ('NOMP-C') is named after the NO-mechano-potential C channel in *Caenorhabditis elegans* and is absent in mammals. In vertebrates, the only animals known to express TRPN are the zebrafish *Danio rerio* and the frog *Xenopus laevis* (Sidi *et al.*, 2003; Shin *et al.*, 2005) [As reviewed by (Clapham, 2003; Venkatachalam and Montell, 2007; Nilius and Owsianik, 2011)].

	<i>Drosophila melanogaster</i>	<i>Caenorhabditis elegans</i> ^b	<i>Ciona intestinalis</i> ^b	<i>Fugu rubripes</i>	<i>Danio rerio</i> ^b	<i>Mus musculus</i>	<i>Homo sapiens</i>
TRPC	3	3	8	8	8	7	6
TRPV	3	5	2	4	4	6	6
TRPM	1	4	2	6	6	8	8
TRPA	4	2	4	1	2	1	1
TRPN	1	1	1	-	1	-	-
TRPML	4	1	9	2	2	3	3
TRPP	1	1	1	4	4	3	3
Total	17	17	27	25	27	28	27

Table 1. TRP channels in the fruit fly (*Drosophila melanogaster*), the worm (*Caenorhabditis elegans*), the sea squirt (*Ciona intestinalis*), the puffer fish (*Fugu rubripes*), the zebrafish (*Danio rerio*), mouse (*Mus musculus*) and human (*Homo sapiens*). The numbers correspond to proteins with distinct channel properties within each subfamily. [From Nilius and Owsianik (Nilius and Owsianik, 2011)]

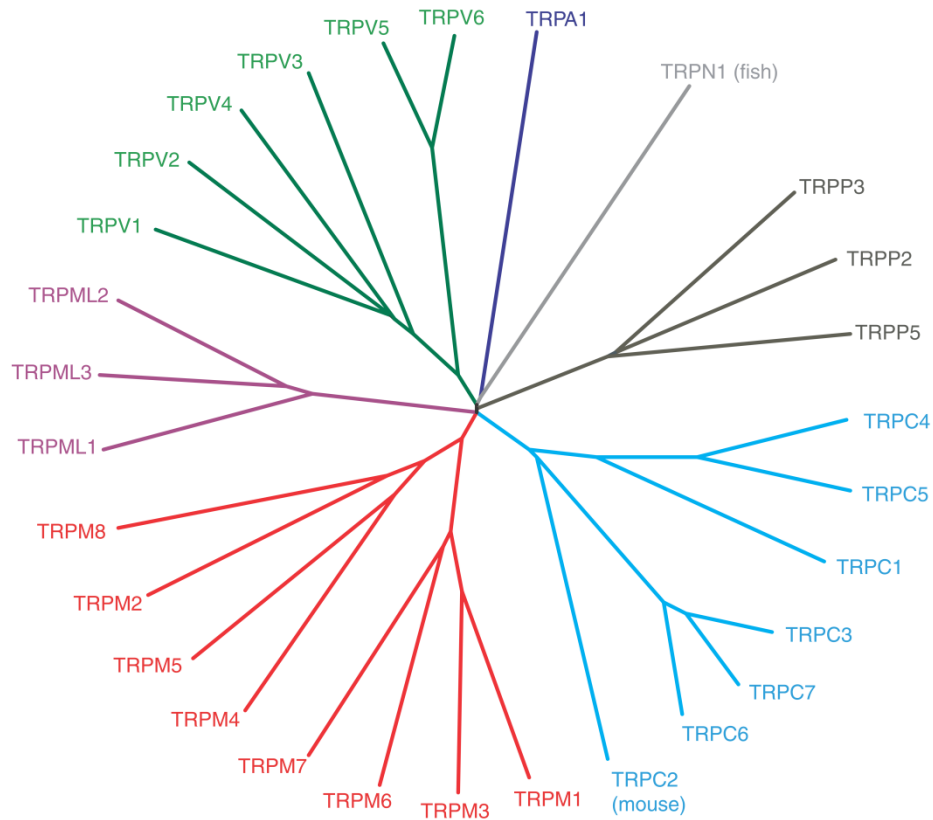


Figure 1. Phylogenetic tree of human TRP channels. Sequence homology analyses show that all TRP channels fall into seven subfamilies that comprise proteins with distinct channel properties. Because TRPC2 is a pseudogene in humans and TRPNs are not present in mammals, mouse TRPC2 and fish TRPN1 were used to show relations between all subfamilies. The TRP subfamilies are represented by different colors. [Adapted from Nilius and Owsianik (Nilius and Owsianik, 2011)].

1.2.2. General TRP structure and permeability

TRP proteins consist of six putative transmembrane (6TM) segments (S1-S6) with large intracellular amino- (N) and carboxyl- (C) termini. It is thought that most TRP proteins assemble as homotetramers to form cation-permeable pores, just as voltage gated K^+ channels whose three dimensional structure they resemble (Cao *et al.*, 2013). Some heteromultimeric channels are reported to form between members of the same subfamily or different subfamilies, although their biological relevance remains unclear (Schaefer, 2005). The reported interaction between subunits of the TRPV1 and TRPA1 ion channel is the latest example of the formation of a functional heteromultimeric TRP channel (Fischer *et al.*, 2014).

In a typical TRP channel, the four centre-facing 2TM elements, S5 and S6, form the gate and selectivity filter of the channel. The reentrant loop between S5 and S6 forms the pore of the channel, while the extracellular side of the pore loop shapes a selectivity filter for the exclusive permeation of certain ions. The cytoplasmic ends of S6 form the lower gate, which opens and closes to regulate cation entry into the channel (Figure 2a,b.). The elements that are outside of the S5-S6 region either function as linkers to elements that control gating or are associated with subunit association (Cao *et al.*, 2013). A significant number of TRP channels are weakly voltage dependent, and gating occurs by the movement of charged elements upon a change in the transmembrane potential. The location of the voltage sensor in TRP channels remains unclear. In a study of TRPM8, charge neutralizing mutations in S4 and the S4-5 linker region reduced the gating charge of the channel, suggesting the involvement of this region in the voltage sensor (Voets *et al.*, 2007). This is in accordance with the location of the voltage sensor in voltage-gated K^+ channels. However, in a recent structural study of TRPV1, S1 to S4 remain stationary upon channel activation, suggesting a less active role in gating (Cao *et al.*, 2013). By performing charge reversal mutations, another group concluded that S4 does not have a separate role in the gating of TRPM8, but rather that voltage sensitivity depends upon an interaction between S3 and S4 (Kuhn *et al.*, 2013).

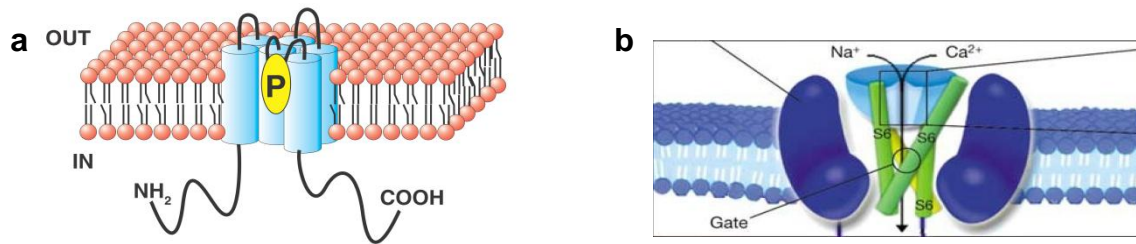


Figure 2 a) All TRP-proteins contain six transmembrane segments (S1 to S6) with a putative pore region (P) between S5 and S6. Amino- and carboxyl-termini are variable in length and contain different sets of domains. [From Nilius and Owsianik (Nilius and Owsianik, 2011)]. **b)** The selectivity filter formed by the extracellular side of the pore loop (light blue) and the cytoplasmic parts of S6 which shape the lower gate shown in more detail. S5 is not shown. [Adapted from Clapham (Clapham, 2003)].

The intracellular N- and C-termini are variable in length and consist of a variety of structural domains. For example, the C-terminal of the TRPC, TRPM and TRPN subfamily contain a highly conserved region of 23-25 amino acids, which is referred to as the TRP-domain. With the exception of TRPM, TRPP and TRPML, the N-terminus of TRP channels contain multiple ankyrin repeats, which is a short sequence motif that typically contains thirty-three amino acid residues. The number of repeats within the ankyrin repeat domain (ARD) ranges from 3-4 in TRPCs to about 29 in TRPNs. They are implicated in channel tetramerization, and may participate in protein-protein interactions and serve as a ligand binding site (Clapham, 2003; Clapham *et al.*, 2005; Venkatachalam and Montell, 2007; Nilius and Owsianik, 2011).

Most TRP channels are non-selective cationic channels and are modestly selective for Ca^{2+} , with permeability ratios relative to Na^+ ($P_{\text{Ca}}/P_{\text{Na}}$) between 0.3 and 10. However, TRPV5 and TRPV6 are highly selective for Ca^{2+} with a $P_{\text{Ca}}/P_{\text{Na}} > 100$. Both TRPM4 and TRPM5 are impermeable to Ca^{2+} and are only permeable to monovalent cations (Owsianik *et al.*, 2006).

1.2.3. Gating, expression and function: TRP channels as ideal polymodal sensors

As stated earlier, an enormous variety of gating mechanisms have been described within the TRP superfamily. They include voltage-, ligand-, mechano- and temperature-gated TRP channels, as well as constitutively active channels. Moreover, many TRP channels are polymodal, which means that the channel can be gated by several different stimuli. Because TRP channels are expressed in nearly all mammalian cell types, they are thought to play important roles in a large variety of biological processes. In particular, by virtue of their multiple gating mechanisms, TRP channels are highly suited to function in receptor cells and thus in sensory physiology. Indeed, they are found to act as sensors to a broad range of environmental and endogenous stimuli, such as temperature, chemical irritants, osmolarity, pheromones and growth factors.

In brief, several TRP channels are involved in *chemosensation*, which is a broad class by definition and involves multiple sensory modalities, such as smell, taste and the detection of chemical compounds. Chemosensation is important for the detection of irritant and poisonous chemicals and as such has a protective or defensive function. TRPA1 is a preeminent example of a TRP channel that is activated by reactive chemicals, and among its chief ligands are a large variety of natural pungent chemicals, such as mustard oil, allicin and cinnamaldehyde. TRPA1 activation is responsible for the pungent feel of many foods (Viana, 2011). In the taste buds of the tongue, TRPM5 is involved in the downstream taste transduction of sweet, bitter and umami receptors (Chandrashekar *et al.*, 2006). Furthermore it has been implicated in the detection of signaling molecules such as pheromones in mouse olfactory sensory neurons (Lin *et al.*, 2007; Oshimoto *et al.*, 2013).

Christened thermoTRPs (Patapoutian *et al.*, 2003), thermosensitive TRP channels, are involved in *thermosensation and nociception*. Located in thermosensory nerve endings that mainly innervate the skin and exposed epithelia (e.g. cornea, tongue), they are responsible for the detection of noxious and innocuous temperatures. The thermal thresholds of activation for several different thermoTRPs range from noxious heat to noxious cold, thereby spanning the entire range of temperatures that are sensed by most mammals (Figure 3) (Belmonte and Viana, 2008; Almaraz *et al.*, 2014). For example, certain members of the TRPV

subfamily are sensitive to temperatures ranging from pleasantly warm to excruciatingly hot, whilst TRPM8 and TRPA1 are sensors for temperatures ranging from pleasantly cool to noxiously cold.

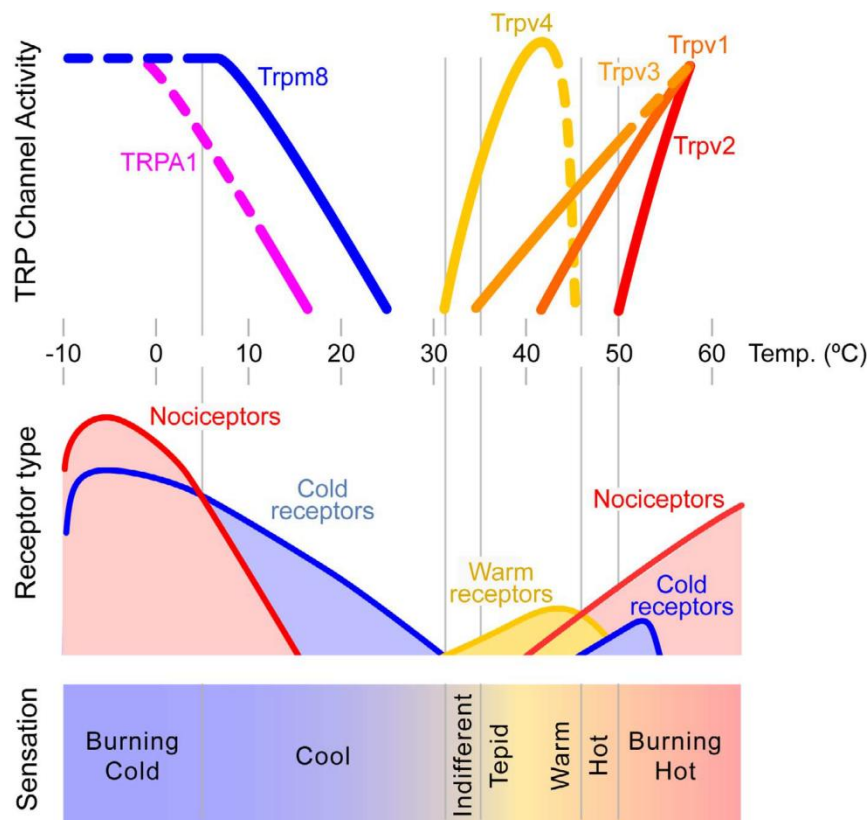


Figure 3. Hypothetical correspondence between activation of TRP channels, body surface temperature and evoked sensations. Upper part: Schematic representation of the thermal activation profile of various TRP channels when expressed in recombinant systems. All of them have been located in sensory neurons and/or skin cells. (Adapted from Patapoutian et al. 2003). Middle part: Schematic representation of impulse activity in various cutaneous sensory receptors during application to their receptive fields of temperatures indicated in the thermal scale. Lower part: Quality of sensations evoked in humans by application to the skin of different temperature values. [From (Belmonte and Viana, 2008)]

In addition to being thermosensors, thermoTRPs can also respond to chemical stimuli. For example, capsaicin, one of the constituents of chili peppers, activates the heat sensing TRPV1, thereby evoking a sensation of heat (Caterina *et al.*, 1997).

Several members of the TRP family have been implicated in *mechanosensation*. An example is TRPC5, which is activated by membrane stretch and hypotonic solutions. However, its physiological role in mechano-transduction and osmotic regulation is not clarified yet (Gomis *et al.*, 2008). TRPV4 (Strotmann *et al.*, 2000), TRPC1 (Maroto *et al.*, 2005) and TRPC6 (Spassova *et al.*, 2006) are other members of the TRP family that are sensors of mechanically and osmotically induced membrane stretch.

Furthermore, TRPC3 seems to play a role in the *phototransduction* cascade of intrinsically photosensitive mammalian retinal ganglion cells (ipRGCs). ipRGCs are involved in nonvisual photoresponses in mammals and studies suggest that TRPC3, the mammalian homolog of the *Drosophila* phototransduction channel, is involved in the light-activation of ipRGCs through melanopsin (Panda *et al.*, 2005; Qiu *et al.*, 2005).

Additionally, TRP channels have important signaling roles in the local cellular environment. In the developing nervous system they have an active part in *growth cone guidance, neurite outgrowth and synaptic activity*. For example, TRPC3 is involved in growth cone guidance, while TRPC5 is implicated in neurite outgrowth (Li *et al.*, 2005). TRPC4 and TRPC1 are involved in postsynaptic responses to activation of metabotropic receptors, reducing or increasing the postsynaptic response (Kim *et al.*, 2003; Munsch *et al.*, 2003). Many TRP channels are expressed in vascular endothelial cells and have been implicated in *endothelial function*. TRPA1 (Earley, 2012; Meseguer *et al.*, 2014) and TRPC4 (Freichel *et al.*, 2001) are implicated in vasorelaxation, while TRPC6 is involved in vascular smooth muscle contractility (Dietrich *et al.*, 2005). Secretion of fluids and hormones is also one of the processes in which TRP channels play a crucial role. TRPC1 is expressed in salivary gland cells and is implicated in the secretion of saliva (Singh *et al.*, 2002; Liu *et al.*, 2007). Four members of the TRPM subfamily, TRPM2, TRPM3, TRPM4 and TRPM5 are expressed in insulin producing pancreatic β -cells. Reducing their functional expression reduces glucose induced insulin secretion (Colsoul *et al.*, 2011). Kidney, bladder and bone function also depend on TRP channels. TRPV1 is involved in the capacity and emptying of the bladder (Birder *et al.*, 2002). Furthermore, TRPV5 is important for Ca^{2+} reabsorption in the kidney. TRPV5 knockout mice excrete high levels of Ca^{2+} in their urine, owing to a defect in Ca^{2+} reabsorption. In the same animals, calcium reabsorption in the bone is also affected (Hoenderop *et al.*, 2003) [for comprehensive reviews, see (Venkatachalam and Montell, 2007; Belmonte and Viana, 2008; Damann *et al.*, 2008; Talavera *et al.*, 2008; Nilius and Owsianik, 2011; Gees *et al.*, 2012)]

1.2.4. TRP channels and disease

Mutations and misregulation of some TRP channels have been linked to pathophysiology and disease, which is perhaps unsurprising considering their large diversity and association with a multitude of biological processes.

When TRP-related diseases are considered, one can distinguish between TRP channelopathies, as diseases caused by channel malfunction are called, and diseases in which TRPs are involved due to their nature as targets for irritants, inflammation products and toxins. To date, mutations in at least six members of the TRP family have been identified as TRP-channel related channelopathies in humans (Moran *et al.*, 2011). Misregulation of TRP channels, such as changes in the number of expressed TRP channels and channel (de)sensitization, can lead to diminished or potentiated responses to stimuli, and may result in disease. Mechanism through which misregulation lead to disease include disruptions in calcium signaling, which plays an important role in many processes, mistuning of sensory input, disturbances in calcium and magnesium homeostasis, disturbed organelle function, trafficking and dysfunctions in the control of cell proliferation and growth. Diseases caused by dysfunction and misregulation of TRP channels make them promising targets for pharmacological modulation. However, the lack of knowledge about the function of many TRP channels and the limited number of available selective modulators has hindered the development of approved drugs that target TRP channels (Nilius, 2007; Nilius *et al.*, 2007; Moran *et al.*, 2011).

1.2.5. ThermoTRPs

The ability of an organism to sense ambient temperature and to avoid harmful extremes is essential to its survival. Thermosensitive ion channels in free nerve endings of peripheral sensory neurons that innervate the skin and mucosa are crucial to temperature sensation, the most notable being a small group of TRP channels that stand out by their extreme sensitivity to temperature. A way to quantify the temperature sensitivity of an ion channel is by measuring the temperature coefficient (Q_{10}), which is the change in the rate of gating by a change in temperature of 10°C. Typical ion channels have a Q_{10} around 3, similar to the effect of temperature on other enzymatic reactions (Hille, 2001). However, temperature sensitive TRP channels have Q_{10} values ≥ 5 . Due to their high temperature dependence, these thermosensitive TRP channels were dubbed thermoTRPs (Patapoutian *et al.*, 2003).

Using Q_{10} values as a criterion, at least eleven TRP channels are categorized as thermosensitive. These are the heat activated thermoTRPs TRPV1 (Caterina *et al.*, 1997), TRPV2 (Caterina *et al.*, 1999), TRPV3 (Peier *et al.*, 2002b), TRPV4 (Watanabe *et al.*, 2002), TRPM2 (Togashi *et al.*, 2006), TRPM3 (Vriens *et al.*, 2011), TRPM4 and TRPM5 (Talavera *et al.*, 2005), and the cold activated thermoTRPs TRPM8 (McKemy *et al.*, 2002; Peier *et al.*, 2002a), TRPA1 (Story *et al.*, 2003) and TRPC5 (Zimmermann *et al.*, 2011). However, the physiological role of several of these thermoTRPs (TRPV2, TRPV3, TRPV4, TRPM2, TRPM4, TRPC5) in thermal sensing or modulation of temperature-dependent physiological processes is not clear (Voets, 2012). In their role as peripheral thermosensors expressed in the nerve terminals of thermosensitive neurons, thermoTRPs have distinct temperature thresholds of activation, spanning the whole range of the perceived temperature spectrum from excruciating cold to burning hot (Figure 3).

1.2.6. Functional organization of peripheral thermotransduction

The peripheral nervous system serves as a target for sensory stimuli, communicating with the central nervous system and providing it with information about the outside world. Peripheral afferent fibers from sensory neurons richly innervate the skin, muscle and other tissue where they detect sensory stimuli (Purves, 2008). Their cell bodies reside in dorsal root ganglia (DRG), which are node-like structures flanking the spinal cord bilaterally from the neck down. DRG central afferents terminate in the dorsal horn of the spinal cord from where ascending pathways further relay sensory information to the central nervous system. The trigeminal ganglia (TG) are analogous in cellular organization to DRG and are located on either side of the base of the cranium from where its peripheral sensory afferents innervate the oral cavity and all tissues in the head, including the face, the cornea and the meninges. Sensory information is relayed to second-order neurons in the spinal cord and to brainstem sensory nuclei. From there the information is carried to higher processing centers. Peripheral afferent fibers are categorized in three main groups based on their conduction velocities. These are the thickly myelinated A β fibers, which have a fast conduction velocity, the thinly myelinated type I and II A δ fibers, which have a lower conduction velocity and the unmyelinated slowly conducting C fibers. Thermoreception in mammals is mediated by A δ and C fibers (Basbaum, 2008). Among these afferents there exist distinct populations which are activated at different

thermal thresholds. Moderate heating is primarily conducted by C-fibers and type II A δ -fibers, whereas type I A δ -fibers mainly respond to noxious heat. Painless cold sensations are conducted by A δ -fibers and noxious cold is conducted by C-fibers (Julius and Basbaum, 2001).

1.3. TRPM8

1.3.1. Identification, structure and permeability

In 1951, Hensel and Zotterman found that menthol potentiates the cold responses of trigeminal sensory fibers by shifting their threshold of thermal activation towards warmer temperatures (Hensel and Zotterman, 1951). These and other experiments provided the first evidence of a receptor for cold and menthol in nerves. Much later, electrophysiological and calcium imaging studies suggested that cold and menthol activated unknown calcium-permeable channels in cultured DRG and TG neurons (Okazawa *et al.*, 2000; Reid and Flonta, 2001a). It was just after this that the molecular identity of the cold and menthol sensor was unknowingly revealed. When screening a cDNA library of cancerous prostate cells for upregulated genes, Tsavaler and colleagues identified and cloned a novel gene that shared high homology with TRP proteins, and designated it *trp-p8* (Tsavaler *et al.*, 2001). In an attempt to unify the nomenclature of the TRP superfamily, *trp-p8* was categorized as part of the TRP melastatin (TRPM) subfamily and renamed TRPM8 (Montell *et al.*, 2002; Montell, 2005). A year after its initial discovery, two groups discovered TRPM8 to be a receptor for cold and menthol. The group of David Julius constructed a cDNA expression library from cold- and menthol-sensitive rat trigeminal sensory neurons. Subsequent functional screening of its protein products revealed a menthol- and cold-sensitive receptor that shared high homology with TRPM8 (McKemy *et al.*, 2002). Independently, and by a different approach, Peier and colleagues found a novel TRP channel by scanning genomic databases for sequences that shared homology with the previously cloned heat sensitive TRPV1 channel. Subsequent amplification and sequencing identified it as TRPM8. Functional studies of heterologously expressed mouse TRPM8 demonstrated it to be cold- and menthol-sensitive (Peier *et al.*, 2002a).

The human and rodent TRPM8 gene is transcribed into a messenger RNA that codes for a protein with a length of 1104 amino acids (Tsavaler *et al.*, 2001; McKemy

et al., 2002; Peier *et al.*, 2002a). Like the other members of the TRP superfamily, TRPM8 is thought to consist of four subunits that each comprise six transmembrane domains with a pore loop between S5 and S6, and on either end intracellular N- and C-termini (Dragoni *et al.*, 2006; Stewart *et al.*, 2010; Janssens and Voets, 2011). The C-terminus, with 120 residues, is rather short compared to other members of the TRPM subfamily. It contains conserved coiled-coil domains, which are structural elements in which an α -helix is coiled on itself, and are thought to be involved in tetramerization of TRPM8 (Erler *et al.*, 2006; Tsuruda *et al.*, 2006). However, another study demonstrated that a mutant of TRPM8 lacking the C-terminus is still able to locate to the membrane as a tetramer. Nevertheless, deleting the C-terminus results in a non-responsive channel and thus is essential for proper channel functioning (Phelps and Gaudet, 2007). Also located in the C-terminus, the highly conserved intracellular TRP domain energetically couples ligand-binding to conformational changes of the channel protein, and thus is important for channel gating (Bandell *et al.*, 2006; Valente *et al.*, 2008). The TRP domain also contains several binding sites for PI(4,5)P₂, a membrane phospholipid that is required to activate TRPM8 channels (Liu and Qin, 2005; Rohacs *et al.*, 2005; Brauchi *et al.*, 2007).

TRPM8 is a voltage dependent channel, but the exact position of the voltage sensor domain remains elusive. Neutralizing positive charges in transmembrane domain S4 and the S4-S5 linker suggest this region to be part of the voltage sensor, but was not enough to completely abolish voltage dependent gating (Voets *et al.*, 2007). Later studies suggest that the voltage dependence of TRPM8 depends on an interaction between S3 and S4 (Kuhn *et al.*, 2013).

The mechanism of temperature-dependent gating is also unknown. Swapping the C-terminal domains of TRPM8 and TRPV1 revealed a chimeric TRPM8 channel that is heat-sensitive, suggesting the involvement the C-terminus in temperature-dependent gating (Brauchi *et al.*, 2006).

The N-terminal domain consists of about 700 amino acids. Unlike other members of the TRP family, the amino terminals of TRPM channels lack ankyrin-like repeats. It contains four so-called TRPM homology regions (MHR) that share homology between all TRPM family members (Fleig and Penner, 2004). An important function of the N-terminal domain is the proper localization of TRPM8 in the plasma membrane (Phelps and Gaudet, 2007) and it has also been suggested to play a role in the *in vivo* stabilization of the channel (Erler *et al.*, 2006). Furthermore, some

residues in the N-terminal are protein kinase A-dependent phosphorylation sites involved in regulating channel activity (Bavencoffe *et al.*, 2010).

Post-translational *N*-glycosylation at residue Asn934, situated near the pore entrance of TRPM8, is important role for the segregation of TRPM8 channels in cholesterol-rich specialized membrane domains known as lipid rafts, but is not absolutely necessary for proper cell surface expression or responsiveness of the channel to agonists. However, it is involved in modulating channel activity (Dragoni *et al.*, 2006; Erler *et al.*, 2006; Morenilla-Palao *et al.*, 2009; Pertusa *et al.*, 2012). Two conserved cysteine residues linked by a disulfide bond flank the glycosylation site at positions Cys-929 and Cys-940 and are essential for channel activity (Dragoni *et al.*, 2006).

Like most members of the TRP superfamily, TRPM8 is a nonselective cation channel. Substituting ions in the extracellular solution while recording current-voltage curves revealed modest permeability to calcium and little selectivity among monovalent cations ($P_{Ca} / P_{Na} = 3.2$; $P_K / P_{Na} = 1.1$; $P_{Cs} / P_K = 1.2$) (McKemy *et al.*, 2002).

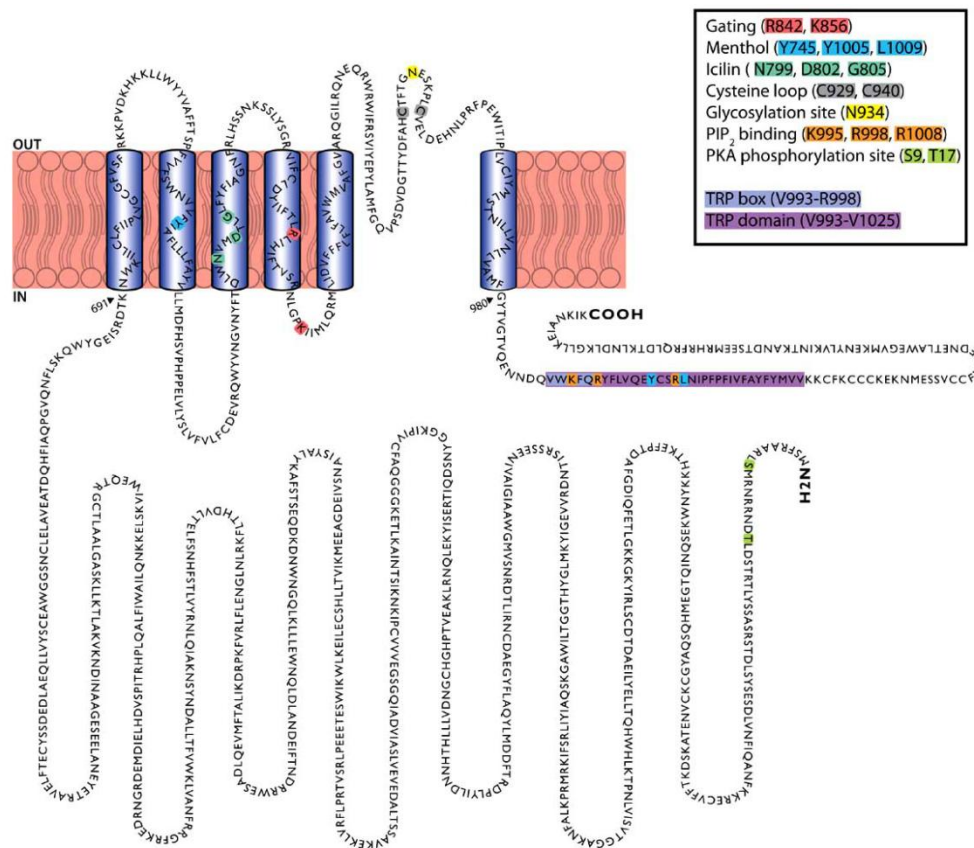


Figure 4. Structure of TRPM8. Schematic representation of human TRPM8 channel subunit topology, showing relevant residues for channel gating and modulation. Individual residues involved in particular aspects of TRPM8 function are highlighted in a color code [From (Malkia *et al.*, 2011)].

1.3.2. TRPM8 gating

Like many enzymatic reactions, the rate of gating of an ion channel increases with temperature (Hille, 2001). However, the cold-sensitive TRPM8 channel is activated by cold temperatures and at first glance seems to defy this basic notion. Voets and colleagues tried to address this apparent paradox by modeling the gating of thermoTRPs (Voets *et al.*, 2004).

Firstly, a characteristic feature of thermoTRPs is a marked outward rectification of the current at positive potentials (Figure 5a). By conducting a tail current protocol, they showed that the TRPM8 channel rapidly closes when stepped to negative potentials from a channel activating positive pre-pulse of +120 mV (Figure 5b). The current-voltage relation right after the step from +120 mV is linear, which indicates that open TRPM8 channels display an ohmic current-voltage relation (Figure 5c). These data reflect a voltage-dependent mechanism of channel closure at negative potentials. In addition, they found that the thermal sensitivity of the channel strongly depends on the transmembrane voltage. By measuring current activation at different holding potentials during slow cooling ramps, they found current activation at depolarized potentials preceding those at more negative potentials. The same principle was true for menthol-induced currents as well. From these results they concluded that temperature and temperature mimetic compounds cause a drastic shift in the voltage dependence of TRPM8 activation towards more negative potentials that are closer to physiological levels (Voets *et al.*, 2004).

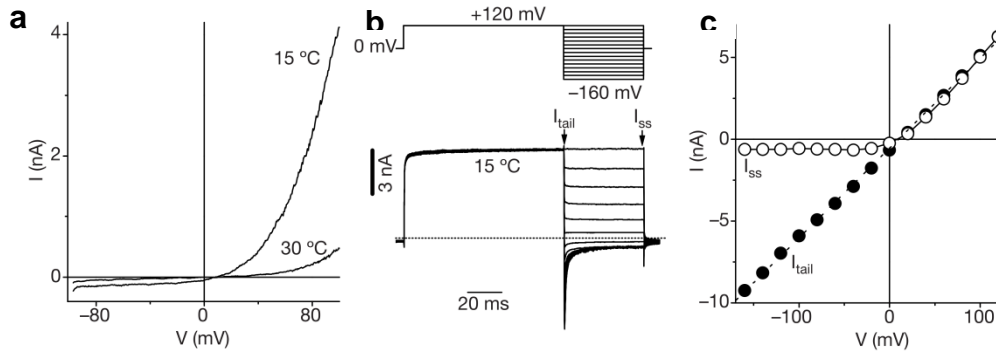


Figure 5. **a)** ThermoTRP channels are marked by a pronounced outward rectification at positive potentials. In the case of the cold-sensitive TRPM8 channel lowering the temperature causes larger inward and outward currents. **b)** By using a tail current protocol it was shown that TRPM8 is activated upon a depolarizing pulse of +120 mV and rapidly closes at negative potentials. **c)** The current-voltage relation obtained immediately after the pre-pulse to +120 mV was linear (black circles), indicating an ohmic current-voltage relation for open TRPM8 channels. This means that the single channel conductance of TRPM8 is independent of voltage [Adapted from Voets *et al.* (Voets *et al.*, 2004)]

Temperature sensing by TRPM8 is a membrane-delimited process, as indicated by the fact that TRPM8 can still be activated in cell-free membrane patches (Voets *et al.*, 2004) and even in artificial bilayers (Zakharian *et al.*, 2010). This precludes a temperature dependent binding of second-messengers as a mechanism for channel activation. Likewise, the fact that the thermal threshold of TRPM8 activation shifts upon changes in transmembrane voltage is not consistent with channel activation by temperature-dependent phase transitions in the lipid membrane, or temperature dependent changes in the channel protein structure, as these theories would predict a single thermal threshold. As an alternative explanation, Voets and colleagues considered a simple two-state model of a voltage-gated channel in which temperature sensitivity is a consequence of a differential effect of temperature on the opening and closing transitions of the channel. The transition from the closed to the open state is voltage dependent, making it more likely for the channel to be in an open state at more positive membrane potentials. Likewise, the opening and closing rates are temperature dependent. In their experiments, Voets and colleagues show that the closing rate of TRPM8 has a steep temperature dependence with a Q_{10} of 9.4, in contrast to the opening rate which is much less temperature dependent, with a Q_{10} of 1.2. The overall effect is that cooling leads to an opening rate that remains constant, but the closing rate sharply decreases, resulting in channel activation (Figure 6).

However, the two-state model is relatively simple and does not properly accommodate some experimental findings, including the effect of saturating thermal, chemical or voltage stimuli on gating (Matta and Ahern, 2007; Yang *et al.*, 2010).

Finally, kinetic analysis of single channel data for TRPM8 provide evidence for multiple open and closed states, which are not predicted by the two-state model (Fernandez *et al.*, 2011). Several allosteric models addressing these limitations have been proposed, which are fashioned under the specific assumption that distinct domains of the channel allosterically act as voltage, agonist and temperature sensors that modulate channel gating (Brauchi *et al.*, 2004; Voets *et al.*, 2007). Nevertheless, the number of free parameters to fit increases significantly when using allosteric models of gating and as such can lead to large errors in parameter estimation (Voets, 2012).

Regardless of the real gating mechanisms, the two-state model is able to predict experimental results obtained for TRPM8 within a temperature range of 10°C to 45°C, and as such is useful as a close approximation of TRPM8 gating under physiological conditions. The thermal activation of the heat-activated TRPV1, TRPM3, TRPM4 and TRPM5 were also found to be voltage dependent and their gating can also be approximated by the two-state model (Voets *et al.*, 2004; Talavera *et al.*, 2005; Vriens *et al.*, 2011).

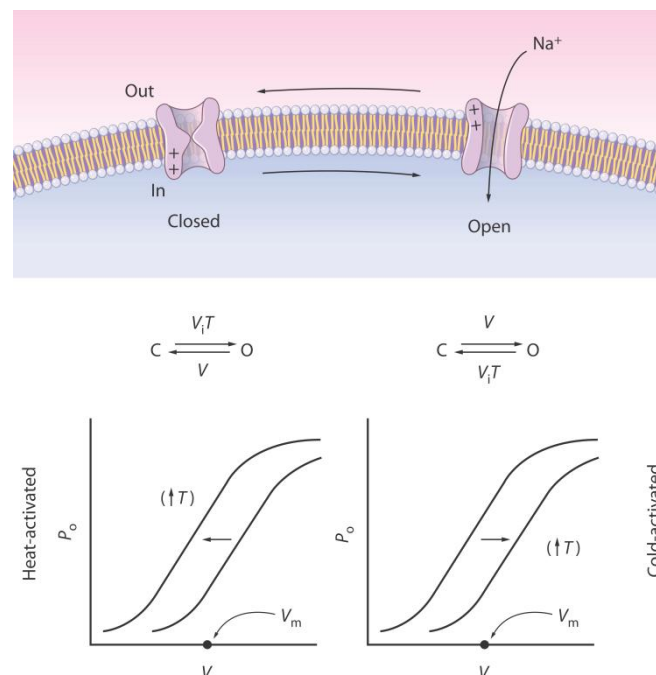


Figure 6. Model for thermal gating of TRP channels. In this simple model, the channel can occupy one of two states—closed and open—and transitions between the two states are sensitive to voltage. Thermosensitivity of the channel results from an asymmetry in the temperature dependence of opening and closing transitions. For the heat-activated channels, the opening transition is more temperature sensitive, whereas for cold-activated channels, the closing transition is more temperature sensitive. This model predicts that the probability that channels are open (P_o) as a function of voltage (V) shifts to the left upon warming for TRPV1 and to the right for TRPM8 [adapted from Liman (Liman, 2006)].

1.3.3. TRPM8 expression profile

TRPM8 is mainly found in primary sensory neurons, where its expression is restricted to a subpopulation of cold-sensitive neurons of small and medium-diameter in the trigeminal and dorsal root ganglia. These neurons are isolectin B4 (IB4)-negative. IB4 is a characteristic marker for non-peptidergic nociceptive neurons (McKemy *et al.*, 2002; Peier *et al.*, 2002a; Abe *et al.*, 2005; Takashima *et al.*, 2007; Dhaka *et al.*, 2008). The peripheral terminals of these neurons innervate the skin, tongue, palate, teeth, cornea, colon and bladder (Takashima *et al.*, 2007; Dhaka *et al.*, 2008; Hayashi *et al.*, 2009; Parra *et al.*, 2010; Harrington *et al.*, 2011). The partial overlap of TRPM8 and certain neurochemical markers indicate that TRPM8 is expressed in unmyelinated C-fibers and lightly myelinated A δ -fibers (Takashima *et al.*, 2007). Studies in cultured sensory neurons suggest that TRPM8 is co-expressed with several nociceptive markers. About half of TRPM8-positive neurons co-express with TRPV1, a marker for nociceptive neurons, as indicated by their response to the TRPV1-agonist capsaicin (McKemy *et al.*, 2002; Viana *et al.*, 2002; Xing *et al.*, 2006; Hjerling-Leffler *et al.*, 2007). Subsequent neurochemical and functional studies of intact fibers corroborated these findings (Takashima *et al.*, 2007; Dhaka *et al.*, 2008; Parra *et al.*, 2010; Harrington *et al.*, 2011). Furthermore, twenty to thirty percent of TRPM8 expressing somatosensory neurons are immunoreactive for calcitonin gene-related peptide (CGRP) (Takashima *et al.*, 2007), a neurotransmitter which is released from the peripheral terminal upon noxious stimulation of nociceptive afferents (Julius and Basbaum, 2001). CGRP release induces vasodilation and causes leakage of proteins and fluids from postcapillary venules (Julius and Basbaum, 2001). Moreover, there exists an extensive overlap of TRPM8 with the GDNF family receptor α 3 (GFR α 3) (Lippoldt *et al.*, 2013), which is activated by the pro-algesic neurotrophic factor artemin. Artemin is implicated in the sensitization of nociceptors to temperature and mechanical stimuli (Elitt *et al.*, 2006; Malin *et al.*, 2006; Lippoldt *et al.*, 2013). The central projections of TRPM8-positive afferents primarily terminate in the superficial lamina I and the outer region of lamina II of the spinal cord dorsal horn, which is in accordance with the termination of CGRP-positive fibers (Takashima *et al.*, 2007).

These results indicate that there are two distinct classes of TRPM8-expressing neurons, one having non-nociceptive properties, whereas the second class

expresses characteristic nociceptive markers. Taken together, these findings suggest that a fraction of TRPM8-positive neurons can be neurochemically considered as nociceptors (Julius and Basbaum, 2001; Basbaum *et al.*, 2009). Indeed, the nerve endings of TRPM8-positive fibers terminate in peripheral structures and zones that mediate both innocuous and noxious cold signaling, giving more substance to the idea of a functionally distinct population of TRPM8-positive fibers (Takashima *et al.*, 2007).

Besides its expression in somatosensory neurons of the dorsal root and trigeminal ganglia, TRPM8 is also found to be expressed in vagal afferents innervating bronchopulmonary tissue, although expression is low (Fajardo *et al.*, 2008; Xing *et al.*, 2008). In non-neuronal tissue, TRPM8 is found in the prostate and testis, which is the site of its original discovery (Tsavaler *et al.*, 2001). Later, it was found to be expressed in the bladder and urogenital tract (Stein *et al.*, 2004), liver (Henshall *et al.*, 2003), lungs (Sabnis *et al.*, 2008b) and vascular smooth muscle (Yang *et al.*, 2006; Johnson *et al.*, 2009). Additionally, functional TRPM8 has been detected in human sperm (De Blas *et al.*, 2009) and more recently in brown adipocytes of mice and white adipocytes in human (Ma *et al.*, 2012; Marco *et al.*, 2013). Furthermore, several cancerous cells like neuroendocrine tumor (NET) cells, human melanoma cells and human uveal melanoma cells also express TRPM8 (Mergler *et al.*, 2004; Yamamura *et al.*, 2008; Louhivuori *et al.*, 2009; Mergler *et al.*, 2014). The function of TRPM8 in many of these tissues is unknown.

1.3.4. TRPM8 pharmacology

Initial studies of TRPM8 showed it to be activated by the natural compounds eucalyptol and menthol, a cyclic monoterpene alcohol found in the leaves of the mint plant of the genus *Mentha*. The synthetic cooling compound icilin was also found to be a potent TRPM8-agonist (McKemy *et al.*, 2002; Peier *et al.*, 2002a). Later, additional natural and synthetic compounds were described as agonists of TRPM8. Among them are the natural odorants linalool, hydroxycitronellal and geraniol as well as synthetic menthol derivatives used in the cosmetics industry such as Frescolat ML, WS-3, frescolatMAG, cooling agent 10, PMD38, WS-23 and CoolactP (McKemy *et al.*, 2002; Behrendt *et al.*, 2004; Bodding *et al.*, 2007). WS-12, another synthetic menthol derivative, is a specific and most potent agonist of TRPM8 known to date (Beck *et al.*, 2007; Bodding *et al.*, 2007). Furthermore, numerous TRPM8-antagonists

have been identified. Several known antagonists of TRPV1 were found to inhibit TRPM8 activation, of which the most widely used is BCTC (Valenzano *et al.*, 2003; Behrendt *et al.*, 2004; Madrid *et al.*, 2006; Malkia *et al.*, 2007). TRPM8-activity is also potently inhibited by SKF96365, a non-specific blocker of various calcium-permeable channels, and by clotrimazole and econazole, members of the imidazole family of antimycotics (Madrid *et al.*, 2006; Malkia *et al.*, 2007; Meseguer *et al.*, 2008).

As mentioned before, menthol acts on TRPM8 by shifting its voltage dependence towards more negative potentials, facilitating TRPM8 opening at physiological potentials (Voets *et al.*, 2004; Malkia *et al.*, 2007). A similar, but opposite effect has been described for several TRPM8 antagonists (Malkia *et al.*, 2007). Co-application of agonist and antagonists can titrate the voltage dependence of TRPM8 to any preferred potential (Malkia *et al.*, 2007).

Several binding sites for agonists of TRPM8 have been discovered. Sensitivity to icilin is conferred by three residues located in the third transmembrane segment of TRPM8, and mutations in either Asn799, Asp802 or Gly805 render the channel insensitive to icilin (Chuang *et al.*, 2004). Furthermore, the amino acids that are involved in menthol sensitivity are Tyr745, which is located in transmembrane segment 2, and Tyr1005 and Leu1009 in the C-terminal of the channel (Bandell *et al.*, 2006; Malkia *et al.*, 2009). Icilin activates TRPM8 in a mechanistically distinct manner from cold or menthol, and requires a simultaneous rise in intracellular Ca^{2+} for TRPM8 activation (Chuang *et al.*, 2004). Some binding sites for antagonists have been uncovered as well, as the menthol binding site at residue Tyr745 is critical for the antagonistic effect of SKF96365 (Malkia *et al.*, 2009).

Ion channel	Agonists	Antagonists
TRPM8	natural compounds	Thio-BCTC ³ , CTPC ⁶ , ethanol ⁶ SB-452533 ⁶ , BCTC ^{3,6,7,8} , capsazepine ^{3,6} , SKF96365 ⁸ , 1,10-phenanthroline ⁸ , NADA ⁹ , anandamide ⁹ , clotrimazole ¹⁰ AMTB ¹¹ , PBMC ¹² , AMG2850 ^{13,14}
	Menthol ^{1,2,3} , eucalyptol ¹ , linalool ³ , hydroxycitronal ³ , geraniol ³	
	synthetic compounds	
	Icilin ¹ , Frescolat ML ³ , FrescolatMAG ³ , Coolact P ³ , cooling agent 10 ³ , PMD 38 ³ , WS-3 ³ , WS-23 ³ WS-12 ^{4,5} , CPS-113 ⁵ , CPS-369 ⁵ , WS-148 ⁵ , WS-30 ⁵	
References: 1) McKemy <i>et al.</i> , 2002 2) Peier <i>et al.</i> , 2002 3) Behrendt <i>et al.</i> , 2004 4) Beck <i>et al.</i> , 2007 5) Boddington <i>et al.</i> , 2007 6) Weil <i>et al.</i> , 2005 7) Madrid <i>et al.</i> , 2006 8) Malkia <i>et al.</i> , 2007 9) De Petrocellis <i>et al.</i> , 2007 10) Meseguer <i>et al.</i> , 2008 11) Lashinger <i>et al.</i> , 2008 12) Knowlton <i>et al.</i> , 2011 13) Gava <i>et al.</i> , 2012 14) Liu <i>et al.</i> , 2013		

Table 2. A selection of TRPM8 agonists and antagonists

1.3.5. Modulation of TRPM8

The thermal thresholds of recombinant TRPM8 channels are found to be consistently lower than that of natively expressed TRPM8. Mean threshold temperatures range from 27°C to 31°C for natively expressed TRPM8 (Reid *et al.*, 2002; Viana *et al.*, 2002; Thut, 2003; Madrid *et al.*, 2006) to 21-26°C for recombinantly expressed TRPM8 (McKemy *et al.*, 2002; Peier *et al.*, 2002a; Malkia *et al.*, 2007). The large discrepancy in the observed thermal thresholds between native and heterologous TRPM8 can be explained by a shift in the voltage-dependent activation of recombinant channels towards more negative potentials (Malkia *et al.*, 2007). This suggests a possible role for endogenous factors that modulate TRPM8 *in vivo* (de la Peña *et al.*, 2005; Malkia *et al.*, 2007).

Cold-sensitive thermoreceptors slowly adapt to sustained cooling. Electrophysiological recordings demonstrate a clear desensitization of cold- and menthol-sensitive TRPM8 currents. This is true for heterologously expressed TRPM8 and TRPM8 expressed in sensory neurons. The desensitization is attributable to an increase in intracellular Ca²⁺, as removing Ca²⁺ from the extracellular medium or chelating intracellular Ca²⁺ prevents desensitization of the current (McKemy *et al.*, 2002; Okazawa *et al.*, 2002; Reid *et al.*, 2002). During adaptation, the temperature-sensitivity of TRPM8 shifts towards lower temperatures. To elicit the same current as before, stronger cooling needs to be applied. Raising intracellular calcium levels

mimics adaptation (Reid *et al.*, 2002). Rising intracellular Ca^{2+} -levels modulate the activity of TRPM8 by the activation of Ca^{2+} dependent phospholipase C (PLC). This enzyme hydrolyzes $\text{PI}(4,5)\text{P}_2$ to form diacyl glycerol (DAG) and inositol 1,4,5-triphosphate (IP_3). As previously described, TRPM8 contains several $\text{PI}(4,5)\text{P}_2$ binding sites and $\text{PI}(4,5)\text{P}_2$ itself is required for TRPM8 activation. Depleting intracellular $\text{PI}(4,5)\text{P}_2$ results in channel desensitization by shifting the voltage dependence of TRPM8 towards more positive potentials (Liu and Qin, 2005; Rohacs *et al.*, 2005; Daniels *et al.*, 2009). Brief exposure to high temperatures shifts the temperature threshold of TRPM8 to warmer temperatures through an unknown interaction with $\text{PI}(4,5)\text{P}_2$, but this does not require the involvement of intracellular Ca^{2+} (Fujita *et al.*, 2013). Another way in which rising intracellular Ca^{2+} -levels modulate TRPM8 is by calcium-dependent protein kinase C (PKC), which initiates dephosphorylation of TRPM8 through activating protein phosphatases (Premkumar *et al.*, 2005; Abe *et al.*, 2006). Additionally, increases in extracellular calcium have been reported to influence the sensitivity of cold sensors (Schafer *et al.*, 1986). This effect has been attributed to the effects of surface charge screening, whereby Ca^{2+} binds to negative charges on the extracellular side of the membrane, thereby altering the potential difference that is applied to the voltage sensor (Hille, 2001). Affecting the TRPM8 voltage sensor by surface charge screening results in a shift towards more positive potentials for the voltage dependent gating of TRPM8 (Hille, 2001; Mahieu *et al.*, 2010).

Furthermore, increases in cAMP through activation of G-protein coupled receptors leads to the activation of protein kinase A (PKA). Two chemical activators of the PKA pathway, forskolin and 8-Br-cAMP, desensitize the response of TRPM8 to menthol and icilin. Selectively inhibiting PKA attenuates this desensitization (De Petrocellis *et al.*, 2007). Consistent with these results is a study that suggests a desensitization of menthol- and cold-induced currents by inflammatory agents that activate PKA or PKC (Linte *et al.*, 2007). Also, activation of calcium-insensitive phospholipase A_2 (iPLA₂) positively modulates TRPM8 (Vanden Abeele *et al.*, 2006; Andersson *et al.*, 2007). iPLA₂ hydrolyzes phospholipids to form polyunsaturated fatty acids, usually arachidonic acid, and lysophospholipids (LPL's) (Akiba and Sato, 2004). LPL's positively modulate TRPM8 activity, whereas arachidonic acid negatively modulates TRPM8. However, reduction of iPLA₂ expression leads to an inhibition of TRPM8 and intracellular application of iPLA₂ activates TRPM8. Given the

overall positive effect of iPLA₂ activation, it is likely that the positive effects of lysophospholipids prevail over the negative effects of arachidonic acid (Vanden Abeele *et al.*, 2006; Andersson *et al.*, 2007).

Inorganic polyphosphate (polyP) is a polymer consisting of many phosphate residues and is present in all eukaryotic cells. PolyP was found to associate with TRPM8 to form a stable complex, thereby modulating its activity. Enzymatic breakdown of polyP reduces TRPM8 activity (Zakharian *et al.*, 2009).

Furthermore, intracellular pH modulates TRPM8 activity. Increasing intracellular pH enhances icilin and cold activation, whilst lowering the pH decreases channel activation. Interestingly, menthol induced activation of TRPM8 is not dependent on pH, at least within the tested range of pH 6.5 to 8 (Andersson *et al.*, 2004).

The specific localization of TRPM8 in the membrane is also of importance for TRPM8 activation. *N*-glycosylation of residue Asn934 facilitates the segregation of TRPM8 into specialized cholesterol-rich membrane domains called lipid rafts. Cholesterol-depletion disturbs the preferential localization of TRPM8 into lipid rafts and results in a significant potentiation of menthol- and cold-mediated responses in heterologous systems and acutely dissociated sensory neurons. This potentiation is based on a shift in the voltage dependent activation of TRPM8 towards more negative potentials. The mechanisms by which TRPM8 is modulated by its localization in lipid rafts are hitherto unknown (Morenilla-Palao *et al.*, 2009).

Recently, a novel membrane protein was discovered called phosphoinositide interacting regulator of TRP (Pirt). It was found to be specifically expressed in peripheral sensory neurons, where it modulates TRPV1 (Kim *et al.*, 2008). Later, it was discovered to modulate TRPM8 as well. Pirt-knockout mice are less sensitive to cooling and when co-expressed with TRPM8, it decreases the cold threshold in HEK293 cells (Tang *et al.*, 2013). Supposedly, Pirt regulates TRPV1 function by binding to both PIP₂ and TRPV1 (Kim *et al.*, 2008). Similarly, Pirt also binds to TRPM8 *in vitro* and it is suggested that the modulation of TRPM8 is mediated by PIP₂ through a physical interaction between the two proteins (Kim *et al.*, 2008; Tang *et al.*, 2013).

Finally, activating a Gq-coupled receptor results in decreased TRPM8 activity. The activated G-protein subunit Gα_q was found to bind directly to TRPM8, preventing TRPM8 activity (Zhang *et al.*, 2012).

1.3.6. Physiological role of TRPM8

TRPM8 as a cold sensor

The main role of TRPM8 *in vivo* is that of a cold sensor. By creating mouse lines deficient in TRPM8, three groups independently showed that TRPM8 is the main transducer of innocuous cold (Bautista *et al.*, 2007; Colburn *et al.*, 2007; Dhaka *et al.*, 2007). Various behavioral tests demonstrated severely attenuated cold mediated behaviors in TRPM8-knockout mice compared to their wild type littermates. The involvement of TRPM8 in cold nociception was less clear. Two groups reported no difference in pain behavior between wild type and TRPM8-knockout mice in a cold plate test (Bautista *et al.*, 2007; Dhaka *et al.*, 2007), whereas another found an increased response latency in TRPM8 knockout mice in the same test (Colburn *et al.*, 2007). A later study found similar results to that of Colburn *et al.*, and suggested that the disparity in results obtained between studies is attributable to methodological issues with the cold plate test. They argue that using lightly restrained animals, with their paws in constant contact with the cold plate, results in less variable responses (Gentry *et al.*, 2010). By using different approaches, some recent studies in TRPM8-knockout and TRPM8-ablated mice strengthen the idea that TRPM8 is involved in the detection of noxious cold. Through creating a line of transgenic mice that specifically express a diphtheria toxin receptor in TRPM8-positive cells, TRPM8-expressing neurons are selectively ablated by the injection of diphtheria toxin into adult transgenic mice. Cells that do not express the diphtheria toxin receptor remain unharmed, as they do not express a receptor that mediates the uptake of the toxin (Knowlton *et al.*, 2013; Pogorzala *et al.*, 2013). Interestingly enough, TRPM8-ablated animals demonstrate more profound deficits in noxious cold sensing than TRPM8-knockout mice. Nevertheless, although noxious cold-induced behavior and cold-evoked responses in sensory neurons from TRPM8-knockout and -ablated mice are attenuated, they do not wholly disappear. This strongly indicates the existence of additional molecular cold sensor(s) that contribute to noxious cold sensing. Possible alternative molecular cold sensors include the cold-sensitive TRPA1-channel (Story *et al.*, 2003), thermosensitive leak or background potassium channels (Reid and Flonta, 2001b; Viana *et al.*, 2002; Madrid *et al.*, 2009; Noel *et al.*, 2009) and a thus far unidentified rapidly adapting cold receptor (Babes *et al.*, 2006).

Briefly, the function of TRPA1 as a noxious cold-sensor *in vitro* is uncontested, yet its role as a physiological noxious cold-sensor in somatic sensory neurons innervating the skin remains a topic of controversy (Story *et al.*, 2003; Kwan and Corey, 2009). However, evidence for its role in mediating cold hypersensitivity after inflammatory or neuropathic injury is overwhelming (Katsura *et al.*, 2006; Petrus *et al.*, 2007; da Costa *et al.*, 2010; del Camino *et al.*, 2010; Chen *et al.*, 2011; Nassini *et al.*, 2011). Furthermore, a role for potassium channels in cold sensing has been established in the peripheral and central nervous system (de la Peña *et al.*, 2012). TREK-1 and TRAAK are thermosensitive background potassium channels that are normally open at physiological temperatures and close upon cooling (Maingret *et al.*, 2000; Kang *et al.*, 2005). Furthermore, a rapidly adapting current was uncovered by applying a fast (<20 ms) 10-s cooling step from 32°C to 18°C in somatosensory neurons. The time course of current adaptation is in the range of a few seconds, and closely corresponds to fast adaptation recorded from intact receptors *in vivo*. As of yet, the molecular identity of this receptor is unknown (Babes *et al.*, 2006).

The involvement of TRPM8 in thermoregulation and thermogenesis

The aforementioned studies (Bautista *et al.*, 2007; Colburn *et al.*, 2007; Dhaka *et al.*, 2007) have demonstrated that TRPM8 mediates the avoidance of innocuous cold, which is a form of behavioral thermoregulation. More recently, a number of studies also revealed a role for TRPM8 in the regulation and maintenance of core body temperature through autonomous physiological thermoeffectors. The TRPM8 agonists menthol and eucalyptol (also known as 1,8-cineole) enhance thermogenesis when injected in mice (Masamoto *et al.*, 2009). Further, it was known that injection of the potent TRPM8 agonist icilin results in an increase in core body temperature in rats, but a definite role for TRPM8 in this effect was not established (Ding *et al.*, 2008). However, a recent report demonstrated that a subcutaneous injection of icilin does not increase core body temperature in TRPM8 knockout mice, in contrast to wild type animals. Intraperitoneal injections with the specific TRPM8 antagonist 1-phenylethyl-4-(benzyloxy)-3-methoxybenzyl(2-aminoethyl)carbamate (PBMC) produces a drop in core body temperature in wild type but not TRPM8-knockout mice (Knowlton *et al.*, 2011). This is highly suggestive for a direct role of TRPM8 in the autonomous regulation of core body temperature. Further studies by other labs corroborate these findings. Orally administering a TRPM8 antagonist produces a

decrease in core body temperature in rats and mice (Gavva *et al.*, 2012) and intravenous injection of a TRPM8 antagonist produces a decrease in core body temperature in rats and mice, but not in TRPM8-knockout mice (Almeida *et al.*, 2012). The decrease in body temperature is partly due to inhibition of peripheral cold signaling which was found to regulate known autonomic thermoeffectors, such as vasoconstriction in the tail and nonshivering thermogenesis in brown adipose tissue (BAT) (Almeida *et al.*, 2012). Possibly, modulation of thermogenesis through TRPM8 is mediated by BAT, as in mice the tissue was found to express TRPM8. Activation of TRPM8 with menthol leads to the upregulation of uncoupling protein 1 (UCP1), the molecular hallmark of BAT activation, in wild-type but not in TRPM8^{-/-} mice (Ma *et al.*, 2012). Also, TRPM8 has been detected in white adipose tissue in humans. Activation of these cells by menthol and icilin leads to a BAT-like phenotype by inducing UCP1 expression and increasing heat production (Marco *et al.*, 2013).

Other physiological roles of TRPM8

As noted before, TRPM8 is also expressed in tissues that are not known to be thermosensitive. It is expressed in vascular smooth muscle, where activating TRPM8 can cause vasoconstriction or vasodilatation, dependent upon the existing degree of vasomotor tone. However, its mechanism of activation and physiological significance remain undetermined (Yang *et al.*, 2006; Johnson *et al.*, 2009). Its expression in the bladder urothelium and afferents innervating the bladder are thought to be involved in the voiding reflex induced by cooling (Stein *et al.*, 2004). The presence of TRPM8 in the urogenital tract, prostate, testis and even in human sperm are suggestive of a possible role in male fertility (Tsavaler *et al.*, 2001; Henshall *et al.*, 2003; Stein *et al.*, 2004; Yang *et al.*, 2006; De Blas *et al.*, 2009; Johnson *et al.*, 2009). TRPM8 expressed in a subpopulation of vagal afferent fibers innervating the airways might provide the mechanism by which inhalation of cold air causes airway constriction (Xing *et al.*, 2008). The role of a truncated variant of TRPM8 expressed in the endoplasmic reticulum of bronchial epithelial cells remains uncertain, but exposing these TRPM8-expressing cells to cold and menthol leads to significant increases in cytokine gene expression (Sabnis *et al.*, 2008a; Sabnis *et al.*, 2008b). The physiological role of TRPM8 in colonic afferent neurons is unknown, but it might be the transducer of the anti-nociceptive properties of peppermint oil in the treatment of irritable bowel syndrome (Harrington *et al.*, 2011). The absence of menthol induced

analgesia in TRPM8 knockout animals after intraperitoneal injections with acetic acid, which normally provokes visceral pain, reinforces this notion (Liu *et al.*, 2013). Finally, TRPM8 is expressed in the terminals of afferents innervating the cornea, where it contributes to regulating basal tear flow (Parra *et al.*, 2010).

1.3.7. Molecular determinants of thermal thresholds and signal propagation

TRPM8 is activated by noxious and innocuous cold and is found in nociceptive and non-nociceptive neurons. Taken together with the results obtained from TRPM8-knockout or -ablated animals it suggests that TRPM8 is involved in both innocuous and noxious cold sensing. But how does a TRPM8-expressing neuron operate over such a wide range of cold temperatures and how does it discriminate between innocuous and noxious cooling?

Mechanistically speaking, opening of TRPM8 provides the receptor potential, that is, a local depolarization of the sensory nerve terminal, to initiate the firing of action potentials. Independently of TRPM8, other molecular players are present that determine the excitability and signal propagation of nerve terminals and afferents (Belmonte *et al.*, 2009).

The reversal potential of potassium ions is negative to the resting membrane potential and opening of potassium channels hyperpolarizes this potential, which is why potassium channels are crucial regulators of neuronal excitability. (Hille, 2001). The first evidence that potassium currents play a role in cold transduction came from studies that indicated that cooling inhibits a potassium conductance and therefore increases neuronal excitability (Reid and Flonta, 2001b; Viana *et al.*, 2002). Moreover, blocking potassium channels rendered previously cold-insensitive neurons cold-sensitive (Viana *et al.*, 2002; Roza *et al.*, 2006).

After the discovery of TRPM8 as the main cold sensor, the contribution of potassium channels to cold sensing was explored further. For example, TREK-1 and TRAAK, two-pore-domain potassium channels that are constitutively open at warm temperatures and act as an excitability break, are temperature sensitive and close during cooling (Maingret *et al.*, 2000; Kang *et al.*, 2005). Deleting both TREK-1 and TRAAK sensitizes cold- and menthol-sensitive neurons to cold. However, it also confers cold, but not menthol-sensitivity to a previously non cold-responding population of neurons (Noel *et al.*, 2009).

Furthermore, by characterizing low- (LT) and high-threshold (HT) cold-sensitive neurons, Madrid and colleagues revealed that their respective thermal thresholds correlate with a variable expression of TRPM8 and Kv1 potassium channels. Dendrotoxin-sensitive Kv1 (e.g. Kv1.1, Kv1.2, Kv1.6) potassium channels act as a brake for neuronal excitability. Therefore, a balance between the expression of Kv1 subunits and TRPM8 results in a variable thermal threshold of TRPM8 expressing cold-sensitive somatosensory neurons. LT cold-sensitive neurons are characterized by a high functional expression of TRPM8 and a low functional expression of Kv1 subunits. The abundance of TRPM8 channels creates a larger receptor potential, whereas the low expression of Kv1 subunits ensures a high excitability, resulting in a neuron that is readily excited by innocuously cold temperatures. The reverse situation presents itself in HT cold-sensitive neurons, with a low functional expression of TRPM8 and a high functional expression of Kv1 subunits, necessitating a more robust thermal stimulus for the few expressed TRPM8 channels to overcome the excitability brake established by the abundance of Kv1 subunits (Madrid *et al.*, 2009). Recently, Kv7 potassium channels were also implicated in modulating cold transduction (Vetter *et al.*, 2013). Kv7 conducts the M-current, which is activated upon depolarization and therefore acts as a brake for repetitive action potential firing (Delmas and Brown, 2005). Blocking the M-current amplifies action potential firing and firing rates in cold-sensitive fibers upon cooling, but does not lead to action potential firing in cold-insensitive fibers (Vetter *et al.*, 2013).

Additionally, sodium channels, which are crucial for action potential generation and propagation, are implicated in cold-sensing (Hille, 2001). In particular, the tetrodotoxin-resistant voltage gated sodium channel Na_v1.8 has an important role in the detection of noxious cold (Akopian *et al.*, 1996). Not because it is a cold sensor *per se*, but because it is unique among voltage-sensitive sodium channels in that it does not inactivate at low temperatures (Zimmermann *et al.*, 2007) and is exclusively expressed in nociceptive sensory neurons. Thus, a cold-sensitive neuron expressing Na_v1.8 maintains its ability to generate action potentials at very cold temperatures (Zimmermann *et al.*, 2007). Consistent with these findings, earlier and subsequent studies demonstrated only minor responses to noxious cold in Na_v1.8 deficient mice (Akopian *et al.*, 1999; Abrahamsen *et al.*, 2008). A more recent study demonstrated that TRPM8-expressing TTX-resistant (TTX_r) DRG neurons retain their ability for

action potential firing at noxiously cold temperatures, as opposed to TRPM8-positive TTX-sensitive (TTX_s) neurons. Moreover, the temperature at which TTX_s neurons started firing action potentials was significantly higher than in TTX_r neurons (Sarría *et al.*, 2012).

Furthermore, hyperpolarization-activated cyclic nucleotide-gated (HCN) channels giving rise to a hyperpolarized-activated inward current (I_h) are present in the majority of sensory neurons (Scroggs *et al.*, 1994; Momin *et al.*, 2008) and are one of the defining features of cold sensitive neurons (Viana *et al.*, 2002). I_h currents play important roles in membrane potential oscillations and they shape neuronal excitability (Pape, 1996). HCN channels are heteromeric and are composed of a combination of different HCN channel subunits (HCN1 to HCN4), of which HCN channels expressed in cold-sensitive neurons consist of a combination of mainly HCN1 and some HCN2 subunits (Orio *et al.*, 2009). Whilst I_h is not essential for the transduction of cold stimuli, it does shape the firing response of cold thermoreceptor nerve endings in which it might play a role in the sensory coding of cold information (Orio *et al.*, 2012).

Taken together, these data emphasize the importance of molecular players other than TRPM8 in the ability of discriminating between noxious and innocuous cold ambient temperatures.

1.3.8. The role of TRPM8 in (an)algesia

In humans, maintained and moderate cooling evokes innocuous cold sensations until a critical temperature is crossed and cooling is perceived as painful (Davis, 1998; Morin and Bushnell, 1998; Davis and Pope, 2002).

As it turns out, the role of TRPM8 in pain and analgesia is a rather complex one. Depending on context, location and stimulus intensity, TRPM8 activation can elicit sensations from pleasurable and soothing cool to painfully cold. As indicated, several studies provide evidence for TRPM8 being involved in transducing painful temperature stimuli. Behavioral studies in mice have implicated TRPM8 for playing a role in this noxious perception of cold (Bautista *et al.*, 2007; Knowlton *et al.*, 2013).

Furthermore, TRPM8 is also implicated in cold-hypersensitivity in the context of chronic pain caused by injury. Damage to peripheral nerves can produce peripheral neuropathic pain, which is characterized by an increase in pain intensity to otherwise normal painful stimuli (hyperalgesia) and pain evoked by stimuli that are

normally non-painful (allodynia) (Schmidt and Willis, 2007; Basbaum *et al.*, 2009). In patients with peripheral nerve disease, innocuous cold stimulation elicits painful sensations (Bowsher and Haggett, 2005). Oxaliplatin, an effective platinum-based chemotherapeutic agent used in the treatment of colorectal cancer, causes cold induced paresthesias and cold hypersensitivity, which severely restricts its dosage and duration of treatment (Lehky *et al.*, 2004). In mice, chronic constriction injury (CCI) of the sciatic nerve or injection of oxaliplatin induces neuropathic pain that is accompanied by cold hypersensitivity (Colburn *et al.*, 2007; Gauchan *et al.*, 2009). Furthermore, cold hypersensitivity develops in Complete Freund's Adjuvant (CFA) induced inflammatory pain (Lehky *et al.*, 2004; Colburn *et al.*, 2007). These models are helpful in elucidating the putative role of TRPM8 in cold hypersensitivity. For example, in the case of CCI induced neuropathic pain, TRPM8-knockout mice do not develop cold hypersensitivity in contrast to wild type mice (Colburn *et al.*, 2007; Knowlton *et al.*, 2011; Su *et al.*, 2011; Knowlton *et al.*, 2013). Similar results in CCI-induced cold hypersensitivity were obtained for mice in which TRPM8-expressing neurons were conditionally ablated (Knowlton *et al.*, 2013). Capsazepine, a non-specific TRPM8 blocker, significantly attenuates CCI induced cold allodynia. (Xing *et al.*, 2007). Similarly, PBMC, a novel specific TRPM8 antagonist also significantly attenuates CCI induced cold allodynia (Knowlton *et al.*, 2011).

Moreover, it has been proposed that TRPM8 is a primary mediator of cold hypersensitivity induced by inflammation, as activation of TRPM8 is modulated by certain inflammatory mediators as protons, phospholipids and bradykinin (Andersson *et al.*, 2004; Premkumar *et al.*, 2005; Rohacs *et al.*, 2005). Indeed, TRPM8-knockout mice fail to exhibit cold hypersensitivity that typically develops in animal models of CFA induced inflammatory pain (Colburn *et al.*, 2007; Knowlton *et al.*, 2011; Knowlton *et al.*, 2013). In contrast, PBMC did not reduce cold allodynia in the oxaliplatin induced model of neuropathic pain, which is in apparent disagreement with the finding that cold hypersensitivity does not develop in oxaliplatin treated TRPM8-knockout mice. However, the authors did not test higher doses due to the hypothermic effect of the drug, which limits the conclusions drawn from this particular result (Knowlton *et al.*, 2011). In the context of neuropathy, the underlying cellular and molecular mechanisms for abnormal cold sensitivity and analgesia remain poorly understood. It is unlikely that a differential expression of TRPM8 expressed in cold sensitive nerve terminals explains cold hypersensitivity after injury, as the expression

of TRPM8 mRNA in several animal models of cold allodynia and cold hyperalgesia correlate poorly with their behavioral responses to cold [reviewed by (Fernández-Peña and Viana, 2013)]. Compounding the issue is that a given level of mRNA does not necessarily predict its protein level and does not reflect channel function.

As pointed out before, TRPM8-activity is modulated by several endogenous factors as well as by a differential co-expression with other ion channels. It follows that these could participate in the development of cold hypersensitivity following injury or inflammation. For example, during inflammation, several pro-algesics are released at the site of injury. Their role in the development of mechanical and heat hyperalgesia have been studied, but their role in the development of cold hypersensitivity is relatively unknown. Recently it was shown that the pro-algesic glial cell-line derived neurotrophic factor (GDNF) family receptor GFR α 3 is preferentially localized to a subset of putative nociceptive TRPM8-expressing neurons. Injecting artemin, the specific natural ligand of GFR α 3, increases cold-sensitivity in wild type but not TRPM8-knockout mice (Lippoldt *et al.*, 2013). Artemin expression is found to be increased in inflamed skin, supporting the notion that it is involved in cold hypersensitivity after injury (Elitt *et al.*, 2006; Lippoldt *et al.*, 2013). Paradoxically, the inflammatory mediators bradykinin and histamine prevent TRPM8 activity by binding to a Gq-coupled receptor, thus activating the G-protein subunit G α_q , which directly inhibits TRPM8 (Zhang *et al.*, 2012). However, bradykinin has no significant effect on cold sensitivity *in vivo* in mice (Lippoldt *et al.*, 2013). These seemingly paradoxical results could be due to a differential effect of artemin and bradykinin on non-nociceptor and nociceptor subpopulations of TRPM8. Whilst the expression of the artemin receptor GFR α 3 is mainly restricted to the putative nociceptors subpopulation of TRPM8 expressing neurons, the bradykinin receptor B2R is widely co-expressed with TRPM8 (Lippoldt *et al.*, 2013).

Furthermore, changes in the ratios of Kv1, NaV_{1.8} and TRPM8 can alter excitability and signal transduction and thus result in altered cold thresholds and changes in signal transduction. Lastly, cold hypersensitivity could be a result of changes in the central processing of nociceptive information (Belmonte *et al.*, 2009).

Although many questions remain, the aforementioned studies successfully uncovered a role for TRPM8 in the development of cold pain. However, cold pain results from extreme conditions, such as intense cooling or neuropathy, which only partly overlap with the physiological context in which TRPM8 operates. On the other

side of the temperature-spectrum, the range of temperatures that cause an organism to feel pleurably cool, cold temperatures have been shown to mediate beneficial effects. Topical application of menthol and mild cooling has been used throughout history as a remedy for pain relief. For example, mild cooling shows beneficial effects on chronic back pain, dental pain, postoperative pain and muscle injuries (Traherne, 1962; Sauls, 1999). Furthermore, menthol is used in preparations for pain relief in sports injuries, arthritis and other painful conditions (Eccles, 1994; Johar *et al.*, 2012). This is highly suggestive for a role of TRPM8 in analgesia. However, one should exercise caution when interpreting results involving menthol-induced anesthesia. Several studies have shown menthol to inhibit neuronal voltage-dependent Ca^{2+} channels and voltage-dependent Na^{+} channels (Swandulla *et al.*, 1987; Sidell *et al.*, 1990; Gaudioso *et al.*, 2012). Furthermore, menthol activates GABA_A-receptors, the main inhibitory neurotransmitter in the mammalian central nervous system, and thus might have a central anti-nociceptive effect (Watt *et al.*, 2008; Zhang *et al.*, 2008). On the other hand, evidence is emerging that menthol-induced analgesia is indeed mediated through TRPM8. A recent study found that menthol-induced analgesia in several mouse models of acute and inflammatory pain was completely absent in TRPM8-knockout animals. Administering the selective TRPM8 antagonist AMG-2850 to wild type animals provided similar results. WS-12, a specific TRPM8 agonist, induced TRPM8-dependent analgesia similar to that of menthol. These results do strongly suggest that TRPM8 is the principal mediator of menthol-induced analgesia in acute and inflammatory pain (Liu *et al.*, 2013). Other studies also provide evidence of TRPM8-mediated analgesia. In a CCI induced model of chronic neuropathic pain, topical or intrathecal application of icilin or menthol produces behavioral analgesia. The specific involvement of TRPM8 was confirmed by the abrogation of icilin-induced analgesia after knocking down TRPM8 with antisense mRNA. Cutaneous cooling in a range of 20°C to 16°C mimicked the effect of topical icilin and menthol application (Proudfoot *et al.*, 2006). Further, cooling attenuates acute nociceptive responses after intra-plantar injections of formalin in wild type but not TRPM8-knockout mice (Dhaka *et al.*, 2007). In the CCI model of neuropathic pain, cooling mediated analgesia was completely absent in TRPM8-knockout and -ablated animals, confirming the findings of the aforesaid studies (Knowlton *et al.*, 2013).

Briefly, depending on context, location and stimulus intensity, TRPM8 activation can elicit sensations from pleasurable and soothing cool to painfully cold. A

possible explanation might be found in the fact that, as reviewed earlier, TRPM8-expressing somatosensory neurons are a functional heterogeneous population, as indicated by its partial co-expression with nociceptive markers and are characterized by widely varying thermal thresholds. In addition, changes in ion channels co-expressed with TRPM8 might alter the activity of TRPM8-expressing nerve terminals. Furthermore, cold hypersensitivity or analgesia could be a result of changes in the central processing of nociceptive information [reviewed by (Belmonte *et al.*, 2009)].

1.3.9. TRPM8 and cancer

TRPM8 was originally identified in a screen for upregulated genes in prostate cancer tissue and it was proposed that it may be an ion channel with oncogene or tumour promoter potential (Tsavaler *et al.*, 2001). Unsurprisingly, this has led to an interest in the study of TRPM8 as a target for the detection and treatment of cancer, and particularly that of prostate cancer (Zhang and Barritt, 2006). Recently, TRPM8 mRNA levels were found to be elevated in blood and urine of patients with metastatic prostate cancer (Bai *et al.*, 2010). TRPM8 is localized in the plasma membrane as well as in the endoplasmic reticulum of prostate cancer cells, suggesting a role for regulating intracellular Ca^{2+} levels that are necessary for the viability and proliferation of prostate cancer cells (Zhang and Barritt, 2004; Monteith *et al.*, 2007). TRPM8 mRNA was detected in three commonly used human prostate cancer cell lines and pharmacological characterization found TRPM8 to be functionally expressed (Valero *et al.*, 2011; Valero *et al.*, 2012). Pharmacological blockade or TRPM8 knockdown by small interference RNA (siRNA) produced a marked reduction in proliferation rate in these cancer cell lines, which is suggestive of a role for TRPM8 in the development of prostate cancer (Valero *et al.*, 2012). Taken together, TRPM8 is developing to be a promising candidate for the detection and therapy of prostate cancer.

After its detection in prostate cancer cells, multiple studies have screened for TRPM8 expression in other types of malignant tumors. In breast cancer cells, functional TRPM8 was detected, and their expression is regulated by estrogen (Chodon *et al.*, 2010). TRPM8 was found to be overexpressed in human melanoma cells, and activation of TRPM8 with menthol produces an influx of Ca^{2+} which reduces its viability (Yamamura *et al.*, 2008). Furthermore, TRPM8 was detected in human neuroendocrine tumor cells (NET) (Mergler *et al.*, 2004). Human uveal

melanoma cells were found to functionally express TRPM8 (Mergler *et al.*, 2014). In a human bladder cancer cell line, TRPM8 is highly expressed and activation by menthol induces cell death (Li *et al.*, 2009).

1.3.10. Therapeutic potential of pharmacological modulators of TRPM8

As discussed before, in recent years evidence has been mounting that TRPM8 is involved in the development of cold hyperalgesia in several diseases and symptoms. On the other hand, there is also evidence that TRPM8 is involved in the analgesic effects of cold- and menthol-activated cold-sensitive thermoreceptors. Furthermore, TRPM8 is expressed in several cancers. Thus, modulating TRPM8 activity holds promise for the successful treatment of aforesaid pathologies. In fact, TRPM8 antagonists successfully alleviated neuropathic cold hypersensitivity in mice (Xing *et al.*, 2007; Knowlton *et al.*, 2011). And although the analgesic benefits of menthol could have been ascribed to its effects on multiple ion channels involved in the transduction and modulation of pain signals, a recent study firmly established a role for TRPM8 as the principal mediator of the analgesic effect of menthol (Liu *et al.*, 2013). Studies have demonstrated that activation of TRPM8 by menthol reduces cell viability in several different cancers (Zhang and Barritt, 2004; Yamamura *et al.*, 2008; Li *et al.*, 2009), whereas silencing TRPM8 has been demonstrated to reduce proliferation of cancerous prostate cells (Valero *et al.*, 2012). Taken together, TRPM8 is a proven and interesting target for therapeutic intervention. This makes it a prime candidate for the development of novel modulators, which in the future could help to treat TRPM8-related pathologies or function as a tool to further elucidate the biophysical and pharmacological characteristics of TRPM8, as well as further uncover its role in health and disease (Malkia *et al.*, 2011).

2. Objectives

The objectives of the presented work are:

2.1. General objectives

Characterize pharmacological modulators of the ion channel TRPM8 by using calcium-imaging and patch-clamp techniques.

2.2. Specific objectives

- Identify and/or characterize new pharmacological agents with agonistic and antagonistic properties on the ion channel TRPM8.
- Characterize the mechanism of action of these pharmacological compounds.
- Study the effects of these compounds on the function of primary sensory neurons that express TRPM8.

3. Materials and methods

For the study of the pharmacology of the ion channel TRPM8 presented in this work I employed the electrophysiological technique known as patch-clamp (Neher *et al.*, 1978), which was used in several different whole-cell and single channel configurations. Furthermore, I used a calcium-imaging technique based on the fluorimetric characteristics of fura-2 (Grynkiewicz *et al.*, 1985; Williams *et al.*, 1985). Both techniques were mainly employed to study rat TRPM8 that was stably transfected into the mammalian cell-line HEK293 (CR#1-cells) and to study TRPM8 natively expressed in cultured neurons from mouse dorsal root ganglia. Furthermore, some electrophysiological and calcium-imaging experiments were conducted on transiently transfected mutant TRPM8 channels, having point mutations in residues that affect their ability to interact with certain agonists. Lastly, a cell-line consisting of Chinese hamster ovary cells stably transfected with TRPA1 was used in one experiment. All cells were maintained in an incubator kept at an ambient temperature of 37°C in a controlled atmosphere containing 5% CO₂.

3.1. HEK293 cells

HEK293 is an immortalized cell line that is originally derived from human embryonic kidney cells and kept in culture. They were used as a transient expression system for the TRPM8 channel and the TRPM8 mutant channels used in this work. The cells were maintained in 25 cm² flasks in medium containing the following ingredients:

- DMEM containing 10% fetal bovine serum (FBS)
- Penicillin (100 U/ml)
- Streptomycin (100 µg/ml)

HEK293 cells were passed weekly according to the following protocol:

- Remove old medium and wash cell with FBS-free medium.
- Remove FBS-free medium and add 1 mL trypsin/EDTA. Make sure all cells are covered. Remove immediately.
- Incubate for aprox. 3 minutes until cells detach.
- Resuspend cells in 5 mL complete medium
- Reseed a new 25cm² flask with 100 µL medium containing cells + 5 mL complete medium.

3.1.1. Transient transfection of TRPM8 mutants

The HEK293 cells that were used in the experiments were transiently transfected with wild type mouse TRPM8 cDNA, the mouse TRPM8-Y745H menthol insensitive mutant cDNA and the icilin insensitive mutant mouse TRPM8-N799A cDNA. The full length cDNA encoding mTRPM8 was expressed in a pcDNA5 vector. Briefly, by site-directed mutagenesis, the menthol insensitive mutant had its tyrosine at position 745 replaced by histidine (Malkia *et al.*, 2009). The icilin insensitive mutant N799A had asparagine replaced by alanine at position 799 (Chuang *et al.*, 2004). The aforementioned plasmids were transfected into HEK293 cells, together with a plasmid coding for a yellow fluorescent protein (YFP), which emits an easily identifiable bright yellow fluorescent light when excited at 470 nm. For the transfection, the following protocol was used:

1. The day prior to transfection, plate 150.000 HEK293 cells in a 2 cm² well (24-well plate)

Protocol on day of transfection (description is for one well):

2. Dilute 2 µL Lipofetamine 2000 (Invitrogen) in 50 µL serum-free DMEM. Stir gently and incubate for 5 minutes at room temperature.
3. Dilute 1-2 µg mTRPM8-cDNA and 0.3 µg YFP in 50 µL serum-free DMEM. Stir gently.
4. Mix diluted Lipofectamine and cDNA within 25 minutes after end of Lipofectamin incubation. Stir gently and incubate for 20 min at room temperature.
5. Add the mixture to the well, stir gently by rocking the plate back and forth.
6. Incubate the cells in an incubator at 37°C for 5 hours, then change medium.
7. After 18-42 hours, trypsinize and replate cells on poly-L-lysine treated coverslips (6mm). Cells will attach and be ready for calcium-imaging or patch-clamp experiments after approx. 2 hours.

3.2. CR#1 cells

The CR#1 cell line consists of HEK293 cells that are stably transfected with rat TRPM8 and was a kind gift to our lab from Dr. Ramón Latorre from the Centro Interdisciplinario de Neurociencia de Valparaíso (Chile). Its generation and characterization is described in a paper by Brauchi and colleagues (Brauchi et al., 2004). Briefly, by using cationic liposomes, HEK293 cells were transfected with the plasmid vector pCDNA3 that also contained the DNA sequence of rat TRPM8. As the pCDNA3 vector also contains a neomycin resistance gene, TRPM8 expressing cells are selected for by exposing them to an analog of neomycin, the antibiotic gentamicin (G418 sulfate), which was added to the medium at a concentration of 800 µg/ml during two weeks.

CR#1 cells were maintained in the following culture medium

- DMEM containing 10% fetal bovine serum
- Penicillin (100 U/ml)
- Streptomycin (100 µg/ml)
- G418 sulfate

The protocol followed for the maintenance of CR#1 cells is the same as followed for the HEK293 cells, with the addition of 50 µL of G418 per 5 mL of culture medium.

3.3. CHO-A1 cells

The CHO-A1 cell line consists of Chinese hamster ovary (CHO) cells stably expressing mouse TRPA1 and was a kind gift to our lab by Dr. Ardem Patapoutian from The Scripps Research Institute, La Jolla, USA. The expression of TRPA1 is inducible by tetracycline. Briefly, a tetracycline-inducible CHO-K1/FRT cell line was co-transfected with the expression vector pcDNA5FRT/TO containing full-length mouse TRPA1 and the Flp recombinase expression plasmid pOG44 and subsequently selected for via hygromycin resistance (Story *et al.*, 2003).

CHO-A1 cells were maintained in the following culture medium:

- DMEM containing 10% fetal bovine serum
- Glutamax® 2%
- Non-essential amino-acids 1%
- Penicilin (100 U/ml)
- Streptomycin (100 µg/ml)
- Hygromycin (200 µg/ml)
- Blastidicin (5 µg/ml)

3.4. Sensory neuron cultures

Dissociated neurons from the DRG and TG are assumed to express membrane receptors and channels that are expressed in their peripheral nerve terminals *in vivo*. As such, cultured sensory neurons serve as a good model of the peripheral nerve terminal (Kress and Reeh, 1996).

In brief, three to twelve week old male mice were anesthetized by inhalation of CO₂ and subsequently decapitated. Using forceps and a pair of scissors, the spine was carefully removed. Under a microscope, the spine is cut in half using a scalpel, and the dorsal root ganglia removed with a fine pair of forceps and deposited in culture medium. When all ganglia are removed, they are further cleaned by using forceps and a scalpel. Subsequently, the cleaned ganglia are transferred to a 1 mL eppendorf containing a mixture of the enzymes collagenase type XI (0.66 mg/ml) and dispase (3 mg/ml). The ganglia are kept in the enzymatic solution for an hour at a temperature of 37°C and in an controlled atmosphere of 5% CO₂. Following the enzymatic dissociation, the ganglia are mechanically dissociated using a fire polished glass pasteur pipette. Then, the enzymatic solution with the dissociated ganglia is

transferred to a centrifuge and spun down for 5 minutes at 1000 RPM. After the centrifugation, the dissociated neurons have formed a pellet on the bottom of the tube. Subsequently, the medium is removed from the tube and the pellet is resuspended in 200 μ L of culture medium. The medium containing the dissociated DRG's is then further plated out on 10 poly-L-lysine (0.01%) treated coverslips with a diameter of 6 mm. After 4 hours in the incubator, 1 mL of medium is gently added to every Petri dish containing the coverslips. After approximately twenty-four hours the cells are ready for experiments.

3.5. TRPM8^{EYFP} transgenic mice

For the identification of TRPM8-expressing somatosensory neurons, I used a transgenic mouse line in which TRPM8-expressing neurons were labelled by the presence of EYFP (Parra *et al.*, 2010).

In brief, a bacterial artificial chromosome (BAC) containing the entire mouse TRPM8 locus was modified by inserting the cDNA encoding for YFP, fused in frame after the first 9 amino acids of the TRPM8-protein, and followed by a stop codon. This prevents the transcription of the TRPM8 sequence contained in the BAC. Subsequently, the BAC was linearized and purified and then injected into fertilized C57Bl/6 mouse oocytes to generate TRPM8:EYFP BAC transgenic mice.

3.6. Reagents

Most drugs were prepared as a stock in dimethyl sulfoxide (DMSO), except for trinitrophenol (TNP), capsaicin and chloroform (CLF). TNP and GsMTx-4 were dissolved in distilled water, capsaicin in ethanol and CLF was directly dissolved in bath solution before use. The final concentration of DMSO in the bath solution was never higher than 0.1% and the final concentration of ethanol was 0.05 %. The required amount of CLF was directly added to a measured amount of bath solution in a glass Erlenmeyer, vigorously shaken for approximately thirty seconds and subsequently transferred to an airtight container made of glass that fed into the bath.

An overview of all used stocks is provided in the following table.

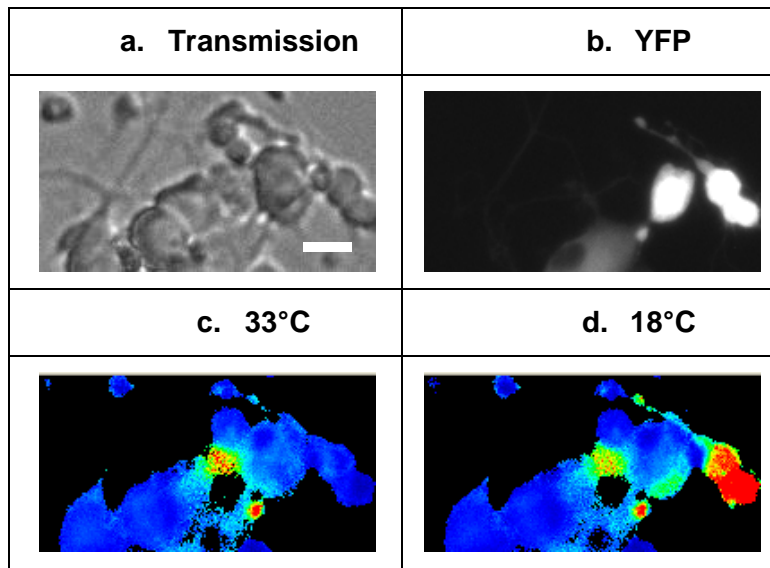
drug	supplier	working concentration	stock	solvent
menthol	Scharlau	20-100 μ M	300 mM	DMSO
icilin	Sigma	10 μ M	10 mM	DMSO
capsaicin	Sigma	500 nM	1 mM	ethanol
AITC	Sigma	100 μ M	100 mM	DMSO
chloroform	Merck	1-20 mM	-	-
5-benzyloxytryptamine	Sigma	1-30 μ M	30 mM	DMSO
BCTC	Grüntal	3 μ M	30 mM	DMSO
GsMTx-4	Peptide Inst.	1 μ M	0.1 mM	d_4 H ₂ O
chlorpromazine	Sigma	10-30 μ M	30 mM	DMSO
trinitrophenol	Sigma	100-200 μ M	57 mM	d_4 H ₂ O

Table 3.1 Overview of all used drugs, their suppliers and their respective solvents.

3.7. Intracellular calcium imaging

Intracellular calcium levels can be determined by the analysis of the fluorescent probe fura-2. Unbound fura-2 has an excitation peak at 362 nm, which shifts to 335 nm upon binding of Ca²⁺ whilst the emission spectrum of the bound and unbound form remains constant. The ratio between the intensity of fluorescence emitted after excitation at 340 and 380 nm (F_{340}/F_{380}) is directly proportional to the concentration of intracellular calcium (Grynkiewicz *et al.*, 1985; Williams *et al.*, 1985).

The cells under study are incubated for approximately one hour at 37°C in standard extracellular solution containing 5 μ M fura-2-acetoxymethyl ester (Fura2-AM). After the incubation period, the glass coverslips containing the cells are transferred to standard external solution (Table 3.2) and held at room temperature before commencing the experiment. The coverslips are then placed in a microchamber continuously perfused with bath solution held at a steady 33°C. Fluorescent measurements are made with a Leica DM IRE2 inverted microscope fitted with a CCD camera (Imago QE Sensicam, Till Photonics). During the experiment, the fura-2 loaded cells are alternatively excited by a wavelength of 340 and 380 nm by a rapidly switching Polychrome IV monochromator (Till Photonics), which is under the control of a computer running the TillVision software package (Till Photonics). After each pulse, the excited fura-2 emits a fluorescent signal at 510 nm. The emitted signal passes through a longpass filter of 510 nm and is detected by the CCD camera. The signal is subsequently sent to a computer, where it is recorded and later analyzed using the TillVision imaging software (Till Photonics).



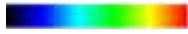
0  2 (F_{340}/F_{380})

Figure 3.1. Example of cultured DRG neurons as seen on a microscope under **a.** visible light and **b.** when excited at 470 nm, with TRPM8-positive neurons emitting a bright fluorescent light. **c-d.** The F_{340}/F_{380} value of these same neurons when held at a normal temperature (**c.**) or when exposed to cold (**d.**). Scale bar, 15 μ m.

3.8. Temperature stimulation

Coverslip glasses with cultured cells were placed in a microchamber and continuously perfused (~ 1 mL/min) with bath solution warmed to around 33°C by a Peltier device (ReidDan Electronics) which is under the control of a temperature controller (model RDTC-1, ReidDan Electronics), connected to a computer through a digitizer. The temperature of the bath-solution is measured by a thermocouple situated directly at the end of the solution-outlet, which is placed near the imaging field. The temperature is recorded using a computer running Clampex 10.2 (Molecular Devices).

3.9. Intra- and extracellular solutions

The contents of the bath solution used in all calcium imaging experiments in this work are described in table 3.2.

Bath solution	
Compound	Concentration (mM)
NaCl	140
KCl	3
CaCl ₂	2.4
MgCl ₂	1.3
Glucose	10
HEPES	10
pH = 7.4	

Table 3.2. Extracellular solution used for calcium imaging

The composition of the bath and pipette solutions used in electrophysiological registrations can differ from the one used in calcium-imaging, and is dependent on the type of experiment.

In the whole-cell patch clamp, a pipette solution was used that mimics intracellular ionic conditions. As the bath solution, a modified standard extracellular solution was used in which calcium is exchanged for sodium and contains the calcium chelator ethylene glycol tetraacetic acid (EGTA). Calcium is excluded from the extracellular solution to prevent calcium-dependent rundown of TRPM8-activity (Liu and Qin, 2005; Rohacs *et al.*, 2005). ATP and GTP are not provided in the

internal solution, as rundown of the current through TRPM8 is contained. Table 3.3 summarizes both solutions.

Pipette solution		Bath solution	
Compound	Concentration (mM)	Compound	Concentration (mM)
CsCl	140	NaCl	142.4
MgCl ₂	0.6	KCl	3
HEPES	10	MgCl ₂	1.3
EGTA	1	Glucose	10
		HEPES	10
		EGTA	1
pH = 7.3		pH = 7.4	

Table 3.3. Pipette and bath solution used for whole-cell voltage clamp recordings.

Table 3.4 provides a summary for the solutions used in cell-attached action current recordings in neurons. The bath solution is identical to the standard solution used for calcium imaging, as is the pipette solution.

Pipette solution		Bath solution	
Compound	Concentration (mM)	Compound	Concentration (mM)
NaCl	140	NaCl	140
KCl	3	KCl	3
CaCl ₂	2.4	CaCl ₂	2.4
MgCl ₂	1.3	MgCl ₂	1.3
Glucose	10	Glucose	10
HEPES	10	HEPES	10
pH = 7.4		pH = 7.4	

Table 3.4. Pipette and bath solution used for cell-attached action current recordings.

Whole-cell current clamp recordings in neurons require a pipette solution that is similar in ionic conditions to the cytosol. As can be seen, the internal solution used for current clamp experiments in neurons differs from the solution used in voltage clamp experiments in CR#1 and HEK293 cells. The main difference is the inclusion of ATP and GTP in the solution. ATP is crucial in preventing run-down of voltage-gated Ca²⁺-channels, whilst the presence of GTP is essential for G-protein

dependent processes (Hille, 2001). In this case, a standard bath solution containing calcium, is used. This is done to provide a more physiological environment for the neurons. Both solutions are summarized in table 3.5.

Pipette solution		Bath solution	
Compound	Concentration (mM)	Compound	Concentration (mM)
KCl	140	NaCl	140
NaCl	10	KCl	3
Mg-ATP	0.4	CaCl ₂	2.4
Na-GTP	0.4	MgCl ₂	1.3
HEPES	10	Glucose	10
		HEPES	10
pH = 7.4		pH = 7.4	

Table 3.5. Pipette and bath solution used for whole-cell current clamp recordings.

For single channel cell-attached and excised patch inside-out recordings, the ionic conditions of the bath solution mimic that of the cytosol. In cell-attached single channel recordings it brings the resting membrane potential close to zero. In excised patch inside-out recordings, the bath solution is on the cytosolic side of the patch and thus should resemble the ionic conditions of the cytosol. The pipette solution used for both type of recordings is the standard extracellular solution without calcium. Table 3.6 contains a description of both solutions.

Pipette solution		Bath solution	
Compound	Concentration (mM)	Compound	Concentration (mM)
NaCl	142.4	KCl	140
KCl	3	MgCl ₂	0.6
MgCl ₂	1.3	HEPES	10
Glucose	10	EGTA	1
HEPES	10		
EGTA	1		
pH = 7.4		pH = 7.4	

Table 3.6. Pipette and bath solution used for single channel recordings.

3.10. Electrophysiological recordings

The advent of the patch clamp technique, developed by Neher and Sakmann in the late 70's and beginning of the 80's (Neher and Sakmann, 1976; Neher *et al.*, 1978; Hamill *et al.*, 1981) made it possible to measure currents through single ion channels or macrocurrents of the whole cell. The technique involves a glass micropipette filled with solution which is in contact with a microelectrode. The glass micropipette is brought into contact with the cell membrane, after which a small piece of the membrane is drawn into the micropipette, forming a tight seal with the glass. The part of membrane that is under the micropipette is referred to as a patch, and this particular configuration is referred to as cell-attached. Forming a tight seal is the first step to successful patch-clamping and from this basic configuration several other patch-clamp configurations can be obtained (Figure 3.2).

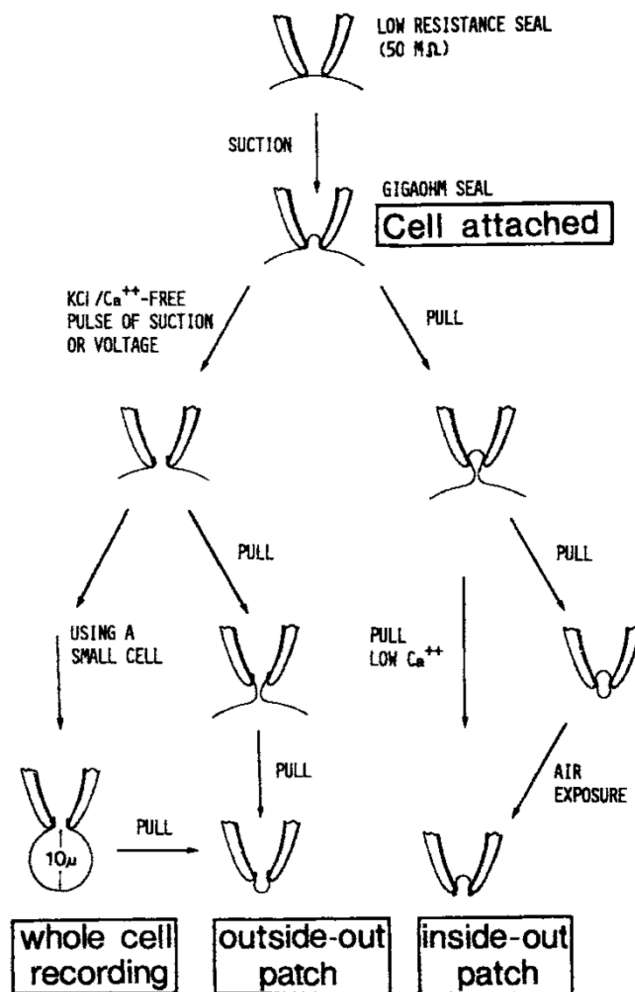


Figure 3.2. All patch-clamp configurations obtainable from the cell-attached configuration. Figure from (Hamill *et al.*, 1981)

In brief, all patch-clamp experiments start with lowering the filled micropipette into the bath, maintaining positive pressure throughout to avoid clogging the tip of the micropipette with debris. Once the micropipette is close to the cell of interest, measure the pipette resistance, which usually has a value between 3 and 6 M Ω . Subsequently, set the pipette offset voltage manually to achieve zero current at a zero pipette potential. Then, slowly approach the cell with the micropipette, aiming for contact at a quarter-diameter distance from the center of the cell, towards the direction of the pipette. This ensures maximal contact between the micropipette and the cell when approaching at an angle, and maximizes the chance for the formation of a tight seal. Once contact is made, as can be inferred from a slight increase in pipette resistance, release the positive pressure. Wait for a tight seal to form, which will regularly reach values above 1 G Ω . If seal formation is not forthcoming, apply slight negative pressure. After seal formation, compensate for the pipette capacitance, visible as capacitance transients on screen. Following the above described procedure will result in the cell-attached configuration, the initial configuration from which all other configuration can be attained (Figure 3.2). All electrophysiological recordings were performed with an Axopatch 200B patch clamp amplifier (Molecular Devices) in conjunction with Clampex, version 10.2 (Molecular Devices). The micropipettes used were pulled from thick-walled borosilicate glass (Harvard Apparatus) with a Flaming/Brown type micropipette puller (P-97, Sutter Instrument) resulting in a pipette with a resistance between 3-6 M Ω when filled with pipette solution and lowered into the bath.

3.10.1. Whole-cell voltage-clamp

In whole-cell patch clamp experiments the interior of the cell is perfused with pipette solution. The whole-cell configuration is attained by rupturing the patch in the cell-attached configuration by applying negative pressure (Figure 3.2). The bath solution is grounded by a chlorided silver pellet (Ag-AgCl), keeping the outside potential at zero. Through the electric access to the interior of the cell, the membrane potential is under the control of the experimenter.

Briefly, once a tight seal with a sufficient seal-resistance (>1G Ω) is attained following the aforementioned procedure, proceed by applying a prolonged pulse (3-5 s) of gentle negative pressure to rupture the patch. If, after repeated attempts, this procedure does not lead to cell access, apply a brief pulse of strong negative

pressure. Once the patch is ruptured and access is gained to the intracellular environment of the cell, a large transient capacitance will appear on screen. This capacitance transient is electronically compensated by manually setting the whole cell capacitance and series resistance until the transient is minimized. Set compensation to around 40% to correct for voltage errors. You are now ready for any type of whole cell voltage-clamp experiment.

Currents were recorded with the software package Clampex 10.2 (Molecular Devices). All whole-cell voltage clamp experiments were performed at a bath temperature between 32°C and 34°C, with the occasional cooling pulse to around 18°C. Solutions used for these type of recordings are found in table 3.3.

3.10.2. Cell-attached voltage clamp in neurons

Cell-attached voltage-clamp recordings provide a way to measure and record the activity of neurons without rupturing the cell membrane (Fenwick *et al.*, 1982). The cell firing activity is recorded in the form of action potential currents, which are the derivatives of the actual action potentials. Currents passing from the amplifier through the patch resistance can influence the firing activity of the neurons, so it is imperative to keep this current at a minimum as not to influence the recording. This is accomplished by switching the amplifier to current clamp mode and reading the command potential at which the measured current is zero pA. The measured potential is subsequently used as the command potential when the amplifier is switched back to voltage clamp mode in order to record action currents. (Perkins, 2006). The pipette solution used for these type of recordings is the same as the extracellular bath solution, and can be found in table 3.4.

3.10.3. Whole-cell current clamp

The whole-cell current clamp is a method in which the current is controlled and the changes in membrane potential are measured. It is a useful technique for measuring action potentials in cells. Before starting a whole-cell current clamp recording, first establish the whole-cell configuration in voltage-clamp mode, with pipette capacitance compensation set. Correction, prediction and whole cell capacitance are of less importance, as they are disabled when switching from voltage-clamp to current-clamp mode. Solutions used in these recordings are found in table 3.5.

3.10.4. Single channel cell-attached and excised inside-out patch

The patch clamp technique allows for high resolution recordings of ionic currents flowing across a patch of membrane that only contains one or a few ion channels. This technique allows for further study into the behavior of ion channels by providing information about its unitary conductance and kinetic behavior.

Single channel currents can be measured in different configurations. The starting configuration is the cell-attached mode. With cell-attached single channel recordings only the potential on the outside of the patch is under direct control of the experimenter. The internal potential of the cell is unknown, which makes it impossible to control the potential across the membrane. To circumvent this problem the bath solution for cell-attached experiments usually consists of a solution that has a similar ionic composition as the cytosol. This brings the resting membrane potential close to zero so the membrane potential across the patch can effectively be set by only controlling the pipette potential. Since the potential is now set at the outside of the patch, the sign of the pipette potential is the reverse from a whole-cell recording and inward and outward currents are indicated by positive and negative currents. For clarity, the single-channel currents displayed in the results section are manually reversed to conform to the standards of displaying inward and outward currents.

Inside-out excised membrane patches are attained by pulling back the micropipette after seal formation. This results in an excised patch whose cytosolic side is in contact with the bath solution. In this configuration, the cytoskeleton is disrupted and the cytosol is lost, along with any intracellular factors that might influence channel function. The experimenter controls the potential on both sides of the patch, thereby being able to set the exact membrane potential. Inside-out recordings were performed in zero calcium conditions, which usually helps to prevent patch resealing (see Figure 3.2). If the patch does reseal, it can briefly be exposed to air. However, this procedure is riskier and can result in losing the patch.

Single channel recordings were performed at 20°C in order to enhance the channel open-probability (P_{open}). Pipettes were coated with Sylgard 184 and cured using an electrically heated coil. Sylgard reduces electric input noise by increasing the pipette capacitance and by preventing bath-solution from creeping up the pipette. After curing, pipette tips were fire polished with a microforge (MF-830, Narishige). The smoothed tip supports the formation of a tight seal, which typically reaches

values >10 G Ω after smoothing. Current signals were digitized at 100 kHz and analogue filtered with the built in -3dB 4-pole Bessel filter at 5 kHz. Subsequently, the recorded signal was digitally filtered with a -3dB 8-pole Bessel filter at 2 kHz. Voltage pulses from +140 to 0 mV at a 20 mV interval with a duration of 2 seconds were applied to provide data for the generation of a conductance plot. Gap-free recordings at -100 mV were performed for recordings that were used for trace idealization and subsequent analysis.

3.11. Data analysis

Electrophysiological data from whole-cell patch clamp recording were analyzed with WINASCD, written by Dr. Guy Droogmans (<ftp://ftp.cc.kuleuven.ac.be/pub/droogmans/winascd.zip>). Data from cell-attached action current recordings, whole-cell current clamp recordings and single-channel recordings were analyzed with Clampfit 10.2 (Molecular Devices). Statistical analysis of the data were performed with GraphPad Prism 5.03 (GraphPad Software). All figures were created using the graphing software OriginPro 8.0 (OriginLab Corporation). Data is expressed as averages \pm S.E.M of n independent experiments. The statistical significance between groups were tested with a paired or unpaired two-tailed student's t-test and, in the case of more than two groups, a one-way ANOVA with a Bonferroni post-hoc test.

3.11.1. Analysis of voltage dependent activation of TRPM8

For an estimation of the shift in the voltage dependence of activation of TRPM8, I-V curves obtained from voltage-ramps were fitted with a function that combines a linear conductance multiplied by a Boltzmann activation term (Nilius *et al.*, 2006; Malkia *et al.*, 2007).

$$I = g \times (V - E_{rev}) / (1 + \exp [(V_{1/2} - V) / k]) \quad (1)$$

Through this formula, one is able to estimate the value of the voltage where the probability of opening for TRPM8 is 50% ($V_{1/2}$), the maximal conductance (g) and the slope factor (k). E_{rev} was fixed for I-V curves that did not display a clear inward current, with a value obtained from an I-V curve with a clear inward current.

Briefly, the fraction of TRPM8 channels in the open state can be described by a Boltzmann activation term. Furthermore, the linear conductance assumed in this

function is based upon the aforementioned observation that open TRPM8 channels display an ohmic current-voltage relation (Voets *et al.*, 2004).

3.11.2. Single channel data analysis

All single-channel records were analyzed using Clampfit (Molecular Devices). The baseline of gap-free recordings were manually adjusted to zero pA. Single-channel conductance was determined by generating an all-points amplitude histogram and subsequent fitting of the open and closed state with a Gaussian curve. The recorded traces were idealized using the 50%-threshold method in Clampfit 10.2, in which the calculated open conductance was used to set the open levels (Sakmann and Neher, 2009). The process of trace idealization is a semi-automated process, and the results were visually inspected during and after idealization.

Briefly, using the 50%-threshold method, the threshold is set at half-amplitude of the fully open channel. Every time the observed current crosses this threshold, the duration of the event is regarded as an estimate of channel-open time. Therefore, it is important to filter the data so as to minimize the occurrence of false events due to noise. Using this method, events shorter than half the risetime of the filter ($T_r / 2$) are missed, because after filtering they never reach threshold levels. Thus, it is in the interest of the experimenter to minimize the amount of filtering that needs to be applied to get a good signal to noise ratio, hence the importance of noise reduction. Once the idealized traces were generated they were used to generate stability plots and to calculate P_{open} , once again using Clampfit 10.2.

3.11.3. Analysis of thermal threshold

The thermal threshold of TRPM8 is determined by calculating the standard deviation of the calcium signal in a 5-second period prior to the cooling pulse. During a cooling pulse, the calcium signal typically decreases slightly as a result of the shift in focus of the microscope due to the cold. The minimum signal value during cooling is determined and the thermal threshold is defined as the point where the calcium signal positively deviates three standard deviations from the minimum. The corresponding temperature is taken as the apparent threshold of activation.

4. Results

4.1. Studying the effects of 5-benzyloxytryptamine on heterologously and natively expressed TRPM8 channels

Recently, 5-benzyloxytryptamine (5-BT), a known ligand of serotonin-receptors with a structural similarity to other TRPM8 antagonists, such as AMTB, was described as a novel antagonist of TRPM8 (DeFalco *et al.*, 2010). Its structural similarity with AMTB is based upon them having in common an aromatic or heteroaromatic core with a benzyl ether and an amine side chain at appropriate positions (Figure 4.1)

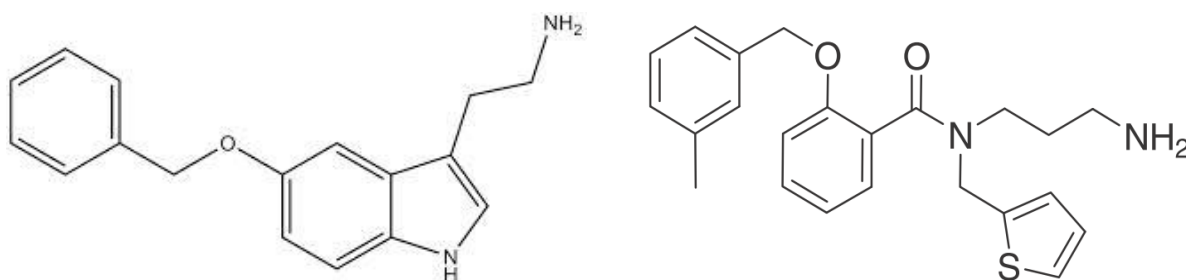


Figure 4.1. Chemical structures of 5-benzyloxytryptamine (left) and AMTB (right).

A potent and selective block of the menthol- and icilin-generated calcium increase through heterologously expressed TRPM8 was observed. However, neither the antagonistic effect of 5-BT on cold-induced calcium increase was tested, nor a further electrophysiological characterization was carried out. Also, no studies concerning TRPM8-mutants that could give more insight into potential important residues through which 5-BT exerts its antagonistic effect were performed. Our objective is to characterize the effect of 5-BT on the cooling induced response of heterologously and natively expressed TRPM8 and to identify potential residues on TRPM8 through which 5-BT may act.

4.1.1. Effects of 5-BT on cold-evoked activity in heterologously and natively expressed TRPM8

The original paper, describing 5-BT as an antagonist of TRPM8 determined its antagonistic effects on the TRPM8 mediated intracellular calcium rise through activation by menthol or icilin. The main physiological role of TRPM8 is that of a cold sensor and thus the first issue to be raised was whether 5-BT also acts as an antagonist of cold-activated TRPM8. Therefore, I tested several concentrations of 5-BT on the cold-evoked intracellular calcium increase in heterologously expressed TRPM8 (Figure 4.2.)

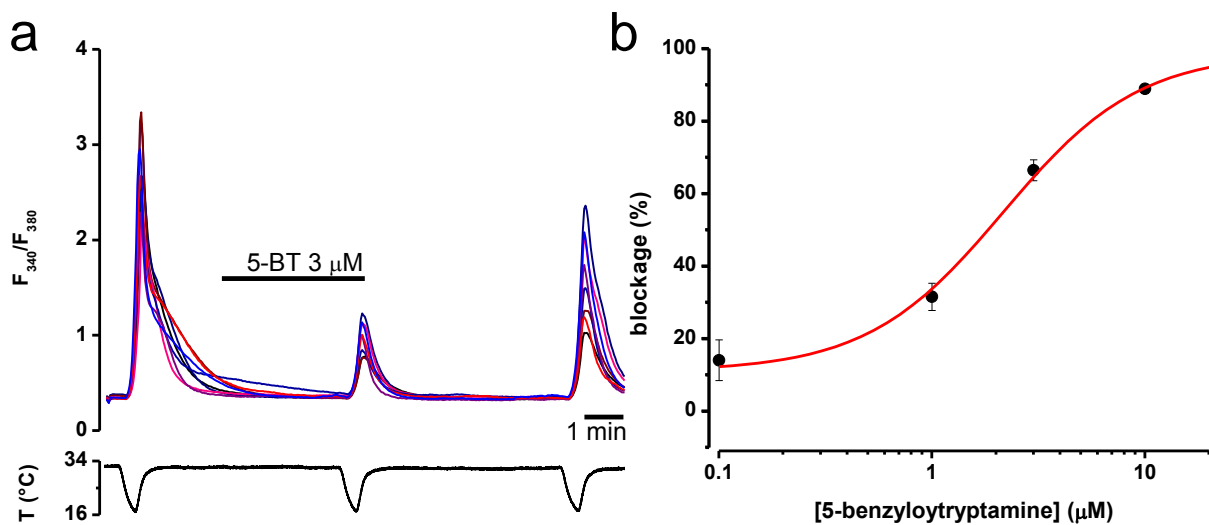


Figure 4.2. 5-BT blocks cold-evoked intracellular calcium increase through TRPM8. a) Time course of cold-evoked intracellular calcium responses in CR#1 cells expressing TRPM8, showing inhibition by 3 μ M 5-BT. **b)** Dose-inhibition curve of various concentrations of 5-BT on the activity of cooling activated TRPM8. The red trace represents the fit to the Hill equation. The calculated IC_{50} was 2.05 with a Hill slope of 1.74 ($n=50-87$ cells per point).

CR#1-cells, stably transfected with rat TRPM8, exhibited a robust response to cooling in control conditions. During the application of 5-BT, the cold-evoked calcium increase is clearly inhibited in a dose-dependent manner. When the data is fitted with the Hill equation, represented by the red curve in figure 4.2., it yields an IC_{50} of 2.05 μ M.

After establishing that 5-BT inhibits cold-evoked calcium increases in CR#1-cells, I investigated whether a similar inhibition of TRPM8 occurs in native cold thermoreceptors. I used a transgenic mouse line expressing the yellow fluorescent protein (YFP) under the control of the TRPM8 promoter (Parra *et al.*, 2010). TRPM8-expressing dorsal root ganglion neurons were identified by their bright fluorescence when excited with 470 nm light. Cold sensitivity was evaluated with fast cooling

ramps from a baseline temperature of 34°C. During the second of three successive cold pulses, 5-BT was applied to the bath (Figure 4.3).

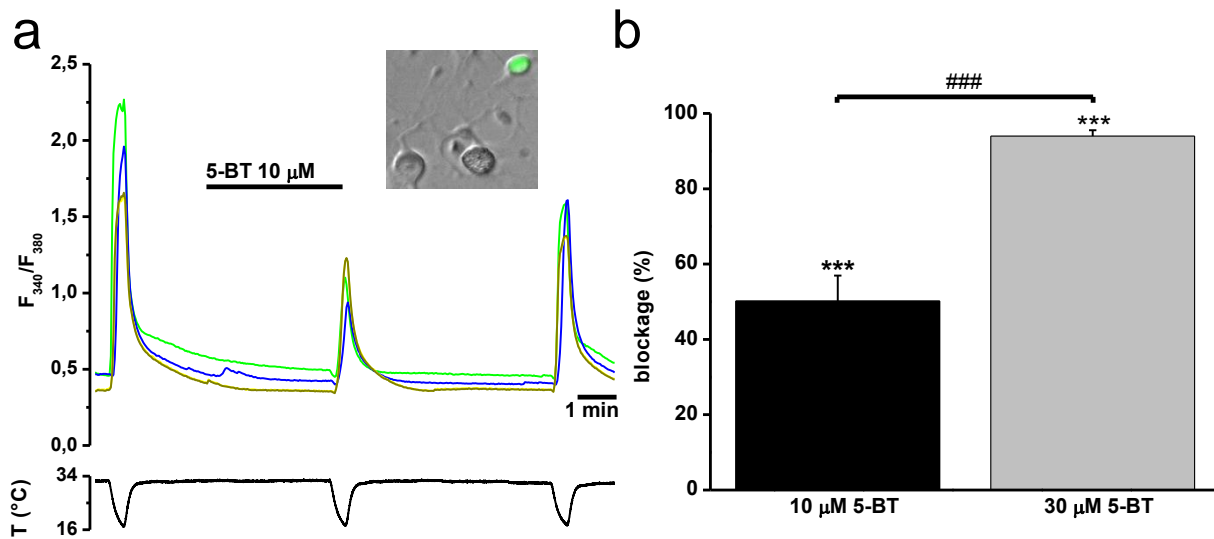


Figure 4.3. 5-BT blocks the cold-evoked intracellular calcium increase in somatosensory neurons natively expressing TRPM8. a) Cold-evoked intracellular calcium responses in TRPM8-YFP positive DRG neurons, showing inhibition by 10 μM 5-BT. *Inset:* example of a TRPM8-YFP fluorescent neuron overlaid in pseudocolour on a regular transmission image. b) Bar-graph summarizing the results obtained from experiments with 10 and 30 μM 5-BT. Data are expressed as average \pm S.E.M. and statistically tested using a two-tailed unpaired t-test, *** = $p < 0.001$. Also the difference between 10 and 30 μM 5-BT was tested with an unpaired t-test, ### = $p < 0.001$. (n=17/12/10 ctrl/10 μM /30 μM)

Native cold receptors normally exhibit a slightly diminished response upon repeated cold-stimulation, which is associated to the calcium-dependent degradation of PIP_2 (Rohacs *et al.*, 2005). To control for this, I compared the cold-pulse during application of 5-BT to a second experimental control in which no 5-BT was applied during the second cold pulse (not shown). In these cold-sensitive DRG neurons, 10 and 30 μM 5-BT inhibit cold-evoked intracellular calcium increases in a dose-dependent manner (Figure 4.3b). Compared to the inhibition observed in CR#1-cells, 5-BT inhibits cold-evoked TRPM8-activity less potently in cold-sensitive (CS) TRPM8-positive somatosensory neurons of the DRG. Thermal thresholds of cold-activated native TRPM8 are lower than that of heterologously expressed TRPM8, which is due to intracellular factors positively modulating TRPM8. As such, the less potent effect of 5-BT on native TRPM8 channels might reflect their intrinsically higher agonist sensitivity (Malkia *et al.*, 2009). Although 5-BT activates the 5-HT_{1D}, 5-HT₂ and 5-HT₆ serotonin receptors (Lyon *et al.*, 1988; Buzzi *et al.*, 1991; Peroutka *et al.*, 1991; Cohen *et al.*, 1992; Boess *et al.*, 1997), of which 5-HT_{1D} and 5-HT₂ are expressed in the DRG (Pierce *et al.*, 1997; Chen *et al.*, 1998; Nicholson *et al.*, 2003), no effects of

5-BT were witnessed on intracellular calcium levels other than the ones described above.

4.1.2. 5-BT shifts the midpoint of voltage activation of TRPM8 to positive values

TRPM8 is weakly voltage-dependent and a number of agonists and antagonist have been shown to modulate TRPM8-activity by shifting its voltage dependence (Voets *et al.*, 2004; Madrid *et al.*, 2006; Malkia *et al.*, 2007; Malkia *et al.*, 2009). The midpoint of voltage activation ($V_{1/2}$) is a measure that specifies the voltage at which half of the channels are open (open-probability = 0.5) (Hille, 2001). The functional result of this change is a shift in the apparent thermal threshold of the cell (e.g. cold receptor). BCTC, a TRPM8 antagonist, shifts the $V_{1/2}$ of TRPM8 towards more positive potentials, counterbalancing the effects of temperature and chemical agonists (Madrid *et al.*, 2006; Malkia *et al.*, 2007; Malkia *et al.*, 2009). The effects of TRPM8-agonists and antagonists on the $V_{1/2}$ are additive and by co-applying various concentrations of agonist and antagonist it can be titrated to any preferred value (Malkia *et al.*, 2007).

This raised the question whether 5-BT inhibits TRPM8 in a similar fashion. The $V_{1/2}$ can be estimated by fitting I-V curves, produced by ramps from -100 to +150 mV, with a function that combines a linear conductance, as is the case for TRPM8, with a Boltzmann activation term (equation (i), see Material and Methods) (Voets *et al.*, 2004; Nilius *et al.*, 2006; Malkia *et al.*, 2007). I chose to investigate the effects of 3 μ M 5-BT on the $V_{1/2}$ of TRPM8, as at this concentration the blocking effect is not saturating, which helps to obtain more reliable fits to equation (i). Furthermore, I used cold and menthol to maximally activate TRPM8 and so be able to observe a potential 5-BT-induced shift in maximum conductance, as has been observed for other antagonists of TRPM8 (Malkia *et al.*, 2007; Malkia *et al.*, 2009).

I proceeded with whole-cell voltage clamp experiments on CR#1 cells, using a protocol in which the potential was held at a steady value -60 mV. Voltage ramps from -100 to +150 mV were applied at various times, from which current-voltage curves were created for fitting with equation (i).

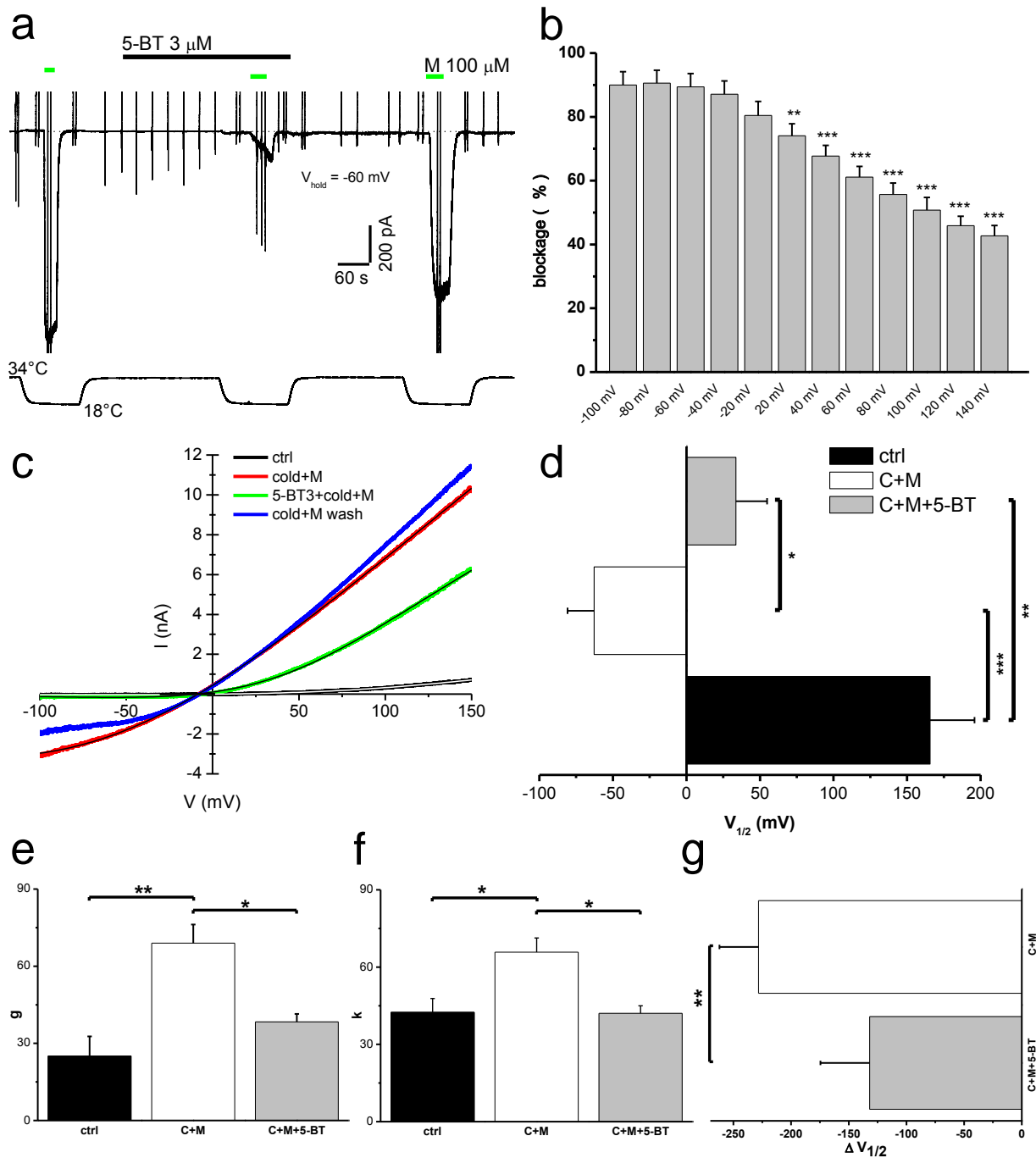


Figure 4.4. 5-BT shifts the $V_{1/2}$ of activation of heterologously expressed TRPM8. **a)** Time course of current development at -60 mV in a CR#1 cell during cooling ramps in the presence of 100 μ M menthol. Voltage ramps from -100 to 150 mV were applied under various experimental conditions and appear as vertical bars in the current trace. **b)** Block of cold and menthol evoked current by 3 μ M 5-BT over various membrane potentials. Statistical significance of block between each studied potential and -100 mV was assessed by a one-way repeated-measures ANOVA ($p < 0.001$) in combination with a Dunnett's post hoc test: ** = $p < 0.01$, *** = $p < 0.001$, ($n = 6$). **c)** Whole-cell I-V curves from voltage ramps (-100 / +150 mV) indicated by vertical bars in panel **a** during menthol and cold application in the presence and absence of 3 μ M 5-BT. A wash trace is included to show the reversible nature of the inhibition. The fits of I-V data to equation (i) are shown as white or black curves within the I-V traces. **d-f)** Parameters obtained from fits of I-V data as shown in **c** to equation (i), $n = 5$ **d)** Average values of the $V_{1/2}$. **e)** Average values of the maximal conductance. **f)** Average values of the slope factor. **g)** Induced shift in $V_{1/2}$ by cold and menthol as compared to control conditions at 33°C and its subsequent rightward shift induced by 3 μ M 5-BT. In panels **d-f)** statistical significance was assessed by a one-way ANOVA with Bonferroni post-hoc: * = $p < 0.05$, ** = $p < 0.01$, *** = $p < 0.001$. In panel **g)** statistical significance was assessed by an unpaired two-tailed t-test: ** = $p < 0.01$.

During the application of cold and menthol, a large inward current develops at -60 mV, as can be observed in figure 4.4a. The development of this inward current is largely blocked by the application of 3 μ M 5-BT, to an extent of $89.4\% \pm 4.2$ (n=6). The block is reversible, showing a complete washout with cold and menthol induced currents reversing to previous levels (Figure 4.4a and c). The antagonistic effect of 5-BT is voltage-dependent, the degree of block diminishing with increasing voltage (Figure 4.4b). Fits to equation (i) reveal a change in absolute $V_{1/2}$ under all different conditions, which supports the notion that cold and menthol act on TRPM8 through shifting its $V_{1/2}$ towards more positive potentials (Figure 4.4d). The negative shift in $V_{1/2}$ caused by simultaneous application of menthol and cold is significantly decreased by 5-BT co-application. Cold and menthol significantly increases both conductance of TRPM8 as well as the slope factor (Figure 4.4e-f). The slope factor (k) is inversely related to the apparent gating charge (z_{app}) ($k = R \cdot T / z_{app} \cdot F$), which means z_{app} decreases. Both changes have been reported before under similar conditions (Malkia *et al.*, 2009). 5-BT significantly decreases the slope factor to previous levels. The maximal conductance significantly decreases when 5-BT is applied, which is also in accordance to the previously mentioned study. In brief, in similar fashion to previously described TRPM8 antagonists, 5-BT exerts its inhibitory effects through shifting TRPM8 voltage dependence towards more positive potentials and by decreasing maximal conductance.

4.1.3. Effects of channel mutations on the ability of 5-BT to antagonize TRPM8 activation

Once it was established that 5-BT is a potent TRPM8-antagonist of cold and menthol-evoked currents, I proceeded to investigate possible structural elements on TRPM8 channel through which 5-BT might exert its antagonistic effect. In a previous study, Malkia and colleagues identified residue 745, located in the middle of putative transmembrane segment 2 and critical for the menthol sensitivity of TRPM8, to be crucial for the antagonistic effects of SKF96365 and partly responsible for the inhibition by capsazepine, clotrimazole and econazole (Malkia *et al.*, 2009). In view of this discovery, I set out probing the involvement of the menthol and icilin binding site. Mutant channels with a neutralized menthol binding site (Y745H) or icilin binding site (N799A) were transfected into HEK293 cells and the antagonistic effects of 5-BT on the cold-evoked responses were tested using Fura2 calcium imaging. By applying various concentrations of 5-BT in a protocol similar to figure 4.2a, I was able to construct a dose-inhibition curve for the two mutants.

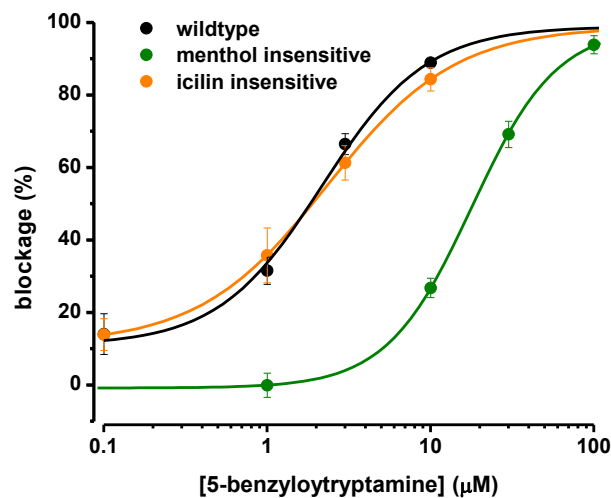


Figure 4.5. 5-BT differentially antagonizes the cold-activation of Y745H-TRPM8 mutant compared to WT and the N799A-TRPM8 mutant. Dose-response curve of WT, N799A and Y745H. Colored curves represent the fits of the Hill equation to the corresponding colored filled circles. Calculated IC_{50} 's: 2.05/2.29/18.04 μ M with Hill slopes of 1.74/1.14/1.64 for WT/N799A/Y745H (n=50-87/10-19/17-43 WT/N799A/Y745H).

As can be seen in figure 4.5, 5-BT preserves its potential to block the cold evoked calcium increase in the icilin insensitive TRPM8-N799A mutant with an IC_{50} of 2.29, virtually indistinguishable from the IC_{50} calculated for the wild type TRPM8 channel. However, the blocking potential exhibited a dramatic decrease when tested on the TRPM8-Y745H mutant, with the dose-response curve demonstrating an unambiguous rightward shift in the order of magnitude, and an IC_{50} of 18.04 μ M.

This result suggests that the menthol binding site at residue 745 is involved in the antagonistic effects of 5-BT.

To further assess channel function more directly, I employed the whole-cell patch clamp technique and tested various concentrations of 5-BT on the cold-evoked current in the Y745H and N799A mutants (Figure 4.6).

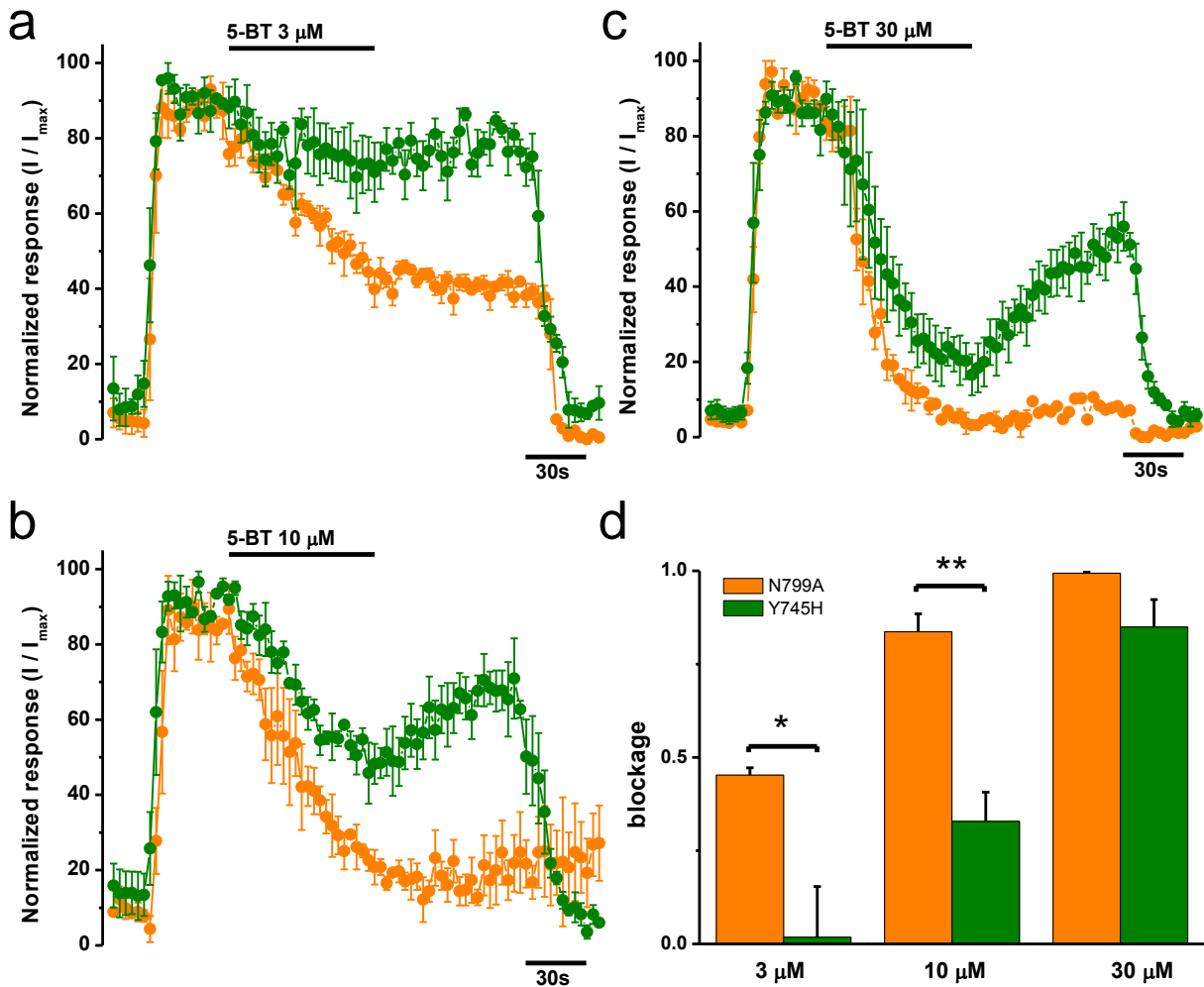


Figure 4.6. Differential effect of the Y745H mutant compared to the N799A mutant on the antagonistic effects of 5-BT on cold-evoked currents. a-c) Average normalized current at +80 mV under control and cold conditions, in the presence of a) 3 μ M 5-BT, b) 10 μ M 5-BT and c) 30 μ M 5-BT. d) Bar-graph summarizing the block results presented in a-c). The block of the cold induced current was compared for each concentration between the Y745H and N799A mutant using a two-tailed unpaired t-test. * = $p < 0.05$, ** = $p < 0.01$ ($n = 2-3/3-4$ N799A/Y745H)

As 5-BT washed out relatively slow, I chose to calculate the block of 5-BT by comparing it to a control in which no 5-BT was applied (not shown). The currents were compared at the end of the application of 5-BT. In close agreement with the calcium imaging experiments, 5-BT differentially antagonizes the cold evoked current in the N799A and Y745H mutant of TRPM8 (Figure 4.6a-d).

Taken together, this data suggests that 5-BT is less efficient in antagonizing the cold evoked response of the TRPM8-Y745H mutant. This could be interpreted as

a decreased affinity of the binding of 5-BT to the TRPM8-channel, or alternatively could be understood as a decreased efficacy of TRPM8-bound 5-BT to antagonize channel activation. Whether the mutation at the menthol binding site affects the ability of 5-BT to bind to TRPM8 or alters its efficacy for channel activation cannot be inferred from concentration-response curves alone (Colquhoun, 1998). However, clues to understanding the interaction of 5-BT with residue 745 might be found in the electrophysiological data. As evidenced in figures 4.6a-c, washout of 5-BT is extremely slow in the N799A mutant, however, a clear yet not complete washout is observed in the Y745H mutant. At concentrations which exert a similar block in current (e.g. compare N799A in figure 4.6a with Y745H in figure 4.6b and N799A in figure 4.6b with Y745H in figure 4.6c), there is still a clear washout in the Y745H as compared to N799A. This might reflect a decreased affinity of 5-BT for TRPM8 in the absence of the menthol binding site, allowing it to wash out more rapidly. Often, the speed of reversibility is dependent on the time it takes for the interaction of an inhibitor with its target to decay (Bindslev, 2008). This would implicate the involvement of the menthol binding site in binding of 5-BT to TRPM8. However, channel antagonism by 5-BT is not completely affected by the Y745H mutation, suggesting at least an additional site on the TRPM8 channel from or through which 5-BT exerts its antagonistic effects.

4.2. Studying the effects of chloroform on heterologously and natively expressed TRPM8 channels

As stated earlier, TRPM8 provides the receptor potential, which ultimately leads to action potential firing through the activation of voltage gated sodium channels. Hyperpolarization of the membrane potential reduces the general excitability of the cell and decreases the chance of action potential generation. The family of background or leak potassium channels is essential in controlling resting membrane potential of excitable and non-excitable cells. Activating these background potassium channels hyperpolarizes the membrane, thus decreasing neuronal excitability. A role for particular potassium conductances on the activity of TRPM8-expressing neurons has been previously elucidated. A differential expression of TRPM8-channels and Kv1 subunits, which form a voltage-gated potassium channel, determines the thermal threshold in cold-thermosensitive neurons. Blocking Kv1 subunit channels resulted in a shift of the thermal threshold towards higher temperatures (Madrid *et al.*, 2009). Furthermore, TRPM8 is a voltage-dependent ion-channel and is negatively modulated by a hyperpolarizing shift in the membrane potential. Lowering the membrane potential additionally results in a decreased open probability for TRPM8, but this effect should be modest as the shift is only in the order of 5 to 10 mV.

TREK-1 (KCNK2) and TREK-2 (KCNK10) are two-pore domain background potassium (K_{2p}) channels that are expressed in neurons of the DRG and TG, where they are important in regulating neuronal excitability. They are activated by many factors, among which is the volatile anesthetic chloroform (CLF) (Figure 4.7) (Patel *et al.*, 1998; Lesage *et al.*, 2000). Furthermore, TRESK (KCNK18), another member of the K_{2p} -family was found to be activated by CLF as well (Callejo *et al.*, 2013).

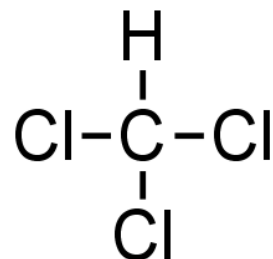


Figure 4.7. Chemical structure of chloroform

Similar to the aforementioned study by Madrid and colleagues, modulating the activity of these background potassium channels should result in an altered threshold

of cold-sensitive neurons. In particular, opening background potassium channels by CLF should lead to membrane hyperpolarization, rendering the neuron less excitable, thus increasing the thermal-threshold. Earlier, such a result was obtained in a study of the thermal modulation of hippocampal activity at the cellular network level (de la Peña *et al.*, 2012).

To investigate whether CLF increases the thermal threshold of cold-thermosensitive neurons, I prepared DRG cultures from transgenic mice expressing YFP under the TRPM8-promoter. This results in YFP-TRPM8-positive neurons that are easily identifiable. For the first experiment, a concentration of 1 mM was used, as this concentration has been shown to be sufficient for activation of TREK-1 and TREK-2 (Patel *et al.*, 1999; Lesage *et al.*, 2000). TRESK required a higher concentration (5 mM), although the effect of a lower concentration was not explored (Callejo *et al.*, 2013).

4.2.1. Effect of low concentrations of CLF on $[Ca^{2+}]_i$ in cold-sensitive neurons from mice DRG

At first I explored the effect of low concentrations of CLF on cold-sensitive (CS) neurons of the mouse DRG. Using the fluorimetric technique of ratiometric calcium imaging, based on the use of fluorescent fura-2, I was able to visualize the effects of CLF on the internal calcium concentration $[Ca^{2+}]_i$ during cooling episodes in cultured DRG neurons (Figure 4.8).

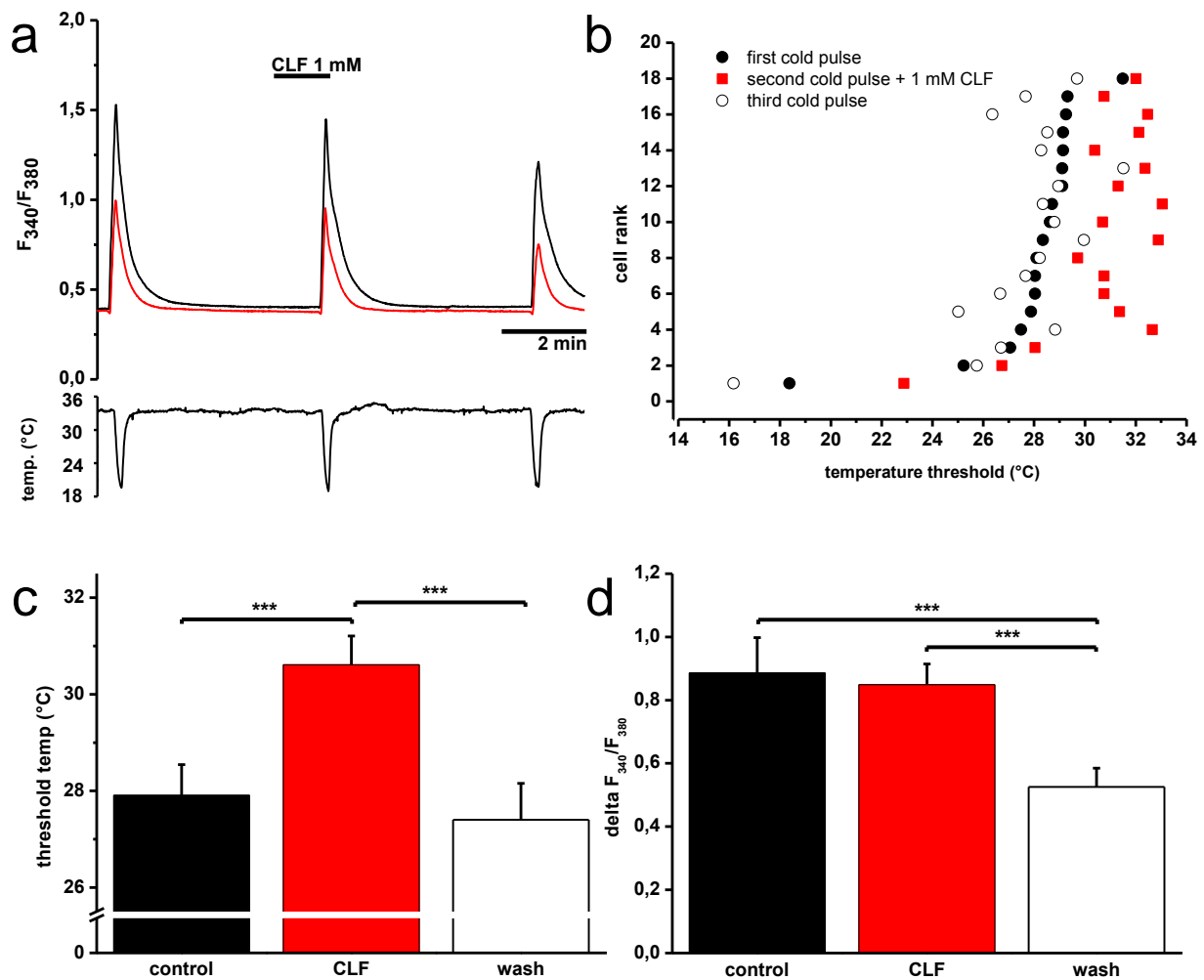


Figure 4.8. CLF lowers the thermal threshold of cold sensitive TRPM8-positive neurons of the DRG. **a)** A representative fluorescent ratiometric calcium imaging recording showing temporal changes of $[Ca^{2+}]_i$ in two CS neurons of the DRG in response to three consecutive cooling pulses, with 1 mM CLF in the bath during the middle pulse. **b)** Graph visualizing all three consecutive cooling thresholds for every individual cold sensitive neuron. **c)** Average cooling thresholds. **d)** Average calcium increase for every cooling pulse. All data expressed as averages \pm S.E.M, n=18; 10 fields. One-way ANOVA with Bonferroni post-hoc, *** indicates $p < 0.001$.

As seen in figure 4.8, CLF decreases the thermal threshold of CS TRPM8-positive neurons. Compared to the first cold pulse, the average cooling threshold decreases significantly with $2.7 \pm 0.3^\circ\text{C}$ in the presence of 1 mM CLF (Figure 4.8b-c), only to

return to control levels after washout. This surprising result is contrary to the hypothesis that CLF indirectly increases the thermal threshold of CS somatosensory neurons through the opening of TREK-1 channels. Whether CLF acts on TREK-1 is not clear from these data, but there is a strong indication for an additional effect of CLF on CS somatosensory neurons that causes its cooling threshold to decrease upon application. The most straightforward hypothesis that could explain such an effect would be that CLF positively modulates TRPM8. To further explore this hypothesis I tested CLF on heterologously expressed TRPM8.

4.2.2. Effect of CLF on $[Ca^{2+}]_i$ in HEK293 cells stably expressing TRPM8

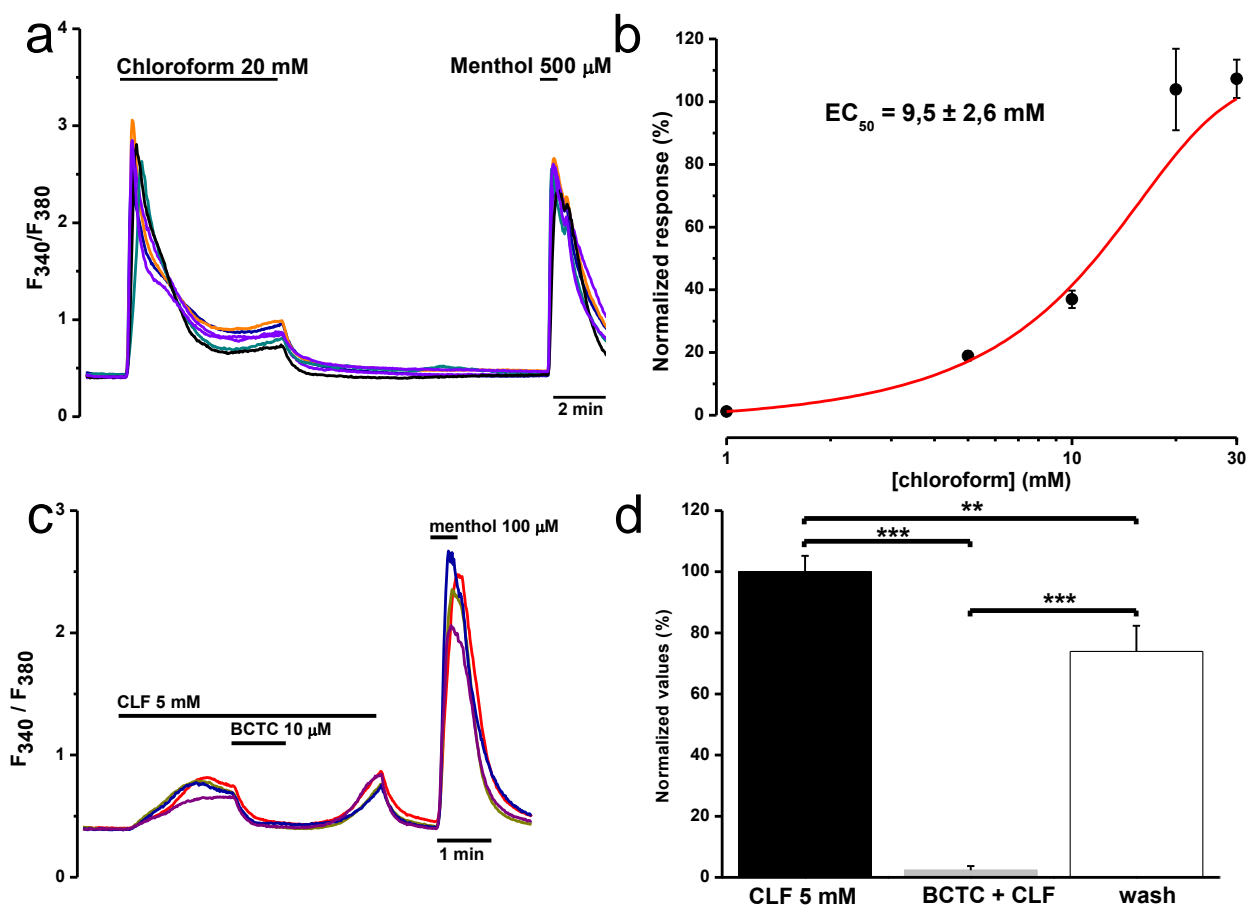


Figure 4.9. CLF activates heterologously expressed TRPM8 **a)** Representative traces of a fluorescent ratiometric calcium imaging recording showing temporal changes of $[Ca^{2+}]_i$ in CR#1 cells in the presence of 20 mM CLF and 500 μ M menthol. **b)** Dose response curve generated by fitting a Hill-curve to normalized CLF responses at different CLF-concentration. n per concentration: 1 = 50, 5 = 56, 10 = 57, 20 = 45, 30 = 50. $EC_{50} = 9,5 \pm 2,6$ mM. **c)** Representative traces of a fluorescent ratiometric calcium imaging recording showing temporal changes of $[Ca^{2+}]_i$ in CR1 cells in the presence of 5 mM CLF, with and without co-application of 10 μ M BCTC. **d)** Results are represented as a percentage of the initial $[Ca^{2+}]_i$ increase as average \pm S.E.M., n=35. Results were tested with a repeated measures ANOVA with a Bonferroni post-hoc correction. (CLF = 100 \pm 5,2 % , CLF+BCTC = 2,4 \pm 1,3 % and wash = 73,9 \pm 8,41 %)

Figure 4.9.a-b describes the results of the application of several different concentrations of CLF to CR#1 cells stably expressing rat TRPM8. The increment of intracellular calcium during CLF application is normalized to a maximal response, achieved by applying a high concentration of menthol, and the subsequent results are plotted in a dose-response graph. Further, the role of TRPM8 in CLF evoked calcium increases were tested, using the TRPM8-antagonist BCTC to try and block the calcium influx (Figure 4.9c-d).

As demonstrated in figure 4.9, CLF increases intracellular calcium levels in CR#1 cells, and this increment exhibits a dose-response relationship. When fitted with the Hill-equation, shown as the red line in figure 4.9b, I obtained an EC_{50} of 9.5 mM. The TRPM8-antagonist BCTC potently and reversibly blocked the CLF induced calcium influx, resulting in a decrease to $2.4\% \pm 1.3$ of control levels. Together, these results strongly suggest a role for CLF as a TRPM8-agonist.

General anesthetics have previously been shown to activate TRPA1 (Matta *et al.*, 2008). To investigate whether CLF also activates TRPA1, I tested CLF on TRPA1 channels stably expressed in CHO cells (CHO-A1). As seen in figure 4.10, CLF evokes a calcium influx, which is reversibly blocked by HC-030031, a selective TRPA1 antagonist (McNamara *et al.*, 2007).

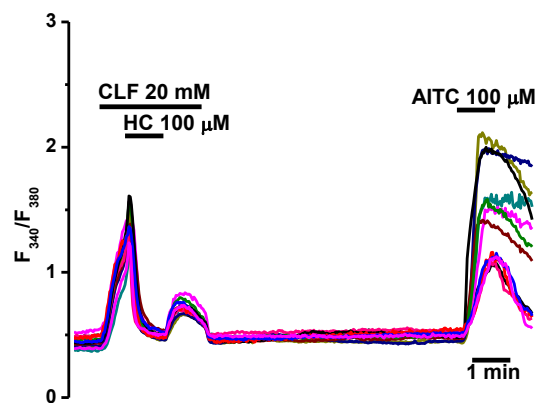


Figure 4.10. CLF increases intracellular calcium levels in TRPA1 expressing CHO cells. a) Representative traces of a fluorescent ratiometric calcium imaging recording showing temporal changes of $[Ca^{2+}]_i$ in CHO-A1 cells, with and without co-application of 100 μ M HC-030031.

4.2.3. Effect of CLF on $[Ca^{2+}]_i$ on cold-sensitive TRPM8-expressing neurons

Having shown that TRPM8-expressing cold-sensitive neurons demonstrate a decrease of their thermal threshold in the presence of 1 mM CLF, I sought to further examine whether higher than previously used concentrations of CLF could activate cultured CS neurons of the DRG.

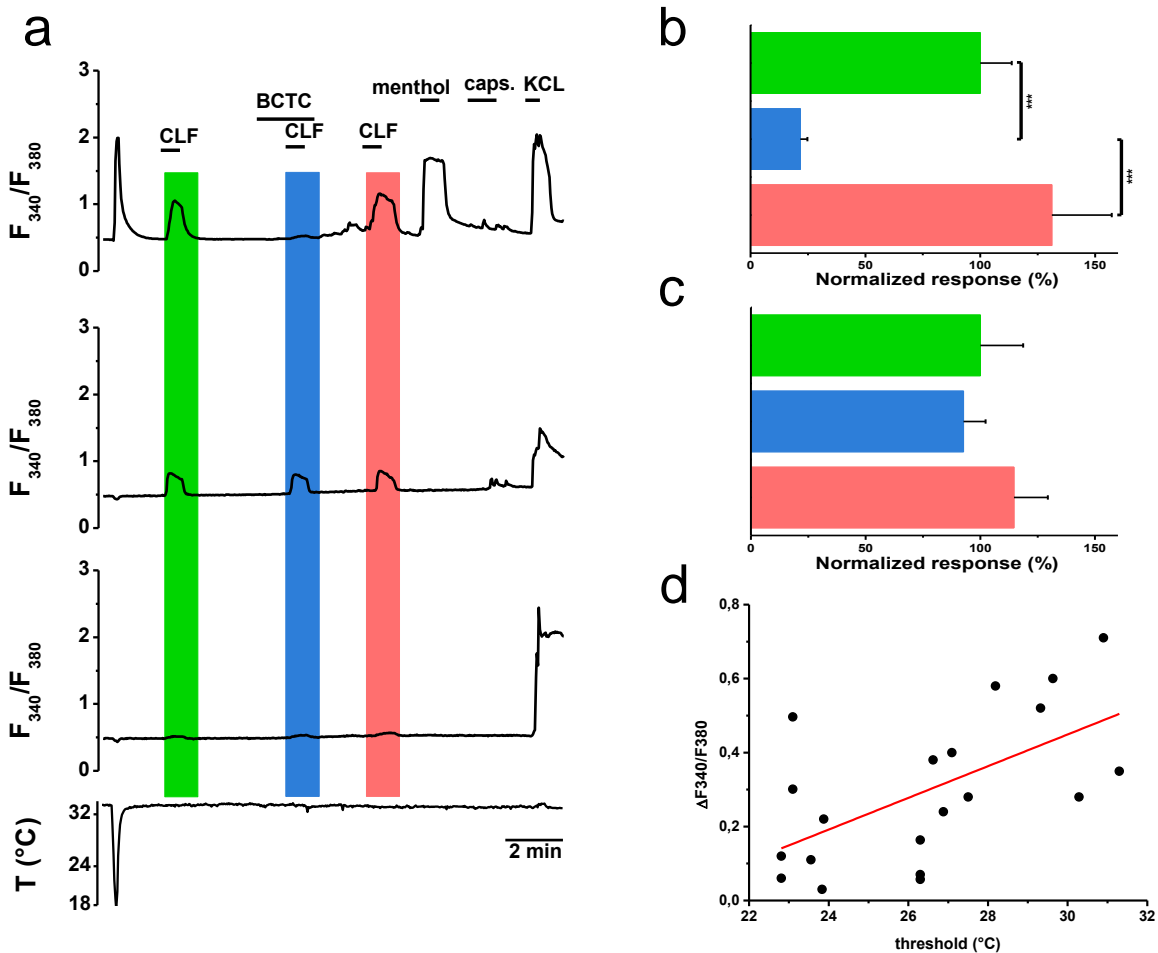


Figure 4.11. 5 mM CLF increases intracellular calcium levels in TRPM8-positive neurons of the DRG. **a)** Representative traces of a fluorescent ratiometric calcium imaging recording showing temporal changes of $[Ca^{2+}]_i$ in acutely dissociated neurons from the DRG after applying 5 mM CLF, with and without co-application of 10 μ M BCTC. *top*: TRPM8-positive neuron that responds to CLF *middle*: TRPM8-negative neuron that responds to CLF *bottom*: TRPM8-negative neuron that does not respond to CLF **b-c.** Normalized responses of TRPM8- and TRPV1-positive neurons, demonstrating the effect of BCTC on the CLF evoked calcium influx. **b)** TRPM8-positive neurons **c)** TRPV1-positive neurons. Data represented as mean \pm S.E.M, n=10/8 TRPM8-positive/TRPV1-positive. **d)** Thermal threshold of CS neurons plotted against their CLF induced intracellular calcium increase. Linear regression to data shown as red line. Correlation was assessed by Pearson's correlation, $r = 0.60$, $p=0.0054$. Results in panels **b** and **c** were statistically tested using a one-way ANOVA with a Bonferroni post-hoc correction.

These experiments were partly conducted with DRG neurons from TRPM8-YFP animals and partly in TRPA1 KO mice. When trying to establish a role for TRPM8 in the CLF evoked calcium increase in CS neurons, CLF co-application with BCTC led to unstable baselines and strong oscillations in most neurons, including TRPM8-

positive neurons. To circumvent this problem, I used DRG neurons obtained from TRPA1 KO, as it was already confirmed that CLF activates TRPA1, for the experiments in which BCTC was used to block the CLF-induced calcium increase in CS neurons. These experiments are shown in figure 4.11a. All data taken together, at a concentration of 5 mM, CLF induces a robust calcium increase in 15 out of 21 CS neurons (71%), when a response is arbitrarily defined as a positive deviation of 0.15 from baseline levels. Following the same definition, 35 out of 94 (37%), of cold-insensitive (CI) neurons respond. When the CI-neurons are divided between TRPV1 and non-TRPV1 expressing neurons, as identified by their response to capsaicin, 13 out of 23 (57%) respond to CLF. In the non-TRPV1 neurons, 22 out of 71, or (31%), responded to CLF. BCTC reversibly inhibits the CLF-induced calcium influx in TRPM8-expressing CS neurons to $21.7\% \pm 3.0$ of the first pulse, indicating a primary role for TRPM8 in this process (Figure 4.11b). However, BCTC is also an antagonist of TRPV1 (Valenzano *et al.*, 2003) but it does not inhibit the CLF-induced calcium influx in TRPV1-positive neurons, indicating no involvement of TRPV1 (Figure 4.11c). BCTC also does not affect the calcium influx in the rest of the neurons (not shown).

Not all TRPM8-positive neurons respond to CLF, which might be the result of a differential expression of TRPM8. As previously described, the cold threshold is the result of a differential expression of TRPM8 and Kv1 potassium channels, where a high thermal threshold in CS-neurons is indicative of a low level of TRPM8-expression (Madrid *et al.*, 2009). When plotting the thermal threshold of all CS-neurons against their response to CLF, a correlation becomes apparent with high threshold neurons having a smaller response compared to low threshold neurons. (Figure 4.11d). This indicates that the differences of response of CS-neurons to CLF could be explained by a differential expression of TRPM8.

4.2.4. Electrophysiological characterization of CLF elicited current through heterologously expressed TRPM8

To further elucidate the TRPM8 mediated response after CLF application I used the patch-clamp technique in the whole-cell configuration on CR#1 cells. This allows for a further characterization of the CLF evoked currents. I repeatedly applied voltage ramps between -100 mV and +100 mV. In order to follow the changes in amplitude of currents during the application of CLF, menthol and cold, I plotted the current at -80 and +80 mV (Figure 4.12a-b).

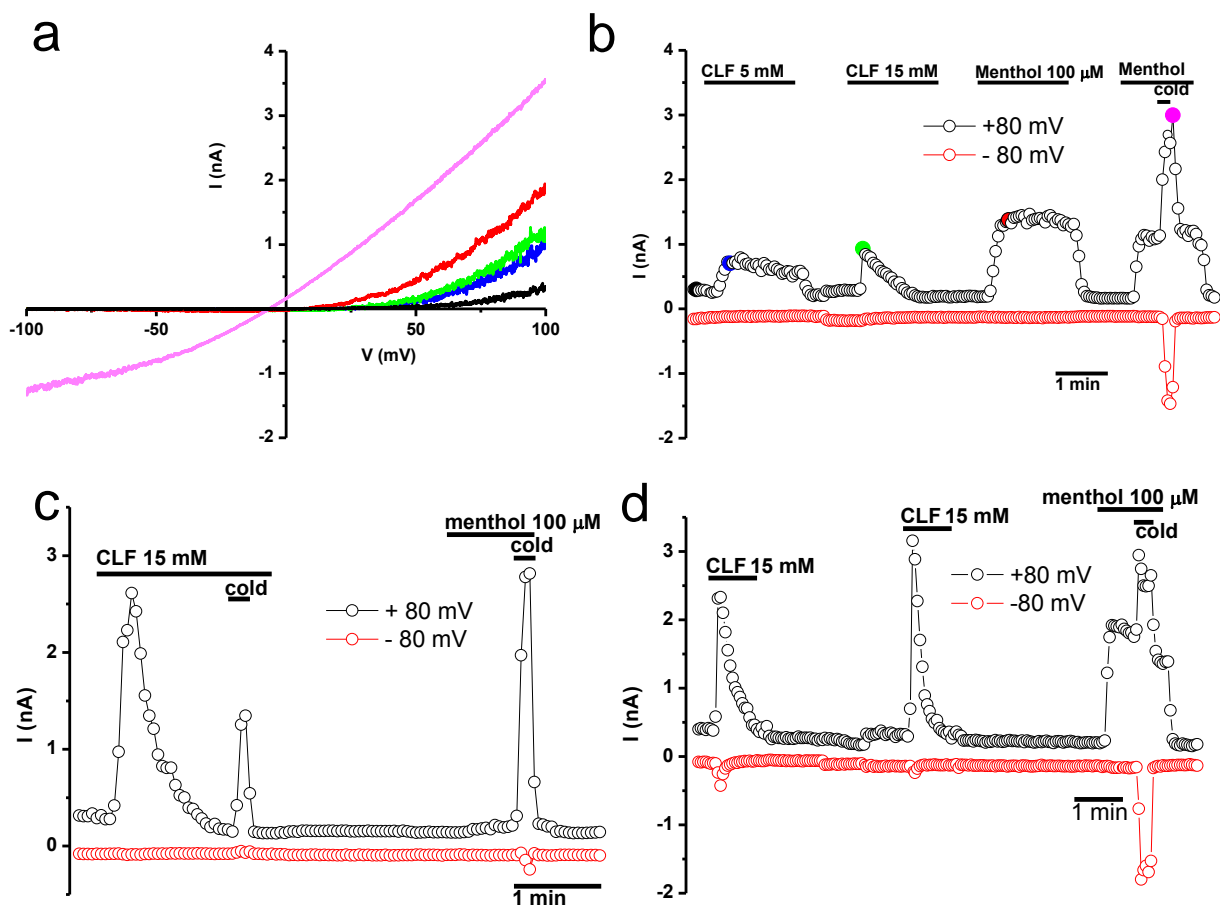


Figure 4.12. CLF elicits typical outwardly rectifying TRPM8-like currents with a near zero reversal potential. a) Example of a current-voltage relation curve obtained by voltage-ramps from -100 to +100 mV. The colored lines refer to the colored circles in **b**. **b-d)** Graphs showing time course of current at -80 and +80 mV for every voltage ramp applied throughout the whole experiment. **b)** Time course showing application of different concentrations of CLF in the same recording in order to compare the residual current after a fixed time of CLF application. **c)** Time course showing application of cold after CLF induced desensitization. **d)** Time course showing a second application of CLF.

A conductance change with voltage is referred to as rectification (Hille, 2001). CLF elicited pronounced outward, but not inward currents. This is referred to as outward rectification and is a typical property of TRPM8 (McKemy *et al.*, 2002; Peier *et al.*, 2002a). The rectification index is a measure of rectification and in this case was

determined at 24.5 ± 4.4 by dividing the absolute current values at -80 mV by those obtained at $+80$ mV (15 mM CLF). Normally, the potential at which the current changes sign is near-zero for TRPM8-currents. Also, CLF elicits a current which reverses at near-zero and was measured at -2.5 ± 1.1 mV (15 mM CLF) (Figure 4.12a). As becomes apparent in figure 4.12, 15 mM CLF elicits a current that rapidly desensitizes. To compare the amount of desensitization between different concentrations of CLF, multiple concentrations of CLF were applied during the timecourse of the experiment. At the end of a long pulse of either 5 mM or 15 mM CLF the percentage of desensitization was calculated as a percentage of the initial CLF-elicited current. The current at 15 mM CLF exhibits a desensitization of more than 100% to $-9,5\% \pm 1.8 \%$. Desensitization with 5 mM CLF is contained to $74,8\% \pm 5.1\%$ of the initial current (Figure 4.12b). Right after desensitization is complete, the application of a short cold-pulse still elicits a current. (Figure 4.12c), indicating that the channel is not in an inactivated state. Furthermore, a repeated stimuli with 15 mM CLF shows that desensitization is also reversible for CLF itself (Figure 4.12d).

In order to confirm that the CLF elicited current is carried through TRPM8, I used the TRPM8-antagonist BCTC to try and block the CLF elicited current. As the current rapidly desensitizes using 15 mM CLF, I used 5 mM CLF to elicit a more sustained current (Figure 4.13).

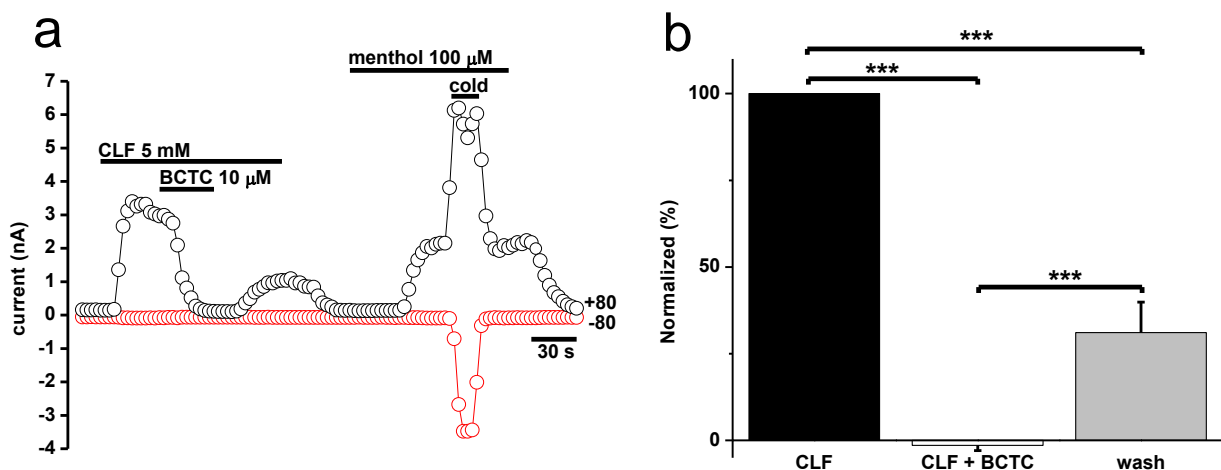


Figure 4.13. CLF induced current is blocked by BCTC, a TRPM8 antagonist. **a)** Graph showing the current at -80 and $+80$ mV for voltage ramps applied every 3 seconds throughout the whole experiment. **b)** Bar graph comparing the normalized block of the CLF induced current by $10 \mu\text{M}$ BCTC. Data were normalized against the current elicited by 5 mM CLF before application of BCTC. Data is expressed as average \pm S.E.M. and were statistically tested using a one-way ANOVA with Bonferroni post-hoc. *** indicates $p < 0.001$, $n = 8$.

The application of BCTC during a continuous CLF pulse rapidly decreases the CLF elicited current to an average of $-1.4 \pm 1.5 \%$ in respect to the original current.

After washing out BCTC, the current returns to an average of 31.1 ± 8.8 %. This result confirms that the current elicited by CLF is indeed carried through TRPM8.

TRPM8 is a voltage-gated channel and most agonists activate TRPM8 by shifting its voltage dependence towards more negative potentials, allowing TRPM8 activation at more physiological potentials (Voets *et al.*, 2004; Malkia *et al.*, 2007). I hypothesize that the same mode of activation is also true for CLF, and to test this I fitted the current-voltage relation curves to equation (1).

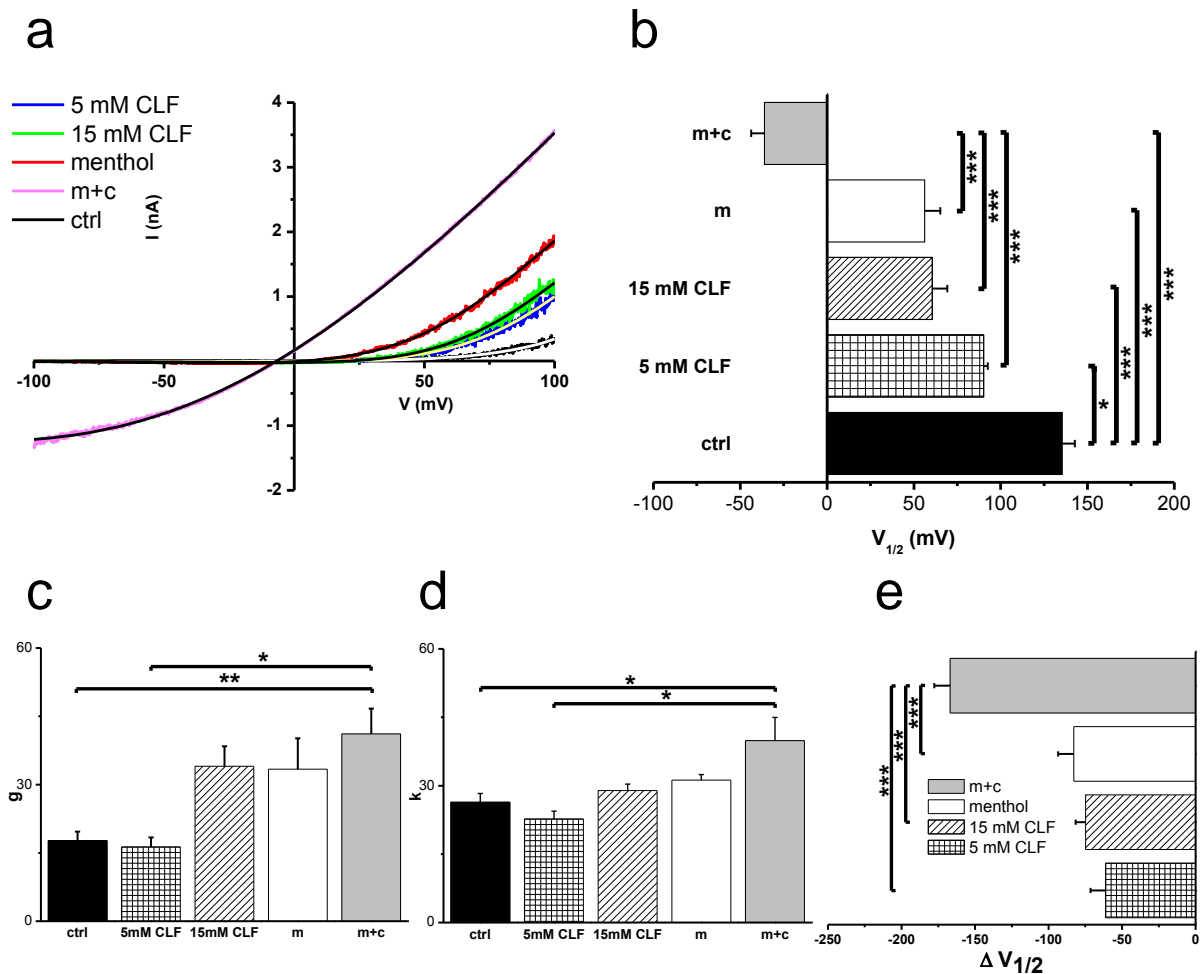


Figure 4.14. CLF produces a shift in the $V_{1/2}$ of heterologously expressed TPM8. **a)** Current-voltage curves resulting from voltage ramps from -100 to 100 mV under various experimental conditions. Voltage curves are fitted to equation (1), which are indicated by black or white curves within the I-V traces. **b-d)** Parameters obtained from fits of I-V data as shown in **a** to equation (1), $n=5-11$ **b)** Average values of the $V_{1/2}$. **c)** Average values of the maximal conductance. **d)** Average values of the slope factor. **e)** Induced shift in $V_{1/2}$ by various experimental conditions as compared to control conditions at 33°C. In panels **b-e** statistical significance was assessed by a one-way ANOVA with Bonferroni post-hoc: * = $p < 0.05$, ** = $p < 0.01$, *** = $p < 0.001$.

As described in figure 4.14.e, CLF does indeed shift the $V_{1/2}$ towards more negative potentials, indicating that CLF activates TRPM8 by shifting its voltage dependence towards more negative potentials.

4.2.5. Electrophysiology in TRPM8 neurons

At this point, the agonistic effect of CLF on heterologously expressed TRPM8 is robustly demonstrated. In addition, CS TRPM8-expressing somatosensory neurons demonstrate a calcium influx upon stimulation with CLF. However, what are the physiological implications of CLF-activated TRPM8, other than increased intracellular calcium levels? As touched upon in the introduction, intracellular calcium increases are indicative of channel activation but is not proof of action potential generation. This is an especially relevant topic of discussion in the case of CLF evoked TRPM8 activity. As aforementioned, CLF opens TREK-1, driving the membrane potential towards more negative potentials, decreasing general excitability and also decreasing the open probability of the voltage-gated TRPM8-channel. Furthermore, CLF targets sodium-channels, which is of particular relevance as they are indispensable for action potential generation and propagation (Hille, 2001). The effect of CLF on sodium currents is a depolarizing shift in the voltage dependence of steady-state activation and a hyperpolarizing shift in the steady-state inactivation (Haydon and Urban, 1983). Taken together this poses the question if activation of TRPM8 by CLF ultimately leads to action potential generation. To answer this question, electrophysiological recordings in the cell-attached mode and in whole-cell current clamp were performed in cold-sensitive TRPM8-positive somatosensory neurons of the DRG, as identified by their expression of YFP.

CLF elicits action currents in cell-attached mode

Cell-attached recordings provide a way to monitor the activity from intact neurons without rupturing the cell membrane and leaving the intracellular milieu undisturbed. Activity is measured in the form of currents passing the membrane, which are the derivatives of action potentials. The pipette was held at a potential that gives a holding current of zero pA, as not to change the intrinsic firing activity of the cell (Perkins, 2006).

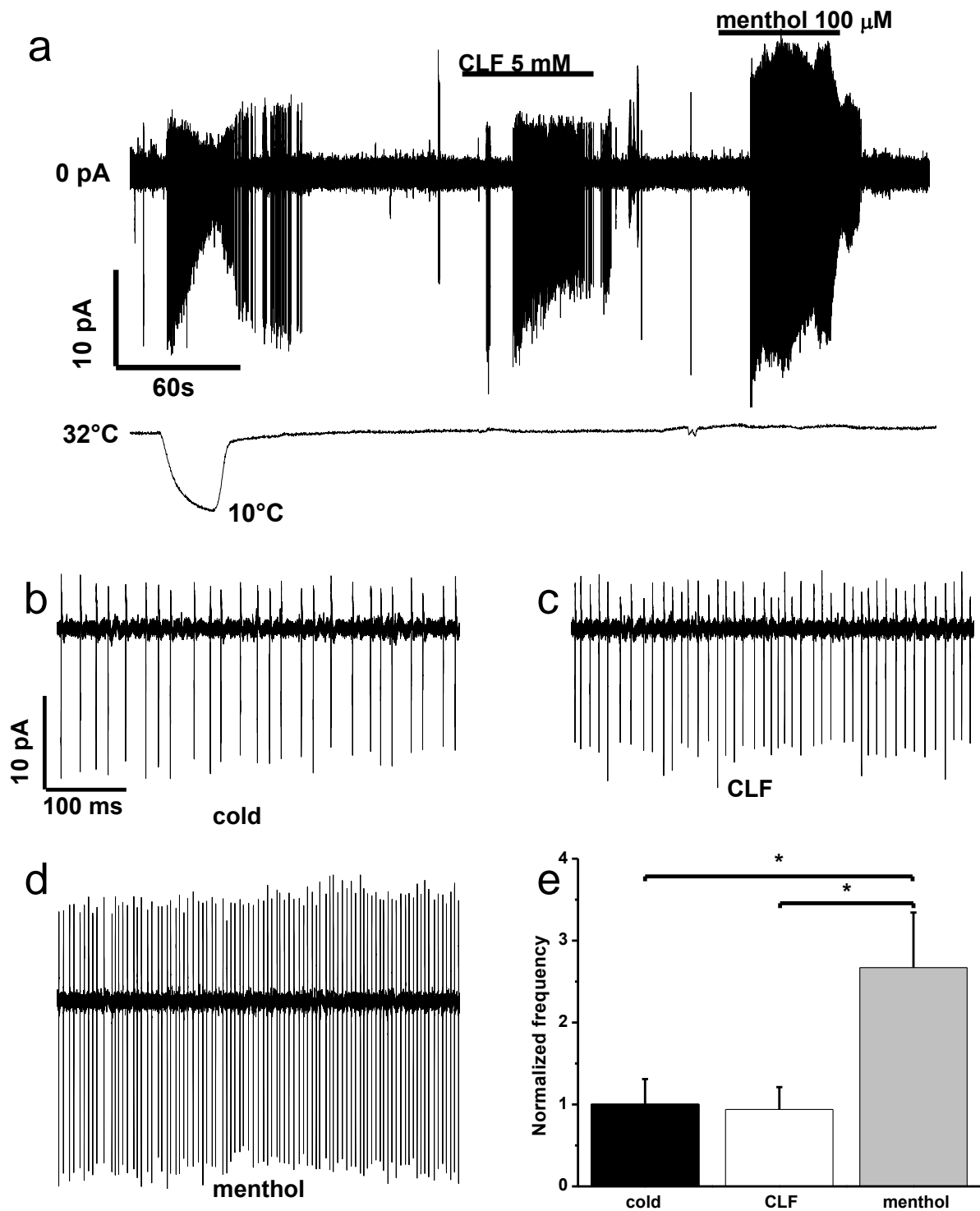


Figure 4.15. CLF elicits action currents in cold-sensitive DRG neurons. **a)** Example trace of an action current recording in a cold-sensitive neuron expressing TRPM8. **b-d)** Parts of **a** shown in a higher temporal resolution of 0.5 seconds. Type of stimulus as indicated under each trace. **e)** Bar graph indicating the normalized firing frequency under different conditions. Data is expressed as average \pm S.E.M. Normalized firing frequency for cold is 1.00 ± 0.31 , CLF 0.94 ± 0.27 and menthol 2.67 ± 0.67 . Data were statistically tested using a one-way ANOVA with Bonferroni's post-hoc test. * indicates $p < 0.05$. cold, $n=5$, CLF, $n=5$, menthol, $n=3$

Cold elicits the generation of action currents that decrease in amplitude upon further cooling, which return to normal levels upon reheating. This effect can be attributed to the general inhibitory effect of cold on sodium-channels, which affects the time

course of the action potential, slowing it down and thus decreasing the first derivative (action currents). This effect is similar to changes, induced by cold, in the shape and amplitude of nerve terminal impulses, recorded from guinea pig corneal terminals. This change is brought about by the increased inactivation of sodium channels, affecting action potential generation and propagation (Carr and Brock, 2002). Both CLF and menthol also elicit the generation of action currents. The firing frequency was normalized to that of the cooling pulse, as the initial cooling induced action current frequency varied from recording to recording. CLF elicits action currents at roughly the same frequency as cooling. In contrast, action current frequency is significantly increased upon stimulation with 100 μM menthol (Figure 4.15).

CLF elicits action potentials in current-clamp mode

The action current recordings demonstrated that CLF is able to elicit action potential firing in cold-sensitive TRPM8-positive neurons. To follow up these results, I also performed patch-clamp recordings in the current clamp mode.

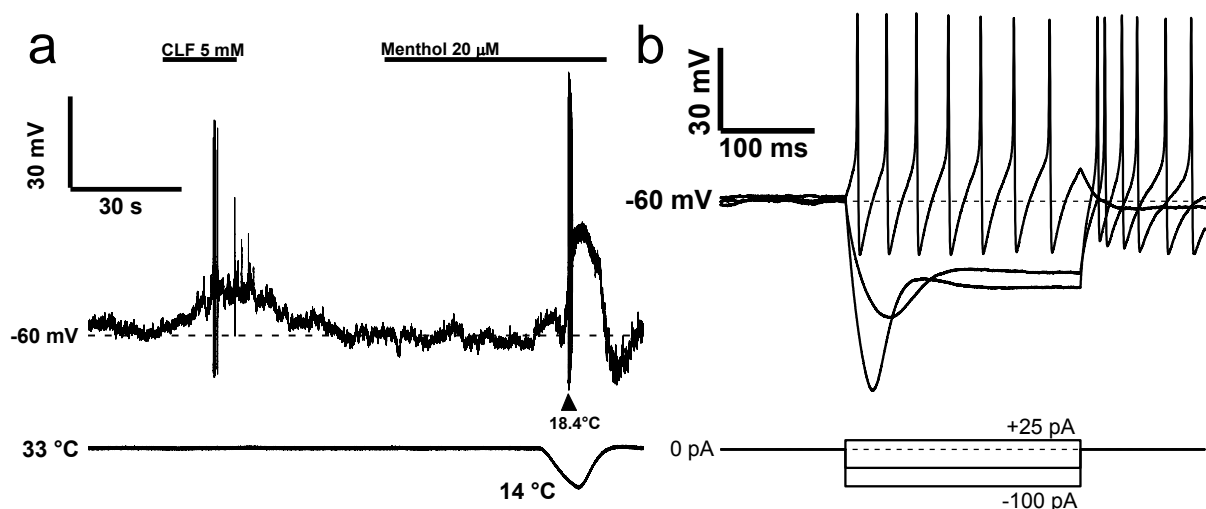


Figure 4.16. CLF elicits action potential firing in cold-sensitive TRPM8-expressing neurons of the DRG. a) Example of a current clamp recording in a cold-sensitive TRPM8-expressing DRG neuron. b) Action potential firing elicited by current injection with the corresponding current injection shown underneath.

Corroborating the earlier results obtained in cell-attached recordings, CLF causes an average membrane depolarization of 13.2 ± 3.2 mV and subsequent action potential firing in cold-sensitive TRPM8-expressing neurons ($n=4$) (Figure 4.16a). The neurons activated by CLF had the electrophysiological characteristics typical of TRPM8-expressing neurons (Viana et al., 2002). Notice the marked and intermittent downward deflection of the measured potential during a current injection of -100 pA

and less so at -50 pA (Figure 4.16b). This is the result of an inward current carried by hyperpolarization activated HCN channels, which are a hallmark of cold-sensitive neurons (Scroggs *et al.*, 1994; Viana *et al.*, 2002), leading to a more depolarized membrane potential. Injecting a current of 25 pA lead to action potential firing in all cases.

Both, results obtained in cell-attached as in current-clamp recordings, reveal that CLF elicits action potential firing in CS TRPM8-positive neurons of the DRG. Clearly, the supposed effects of CLF on sodium- and leak potassium channels are not potent enough at the used concentration to prevent action potential firing.

4.2.6. Effect of CLF on several mutants of TRPM8

A first interest is taken into specific agonist binding sites of TRPM8. For this purpose, I transfected HEK293 cells with mutant TRPM8 in which the binding site for menthol is rendered inactive by a mutation at position Tyr745 and a mutant in which the binding site for icilin is rendered inactive by a mutation at position Asn799. These mutants are still readily activated by cold, but fail to be activated by their respective agonists menthol and icilin (not shown).

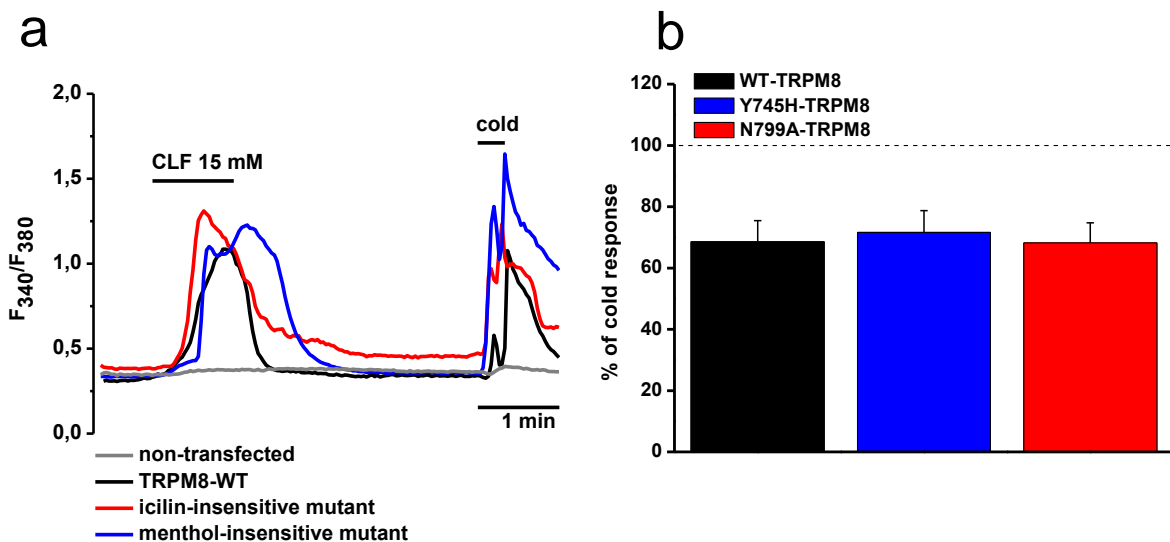


Figure 4.17. CLF activates menthol- and icilin-binding site mutants normally. **a)** A representative fluorescent ratiometric calcium imaging recording showing temporal changes of $[Ca^{2+}]_i$ in HEK293 cells transfected with the wild type, N799A or Y745H mutant of rat TRPM8 in response to a pulse of 15 mM CLF, later followed by a cold pulse. Also shown is a trace of an untransfected HEK293 cell present in the same field. **b)** Bar graph summarizing the effects of CLF induced $[Ca^{2+}]_i$ increases, expressed as a percentage of the cooling response. n=15/24/21 wt/Y745H/N799A. Data represented as mean \pm S.E.M. Statistics are one-way ANOVA with Bonferroni post-hoc analysis.

The results in figure 4.17 show that CLF normally activates both TRPM8 mutants, compared to wild type TRPM8. Thus, I can conclude that these particular binding sites do not play a significant role in CLF-induced TRPM8 activity.

4.2.7. Effect of bilayer curvature altering agents on activation of TRPM8 by CLF

CLF is a lipophilic compound and its effect on lipid bilayers has been the subject of multiple studies (Lieb *et al.*, 1982; Engelke *et al.*, 1997; Mishima *et al.*, 2003; Turkyilmaz *et al.*, 2011; Reigada, 2013). As it inserts into the lipid bilayer, it is thought to modulate membrane bilayer properties, which in turn could affect ion channel functioning. In the case of TREK-1, these membrane-modulating properties are thought to be responsible for its activation by CLF. More specifically, CLF's agonistic effects were reversibly blocked by the addition of chlorpromazine (CPZ), a cationic amphiphatic molecule that alters the membrane curvature. CLF and trinitrophenol (TNP), an anionic amphiphatic, readily activate TREK-1. These results suggest that CLF activates TREK-1 through modulating lipid membrane properties, specifically by changing membrane curvature (Patel *et al.*, 1998). Thus, my initial hypothesis was that CLF might act in a similar fashion to activate TRPM8. To test this idea, I explored the effects of CPZ and TNP on the ability of CLF to activate TRPM8.

Amphiphatic molecules such as CPZ and TNP are part hydrophobic and part hydrophilic, which give them the ability to easily segregate into lipid membranes. Chlorpromazine is positively charged and when segregating into the membrane prefers the inner leaflet that directly borders the negatively charged cytosol. Trinitrophenol is negatively charged and thus prefers the outer leaflet of the lipid bilayer (Deuticke, 1968; Sheetz and Singer, 1976).

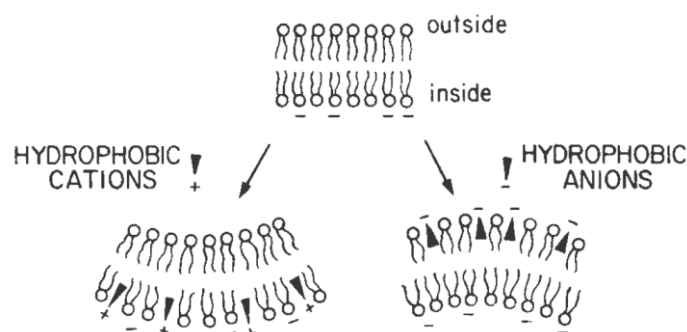


Figure 4.18. Illustration of the principle of the bilayer couple model (from Martinac, Adler and Kung., 1990)

According to the bilayer couple hypothesis, these molecules shape membrane curvature due to an unequal distribution over the membrane leaflets, causing one monolayer to expand relative to the other, changing membrane curvature. Chlorpromazine causes the membrane to bend inwards (cup-forming) whilst TNP causes it to bend outwards (crenating) (Sheetz and Singer, 1974) (Figure 4.18). Making use of their curvature altering properties, these molecules have also been used in classic studies of mechanosensitive gated ion channels in bacteria (Martinac *et al.*, 1990). Similarly, I studied the effects of CPZ and TNP on the CLF induced calcium increase in CR#1 cells.

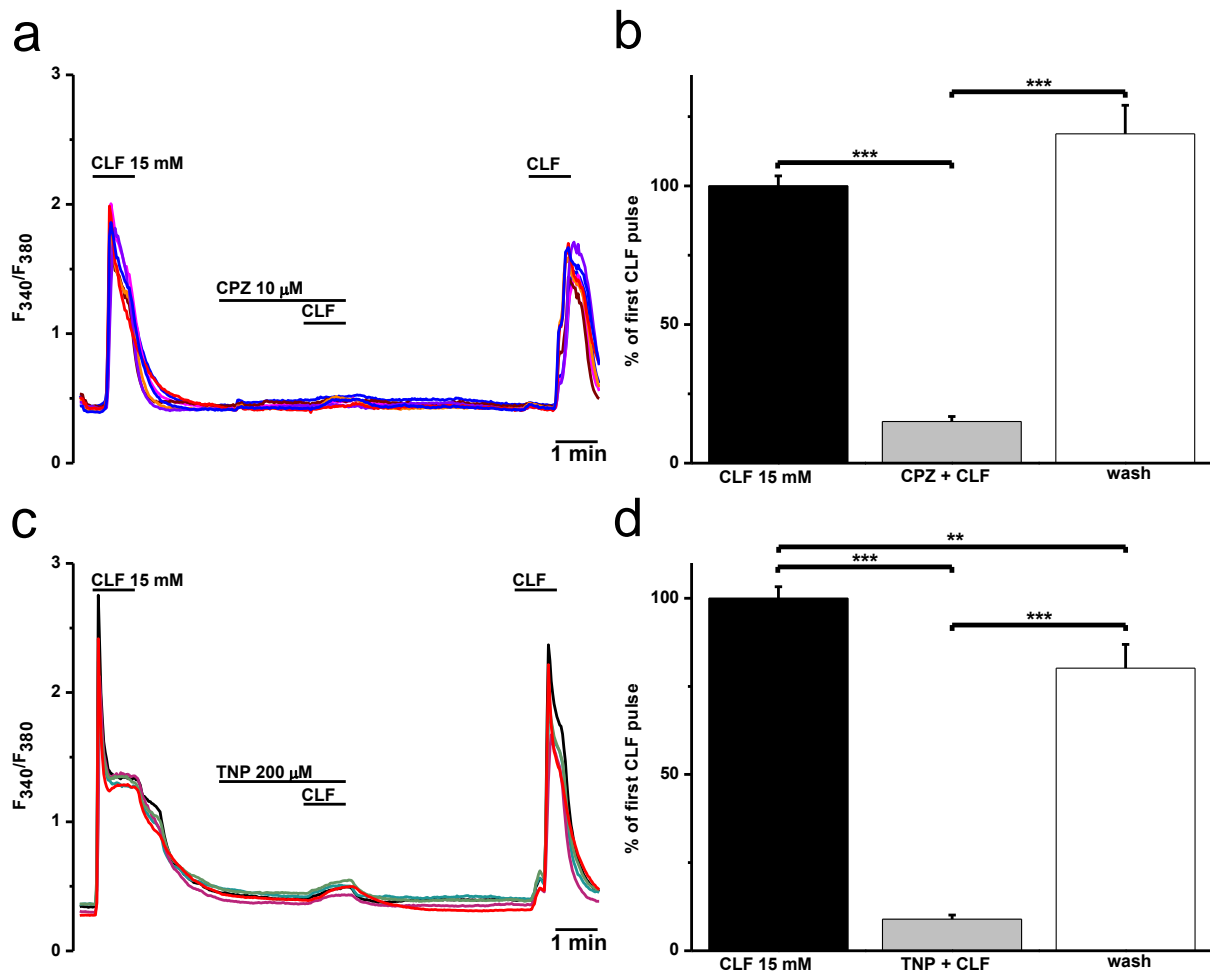


Figure 4.19. The amphipaths CPZ and TNP both block CLF induced intracellular calcium increases. **a)** representative fluorescent ratiometric calcium imaging recording showing temporal changes of $[Ca^{2+}]_i$ in a CR#1 cell in response to pulses of 15 mM CLF with and without the presence of 10 μ M CPZ. **b)** Bar graph summarizing the effects of CPZ on CLF induced $[Ca^{2+}]_i$ increases. **c)** A representative fluorescent ratiometric calcium imaging recording showing temporal changes of $[Ca^{2+}]_i$ in a CR#1 cell in response to pulses of 15 mM CLF with and without the presence of 200 μ M TNP **d)** Bar graph of summary of three CLF pulses without TNP. Data represented as mean \pm S.E.M. Statistics are one-way ANOVA with Bonferroni post-hoc analysis. * = $p < 0.05$, ***= $p < 0.001$ n=68/55 CPZ/TNP

CPZ effectively blocked intracellular calcium increases by CLF, to 15.0 ± 1.8 % of the first CLF pulse. TNP was similarly effective, blocking the CLF evoked calcium influx to 8.6 ± 1.2 % of the original CLF pulse (Figure 4.19). These results are contradictory to the previously mentioned results in TREK-1, in which CPZ and TNP have opposite effects, and TNP mimics activation of TREK-1 by CLF. Our results at least indicate that the sign (i.e. crenating or cup-forming) of the curvature does not determine the blocking effect of both amphiphats. Experiments with mechanosensitive bacterial channels have shown that CPZ and TNP compensate for each other's activating effect (Martinac *et al.*, 1990). Thus, if membrane curvature blocks CLF induced TRPM8-activity, simultaneous application of both amphiphats should result in less block of the CLF elicited calcium increase, as the extent of membrane curvature should be less than when one of the two amphiphats is applied alone. To test whether this is the case, I simultaneously applied CPZ and TNP, following a similar protocol as in figure 4.19.

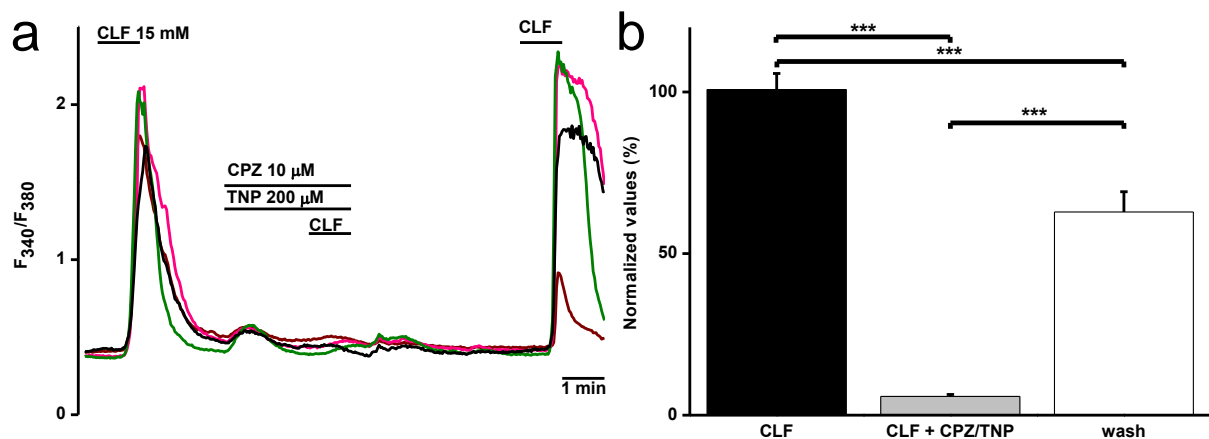


Figure 4.20. Simultaneous application of CPZ and TNP blocks CLF induced calcium increases. a) A representative fluorescent ratiometric calcium imaging recording showing temporal changes of $[Ca^{2+}]_i$ in a CR#1 cell in response to pulses of 15 mM CLF with and without the simultaneous presence of 10 μ M CPZ and 200 μ M TNP. b) Bar graph summarizing the effects of CPZ and TNP on CLF induced $[Ca^{2+}]_i$ increases. Data represented as mean \pm S.E.M. Statistics are one-way ANOVA with Bonferroni post-hoc analysis. ***= $p < 0.001$, $n = 63$, 3 fields

Simultaneous application of CPZ and TNP does not result in any perceptible change in the amount of block when compared to the results of CPZ or TNP alone, resulting in a block of the CLF-evoked calcium influx to 5.8 ± 0.6 % (Figure 4.20). This is an indication that neither membrane-curvature nor its sign seem to have an important role in the effects of CPZ and TNP on the CLF elicited calcium influx.

To test whether these results were particular to TRPM8 channels expressed in heterologous cells or could be extended to natively expressed TRPM8, the

experiments were repeated in cold-sensitive TRPM8-expressing somatosensory neurons of the DRG.

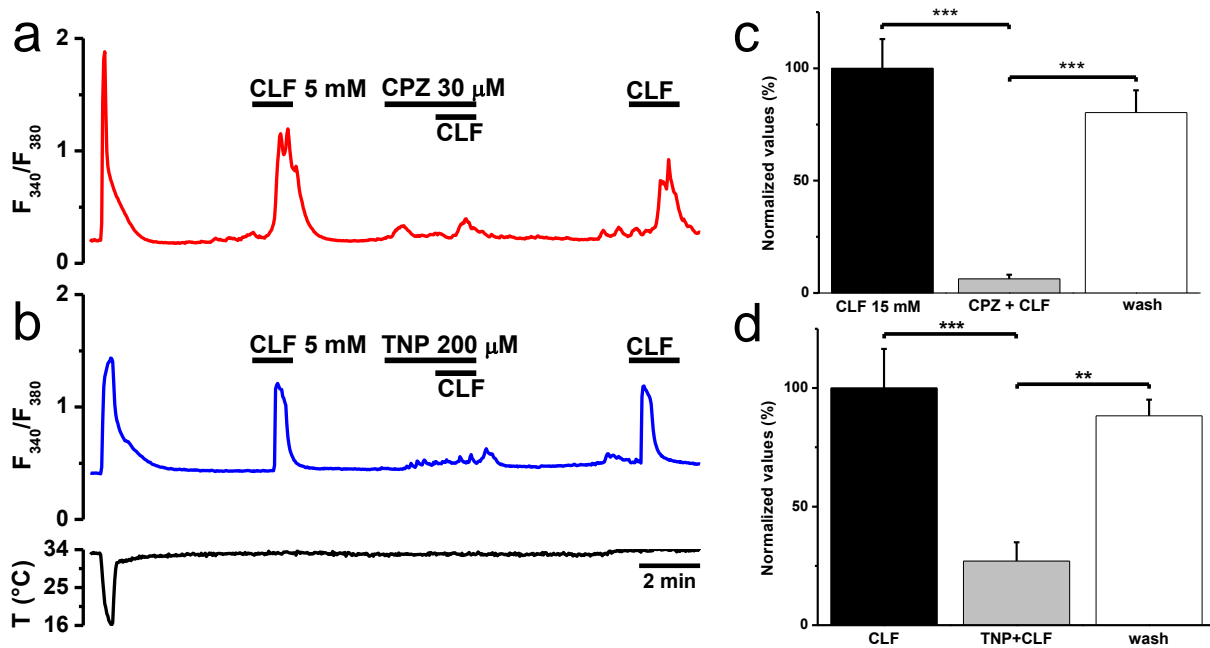


Figure 4.21. CPZ and TNP block CLF induced calcium influx in cold-sensitive neurons of the DRG a-b). Representative fluorescent ratiometric calcium imaging recordings showing temporal changes of $[\text{Ca}^{2+}]_i$ in a TRPM8-YFP neuron in response to pulses of 5 mM CLF with and without the presence of **a.** 30 μ M CPZ or **b.** 200 μ M TNP. **c-d)** Bar graphs summarizing the effects of CPZ and TNP on CLF induced $[\text{Ca}^{2+}]_i$ increases. Graph corresponds to traces shown immediately to the left. Data represented as mean \pm S.E.M. Significance was assessed by a one-way ANOVA with Bonferroni post-hoc analysis. ***= $p < 0.001$ $n=13/10$ CPZ/TNP.

As in CR#1 cells, CPZ and TNP greatly reduced the CLF induced intracellular calcium increases in DRG neurons expressing TRPM8, evidencing that both are good antagonists to the effects of CLF on natively expressed TRPM8 as well.

As both amphiphats have an effect and do not compensate for each other's effect, membrane curvature change is seemingly not involved in their blocking effects. This makes interpreting the results in the context of a possible mechanism difficult. When trying to experimentally modify a certain lipid bilayer property, such as the membrane curvature through the addition of charged amphiphats, it is likely that other bilayer properties, like bilayer compression and thickness, are altered as well (Lundbaek *et al.*, 2010). In fact, CPZ has been found to also change the lateral organization of the lipid bilayer, affecting the lateral pressure profile of the membrane (Jutila *et al.*, 2001). Changes in lateral pressure profiles have been hypothesized to be important for the energetics of channel gating, and redistribution of lateral stresses exerted by the bilayer may alter the amount of mechanical work involved in

a conformational change of a membrane embedded protein, such as an ion channel (Cantor, 1997, 1999). TRPC5 and TRPC6 are examples of TRP channels in which mechanical sensing is thought to involve lateral-lipid tension (Spassova *et al.*, 2006; Gomis *et al.*, 2008). Interestingly, CLF inhibits activation of TRPC5 by lysophospholipids, which supposedly gate TRPC5 through changes in the lipid bilayer (Bahnasi *et al.*, 2008; Beech, 2012). Mechanical activation of both channels is also blocked by GsMTx-4, a peptide found in the venom of the Chilean rose tarantula spider (*Grammostola spatulata*) (Spassova *et al.*, 2006; Gomis *et al.*, 2008). GsMTx-4 is a specific blocker of mechanosensitive channels and thought to exert its inhibitory action by insertion between the channel protein and the boundary lipids, relieving mechanical stress (Suchyna *et al.*, 2004).

To examine the possible role of the lipid bilayer in CLF activation of TRPM8, I investigated whether GsMTx-4 could block the CLF induced calcium increase through TRPM8 (Figure 4.22).

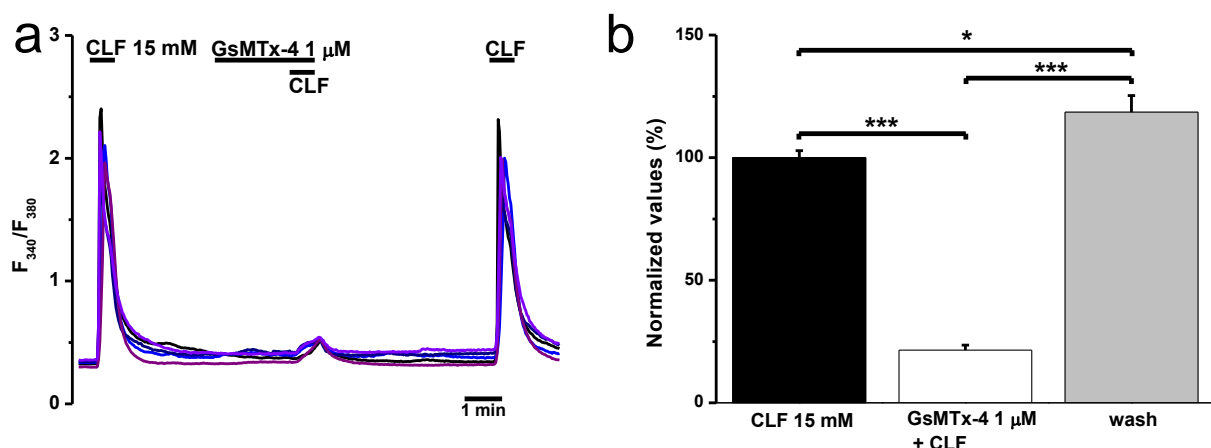


Figure 4.22. a) A representative fluorescent ratiometric calcium imaging recording showing temporal changes of $[Ca^{2+}]_i$ in a CR#1 cells in response to pulses of 15 mM CLF with and without the presence of 1 μ M GsMTX-4. **b)** Bar graph summarizing the effects of GsMTX-4 on CLF induced $[Ca^{2+}]_i$ increases. Data represented as mean \pm S.E.M. Statistics are one-way ANOVA with Bonferroni post-hoc analysis. * = $p < 0.05$, ***= $p < 0.001$. Data from 3 independent fields, $n = 114$. In a three pulse protocol without the presence of GsMTx-4 the three pulses show no significant difference between each other, $n = 67$. Data not shown.

Clearly, GsMTx-4 is a very potent blocker of CLF induced intracellular calcium increases in CR#1 cells, reducing the CLF-evoked calcium response to 21% of the original CLF pulse. This result indicates that changes in the lipid bilayer properties are indeed involved in the activation of TRPM8 by CLF. However, to exclude the possibility that GsMTx-4 functions as a general TRPM8-blocker, I performed additional experiments with more traditional agonists of TRPM8. First, I tested whether GsMTx-4 could inhibit cold-induced TRPM8 activity (Figure 4.23).

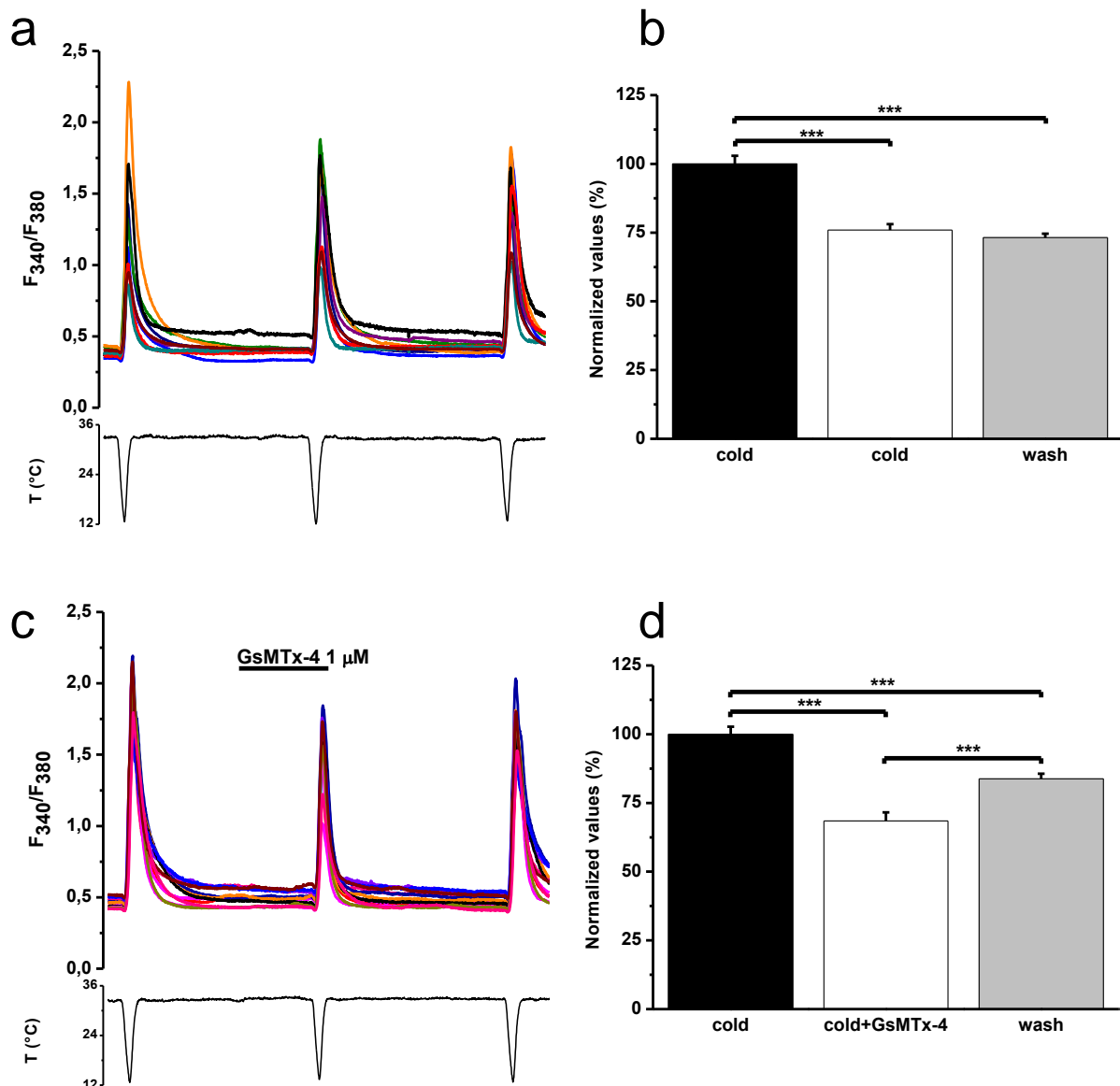


Figure 4.23. GsMTx-4 weakly blocks cold-induced calcium influx in CR#1 cells Representative fluorescent ratiometric calcium imaging recording showing temporal changes of $[Ca^{2+}]_i$ in CR#1 cells in response to **a**) three consecutive cooling pulses and **c**) cooling responses with and without the presence of 1 μ M GsMTx-4. **b and d**) Bar graphs summarizing the results from **a** and **c**. Data represented as mean \pm S.E.M. Statistics are one-way ANOVA with Bonferroni post-hoc analysis. ***= $p < 0.001$. $n = \text{ctrl/GsMTx-4 } 45/42$.

In the experiments where only cold was applied, the second and third response are decreased compared to the first cold-response. The difference between the second and third pulse is not significant, so this can be used to determine the effect of GsMTx-4. When comparing the effect of GsMTx-4 to the washout, it implies a small blocking effect upon cooling induced TRPM8-activation. Also, comparing the second pulse of figure 4.23b and d reveal an effect of GsMTx-4, significantly decreasing the cold-evoked calcium increase from $75.9 \pm 2.1\%$ to $68.4 \pm 3.1\%$ of the first pulse (unpaired two-tailed t-test, $p = 0.049$). These experiments reveal an effect of GsMTx-4 on the cold evoked calcium response in CR#1 cells, but when compared to the

effect on the CLF-induced calcium response it is rather small. Furthermore, I wanted to test the effect of GsMTx-4 on the menthol induced activity of TRPM8, which is shown in figure 4.24.

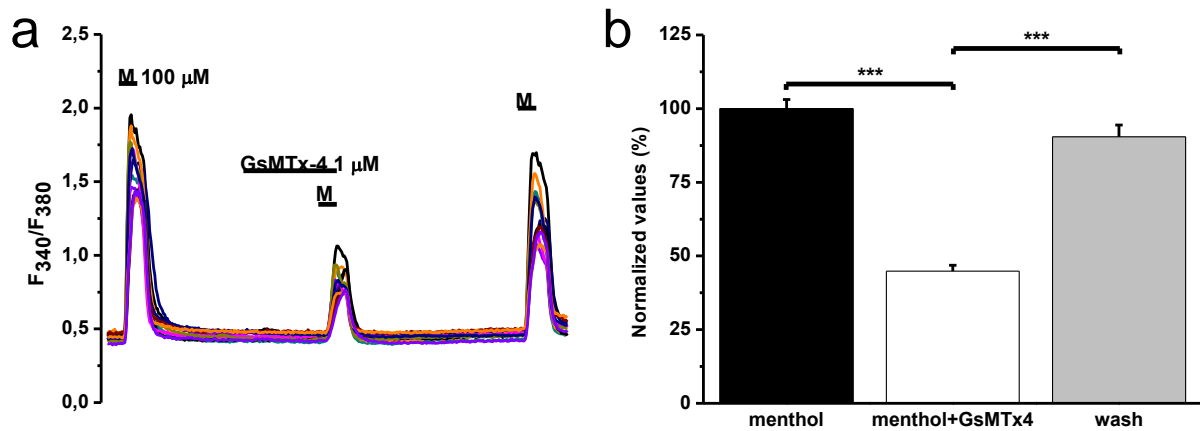


Figure 4.24. GsMTx-4 partly blocks the menthol-induced intracellular calcium increase in CR#1 cells. a) A representative fluorescent ratiometric calcium imaging recording showing temporal changes of $[Ca^{2+}]_i$ in CR#1 cells in response to the application of 100 μ M menthol with and without the presence of 1 μ M GsMTX-4. b) Bar graph summarizing the effects of menthol induced $[Ca^{2+}]_i$ increases. Data represented as mean \pm S.E.M. Statistics are one-way ANOVA with Bonferroni post-hoc analysis. n=49. ***=p<0.001.

The inhibitory effect of GsMTx-4 on the menthol induced calcium flux is larger when compared to the cold induced flux, but smaller than its effect on the CLF induced flux. However, menthol belongs to the family of monoterpenes, which are lipophilic cyclic hydrocarbons. These compounds have the ability to accumulate into the lipid bilayer according to their compound specific partition coefficient (Sikkema *et al.*, 1994) and can also enhance membrane fluidity (Bard *et al.*, 1988). A more recent paper specifically found that menthol partitions into the membrane and changes the phase behavior of the lipid bilayer (Laub *et al.*, 2012). The menthol binding site at residue 745 is evidently involved in menthol-elicited TRPM8-activity (Malkia *et al.*, 2009), but potential effects of menthol on the lipid bilayer cannot be excluded, thus hampering the interpretation of this result. In order to separate the possible effect of menthol induced lipid bilayer disturbance on general TRPM8-activity, I repeated the experiment with a TRPM8-agonist which is not known to have similar effects on the lipid-bilayer. Many natural TRPM8 agonists are structurally related to menthol and thus can be expected to have similar chemical properties. Icilin is a synthetic cooling compound and is structurally unrelated to menthol. It is not known for altering lipid bilayer properties and is less lipophilic than menthol. For these reasons I chose to test GsMTx-4 on the icilin evoked calcium response in CR#1 cells (Figure 4.25).

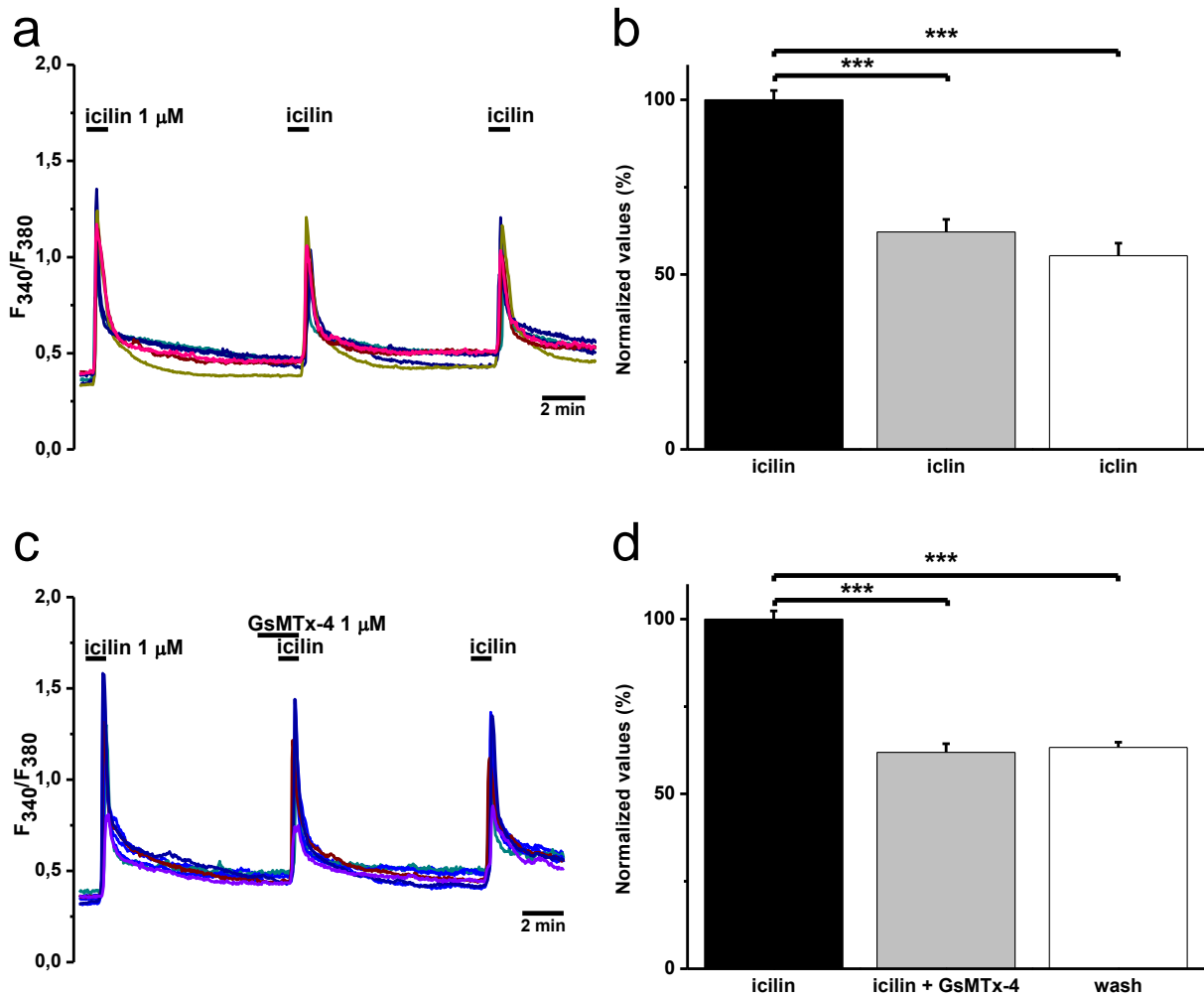


Figure 4.25. GsMTx-4 does not inhibit the icilin-evoked intracellular calcium increase in CR#1 cells **a.** A representative fluorescent ratiometric calcium imaging recording showing temporal changes of $[Ca^{2+}]_i$ in CR#1 cells in response to the application of 1 μ M icilin. **b.** Bar graph summarizing the effects of icilin induced $[Ca^{2+}]_i$ increases. **c.** A representative fluorescent ratiometric calcium imaging recording showing temporal changes of $[Ca^{2+}]_i$ in CR#1 cells in response to the application of 1 μ M icilin with and without the presence of 1 μ M GsMTx-4. **d.** Bar graph summarizing the effects of icilin induced $[Ca^{2+}]_i$ increases shown in c. Data represented as mean \pm S.E.M. Statistics are one-way ANOVA with Bonferroni post-hoc analysis. ***= $p < 0.001$. $n = 70/109$ icilin-ctrl/icilin-GsMTx-4

As the results indicate, the second and third pulse of icilin elicits a smaller calcium increase than the first. However, there is no statistical difference between the 2nd control pulse (Figure 4.25b) and the pulse that included GsMTx-4 (Figure 4.25d). Furthermore, there are no statistical differences between the simultaneous application of icilin/GsMTx-4 and the subsequent wash (both tested with unpaired two-tailed test). In brief, GsMTx-4 blocks CLF-induced, menthol-induced and cold-induced calcium responses in CR#1 cells but has no effect on icilin-induced responses. Moreover, the exerted inhibitory effect was most pronounced on the CLF-induced response, whereas the effect on cold-evoked responses was weak.

4.2.8. Effects of CLF on single channel currents in the cell-attached and inside-out configuration

To gain further insight into the mechanisms of TRPM8 activation by CLF, I recorded single channel activity in membrane patches. I used the cell-attached and the inside-out configuration of the patch-clamp technique, which gives information on open-probability and conductance of a single channel. By using an extracellular solution with a potassium concentration that is typical for the cytosol, the transmembrane potential is brought close to zero in the cell-attached recordings. In all experiments shown below I was unable to record the activity from just a single channel, which is probably due to overexpression of TRPM8 in the CR#1 cell line resulting in multiple channels in the patch of membrane being studied.

For the continuous recordings, the membrane potential at the patch was held at approximately 100 mV, taking into account that the potential difference is unknown but close to zero. Before analyzing the continuous recording, the baseline of the recording was manually adjusted to zero pA. The single channel current was estimated by creating all-points histograms of parts of the trace and subsequently fitted with a Gaussian for the open and closed state of the channel. The trace was idealized by detecting channel openings using the half-amplitude threshold method (Sakmann and Neher, 2009). The threshold was set-up using the measured channel current for each condition. The open probability (P_{open}) was calculated based upon the idealized trace and the estimate of number of channels in the patch. Also, voltage pulses from +140 to 0 mV with a duration of two seconds were applied under all different experimental conditions. As the open probability of the channel decreases, along with the amplitude of the current, calculating the single channel current at levels lower than +100 mV became increasingly difficult. Together with the flickering behavior of TRPM8 channels this leads to channels not reaching full open levels, which can lead to underestimation of the current. For this reason, I restricted measuring the open-channel current to the range of +100 to +140 mV. The measured open-channel currents were plotted and the slope-conductance was calculated by performing a linear fit, forcing it through the origin (0 mV = 0 pA).

First, I conducted single-channel recordings in the cell-attached configuration, holding the temperature at a steady 20°C for increased P_{open} (Figure 4.26).

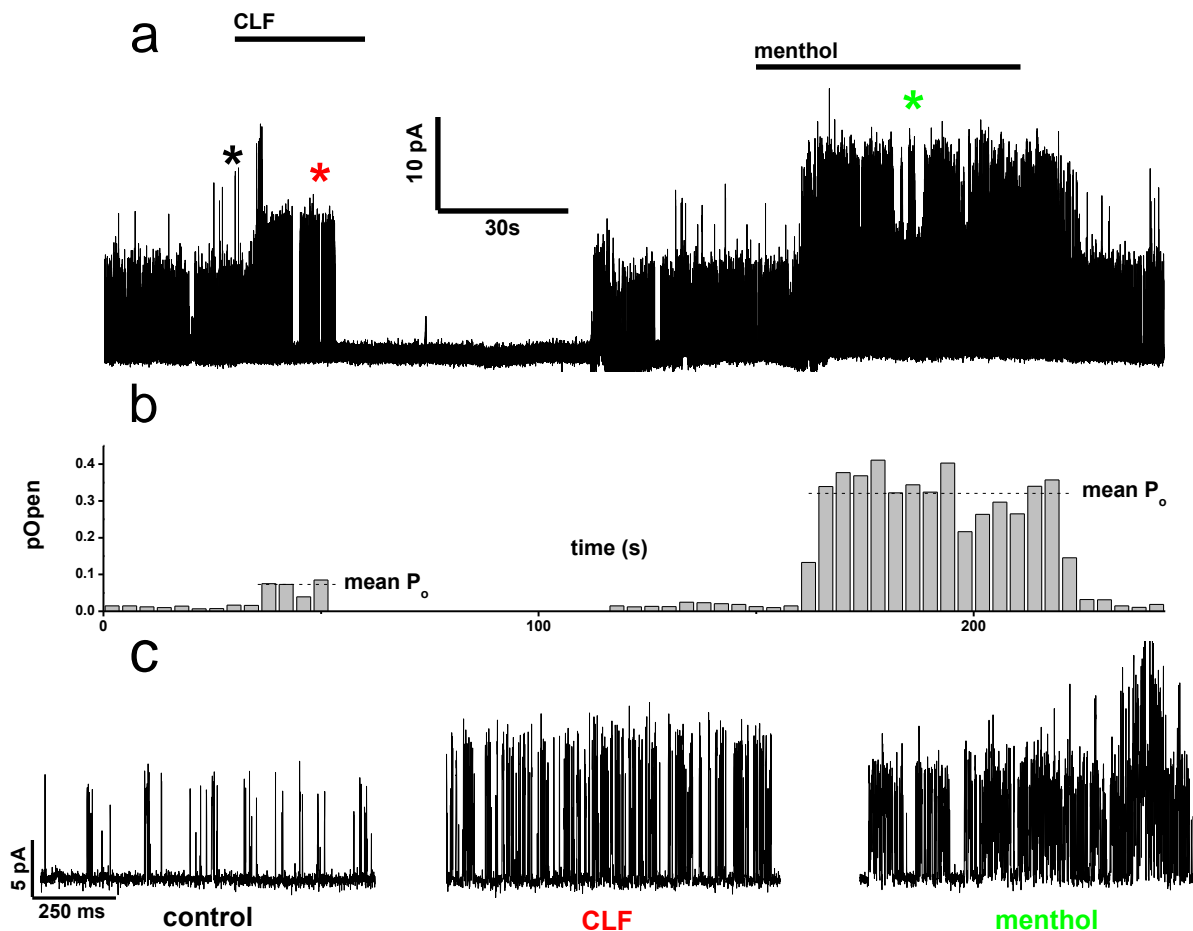


Figure 4.26. CLF increases the open probability and single channel conductance of TRPM8 in the cell-attached configuration. **a)** Complete gap-free trace of a single channel recording in the cell-attached configuration. The trace was digitized at 10 kHz and filtered analogously at 5 kHz (-3dB 4-pole Bessel filter), which later was digitally filtered back to 3 kHz. **b)** Graph indicating the open probability with a 4s-interval. The x-axis is the same as in **a**. **c.** Part of **a**, on a different scale, representing 1-s periods. Approximate region that recording is taken from is indicated by colored asterisk in **a**, which correspond to colored writing.

As can be seen in figure 4.26a and b, upon application of CLF the open probability of TRPM8 clearly rises, although, compared to 100 μ M menthol, this increment is rather small. The open probability is expressed as a ratio of control, as the open probabilities vary significantly from one patch to the other. CLF increases the ratio of P_{open} to 6.4 ± 1.3 ($n = 5$), whereas for menthol it increases to 20.2 ± 4.3 ($n = 5$) (Figure. 4.27f). Of note is the rather abrupt halt of TRPM8-activity during CLF application, and was observed in all cell-attached recordings. This result is in line with the rapid current desensitization that was observed in whole-cell voltage clamp experiments. When changing the scale of the recording, as seen in figure 4.26c, it appears that the single channel conductance increases upon CLF application when compared to control and menthol. The data, when expressed in all-point histograms, confirm this finding (Figure 4.27a-c). When the unitary current at 100 mV is compared, it immediately becomes apparent that CLF increases single-channel

currents, from an average of 7.7 ± 0.1 pA for control (or 8.0 ± 0.2 pA for menthol) to 10.5 ± 0.1 (Figure 4.27d). Compared to control levels, this is an increase of 35,8%. The calculated slope conductance gives similar numbers (Figure 4.27e).

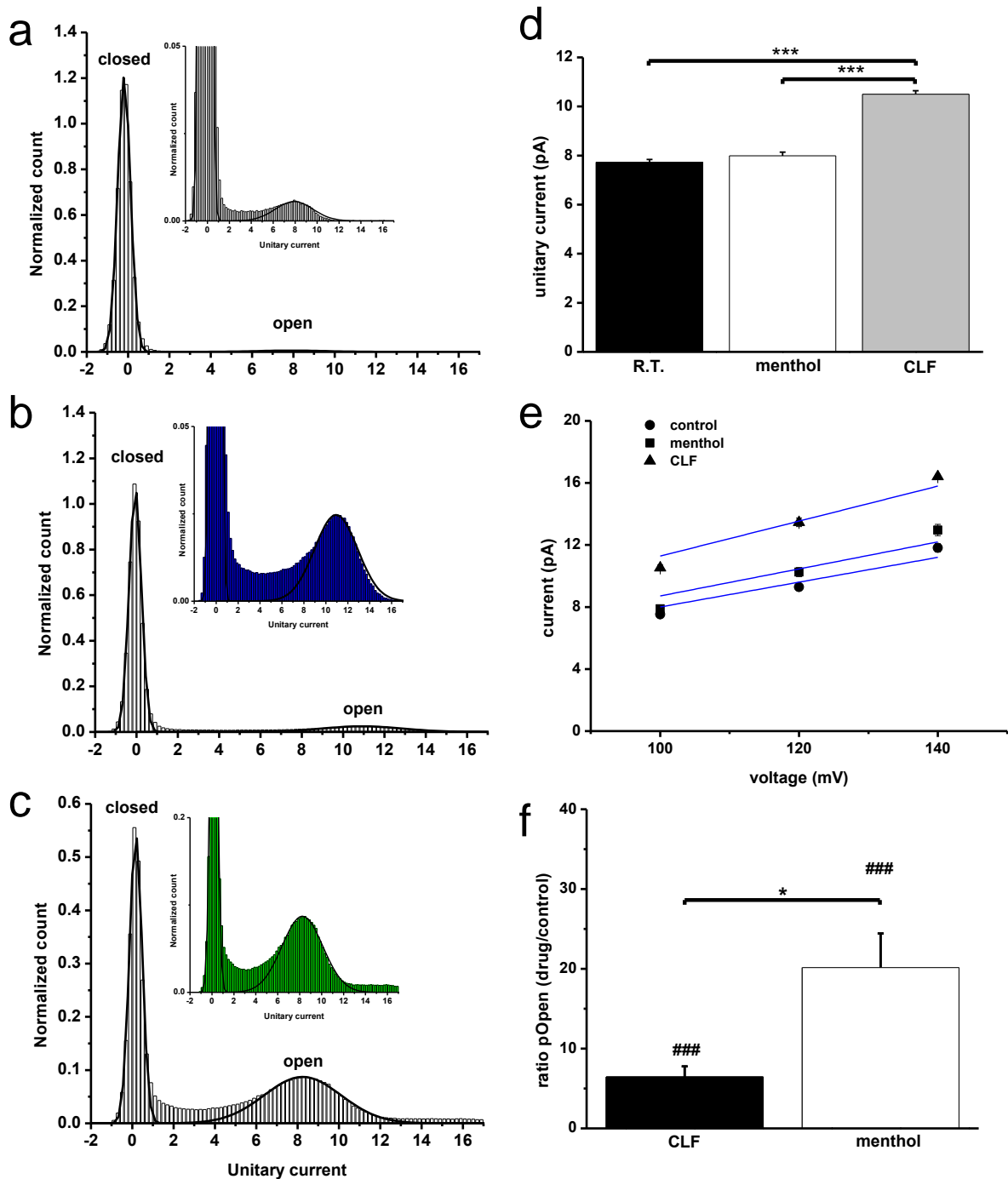


Figure 4.27. a-c) All-point histograms calculated from the trace in figure 4.26. All conditions are represented by color. Insets shows same graph, but on a different scale, to allow for an accurate representation of the histogram in the open state. **d**) Bar graph representing the single channel current at a potential of 100 mV. Data represented as mean \pm S.E.M. Statistically tested with a repeated measurements one-way ANOVA with Bonferroni post-hoc analysis. ***= $p < 0.001$, $n = 10, 9, 10$. **e**) Linear regression drawn through the unitary currents measured at the indicated holding potentials, assuming a reversal potential of 0 mV. Slope of the linear fit represent the slope-conductance. Calculated slope conductance for control: 80,0 pS, menthol: 87,1 pS, CLF: 112,8 pS, ($n =$ at least 5 for each data point). **f**) Bar graph representing the average open probability of TRPM8 with menthol or CLF in the bath, represented as a factor of control, as the basal open-probability varied greatly between membrane patches. Data represented as average \pm S.E.M. Statistically tested with a paired t-test and a one-sample t-test. ### = $p < 0.001$, * = $p < 0.05$.

Now that it was established that TRPM8 open probability and conductance increases upon stimulation with CLF, I continued with single channel recordings in the inside-out configuration, of which the results are presented in figures 4.28 and 4.29. The inside-out configuration is an excised patch configuration in which the intracellular side of the patch is in contact with the bath. This ensures the loss of the cytosolic environment, including any factors that modulate TRPM8, as well as disrupts the cytoskeleton.

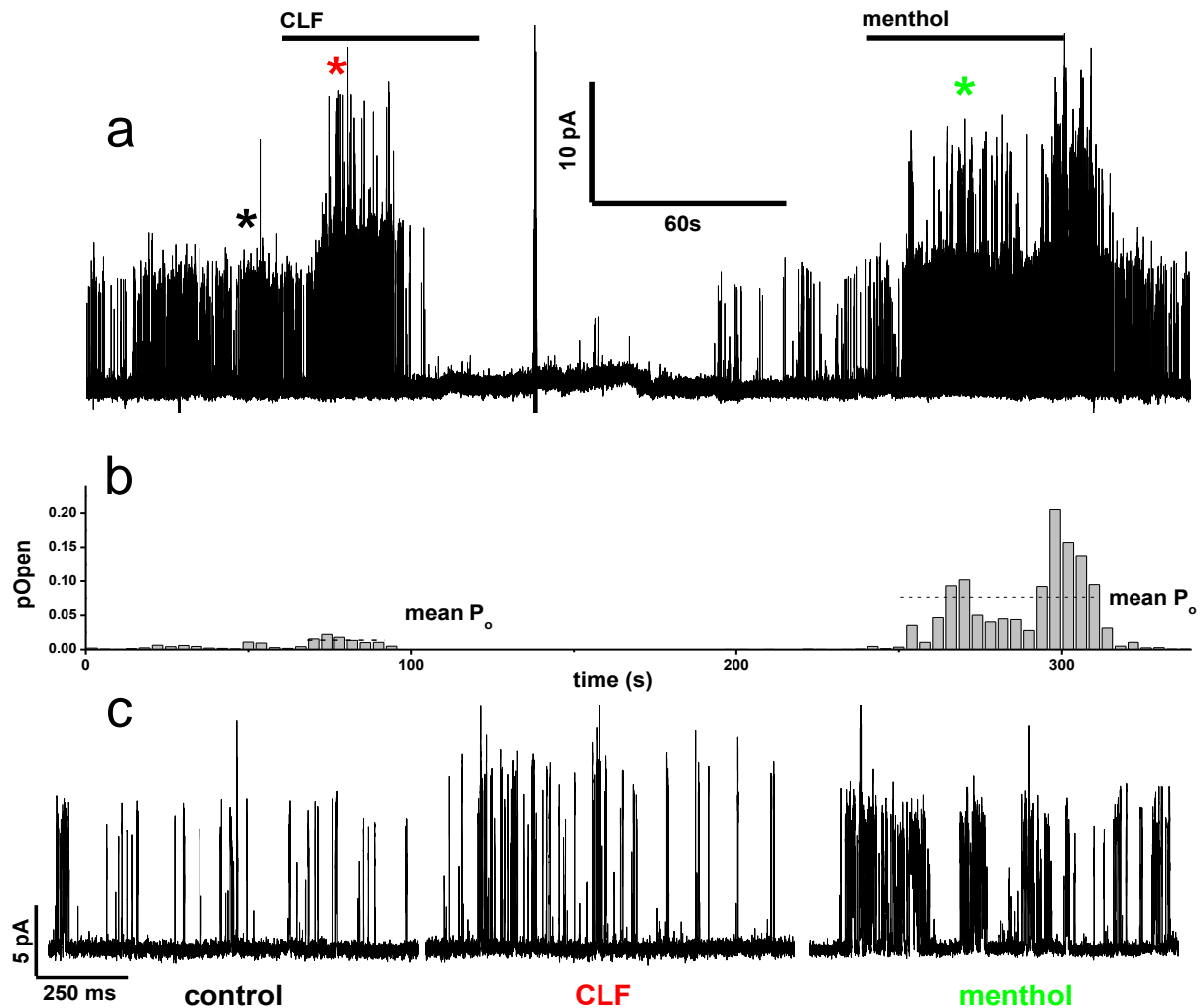


Figure 4.28. CLF increases the open probability and single channel conductance of TRPM8 in excised patches in the inside-out configuration. a) Complete gap-free trace of a single channel recording in the inside-out configuration. The trace was digitized at 10 kHz and filtered analogly at 5 kHz, which later was digitally filtered back to 3 kHz. **b)** Graph indicating the open probability with a 4s-interval. The x-axis is the same as in a. **c)** Showing parts of the recording in a. in more detail in short periods of 1s. Approximate region that recording is taken from is indicated by colored asterisk, which correspond to colored writing.

Also in the inside-out configuration, the application of CLF results in heightened TRPM8 activity as well as in a higher single channel conductance compared to control and menthol (Figures 4.28 and 4.29). The results obtained for single channel conductance are identical for the cell-attached and inside-out configuration at +100

mV (unpaired two-tailed t-test, not shown). Furthermore, just as for cell-attached recordings, an abrupt decrease of TRPM8 P_{open} to zero were observed in all recordings.

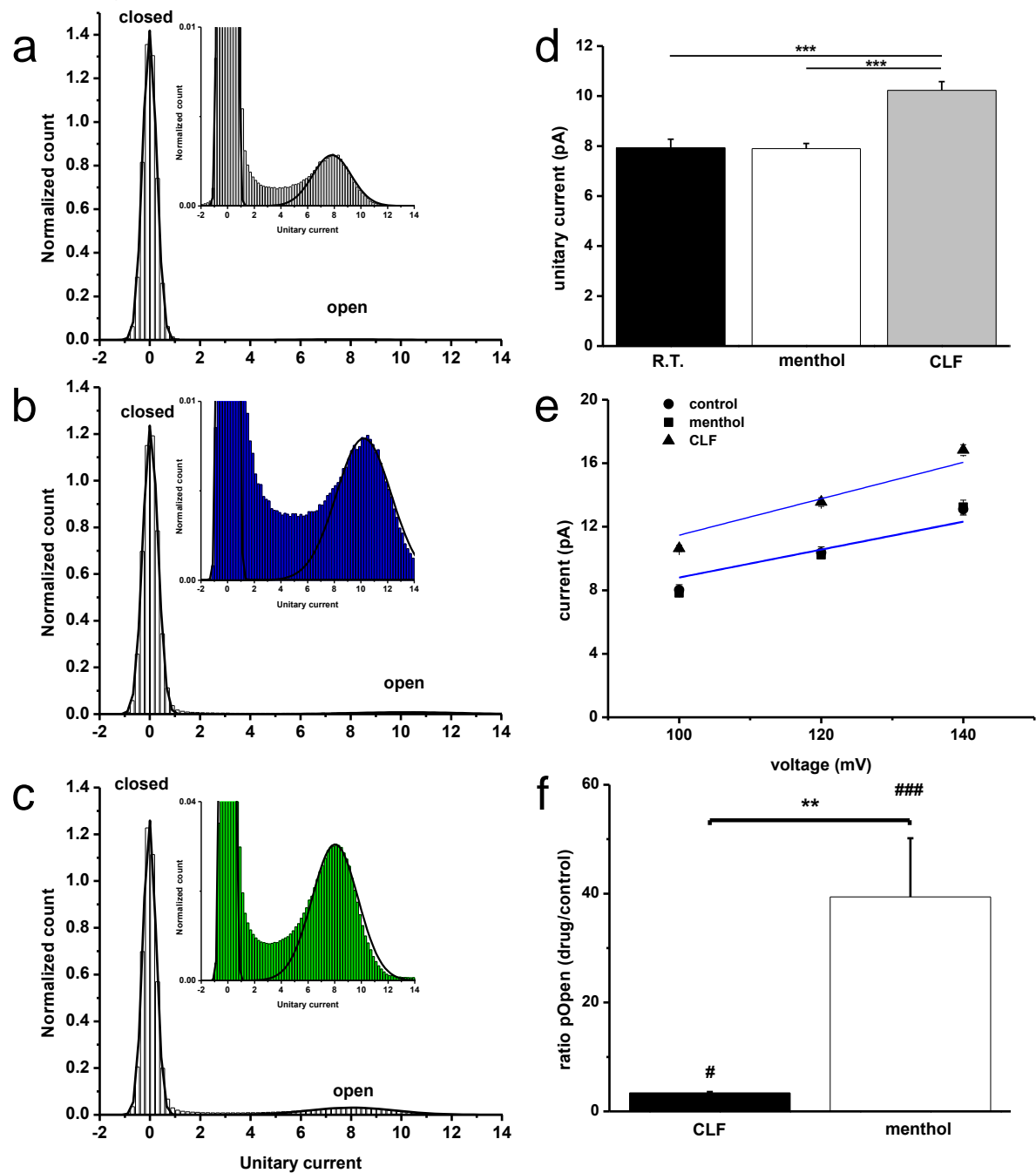


Figure 4.29. a-c) All-point histograms calculated from the trace in figure 4.28a. All conditions are represented by color. Insets shows same graph, but zoomed in to allow for an accurate representation of the histogram in the open state. **d)** Bar graph representing the single channel current at a potential of 100 mV. Data represented as mean \pm S.E.M. Statistically tested with a repeated measurements one-way ANOVA with Bonferroni post-hoc analysis. ***= $p < 0.001$, $n = 10, 9, 10$. Control: $77,3 \pm 1,1$ pA, menthol: $79,9 \pm 1,5$ pA, CLF: $105,0 \pm 1,4$ pA. **e)** Linear regression drawn through the unitary currents measured at the indicated holding potentials, assuming a reversal potential of 0 mV. Slope of the linear fit represent the slope-conductance. Calculated slope conductance for control: 80,02 pS, $n =$ at least 5, menthol: 87,1 pS, $n =$ at least 5, CLF: 112,8 pS, $n =$ at least 5. **f)** Bar graph representing the average open probability of TRPM8 with menthol or CLF in the bath, represented as a factor of control, as the basal open-probability varied greatly between membrane patches.

Taken together, these results indicate that CLF activates TRPM8 in the cell-attached and in the inside-out configuration. The single channel conductance increased for both configurations in a similar fashion. Also, a decrease of the open-probability to zero was observed in both configurations. Given the absence of intracellular modulating factors of TRPM8 in the inside-out configuration, it is reasonable to assume that CLF activates TRPM8 in a membrane-delimited manner. Formation of inside-out patches also disrupt the cytoskeleton, which indicates that also the cytoskeleton is not involved in the activation of TRPM8 by CLF. Moreover, desensitization remains in inside-out patches, again ruling out intracellular modulating factors or the cytoskeleton being involved in this process. The rather abrupt decline in P_{open} to zero indicates that the desensitization observed in whole-cell patch clamp experiments is due to rapid closure of TRPM8-channels in the whole cell and not due to a gradual decrease in single-channel conductance.

5. Discussion

5.1. Inhibition of TRPM8 by 5-BT

The main conclusion of the work presented on 5-BT is that it is an antagonist for cold-induced activity of heterologously and natively expressed TRPM8 channels. As previously shown for other TRPM8-antagonists (Malkia *et al.*, 2007; Malkia *et al.*, 2009), 5-BT exerts its inhibitory effect by shifting the voltage-dependence of activation of TRPM8 rightwards towards more positive potentials, decreasing its open probability at physiological potentials. The inhibitory effect of 5-BT was less potent in native TRPM8 compared to TRPM8 expressed in HEK293 cells, which most likely is the result of the intrinsically higher agonist sensitivity due to additional modulating factors intrinsic to somatosensory neurons. Studies of heterologously expressed TRPM8 channels with mutated binding sites for either menthol or icilin indicated that the menthol binding site is involved in its inhibitory effect, as it was decreased in the menthol-insensitive TRPM8 mutant. The more efficient washout, as observed in whole-cell current recordings of the cold-activated menthol-insensitive mutant when compared to the icilin-insensitive mutant, indicates that 5-BT interacts with the menthol binding site. However, the inhibitory effect of 5-BT is not completely absent, indicating the presence of at least one other site through which 5-BT exerts its effect.

The exact interaction of 5-BT with the menthol binding site is unknown. Previously, *in silico* molecular docking studies of SKF96365 and menthol to a TRPM8 model protein confirmed the interaction of these molecules with the menthol binding site at residue Tyr745, in support of previously gathered experimental data (Malkia *et al.*, 2009). This technique can be useful to probe the putative interaction of 5-BT with the menthol binding site.

In their original study, DeFalco *et al.* demonstrated the importance of the benzyl ether and the amino group of 5-BT for TRPM8 antagonism. Substituting the benzyl ether for a methyl ether shifted the IC_{50} about 40-fold to a higher value, while changing its position relative to the heteroaromatic core changed the IC_{50} about 10-fold. Replacing or deleting the amino group led to similar shifts of the IC_{50} or even to an absence of inhibitory activity (DeFalco *et al.*, 2010). They also noted the structural similarity of 5-BT and AMTB, having in common the aromatic or heteroaromatic core with a benzyl ether and an amine side chain at appropriate positions (Figure 5.1).

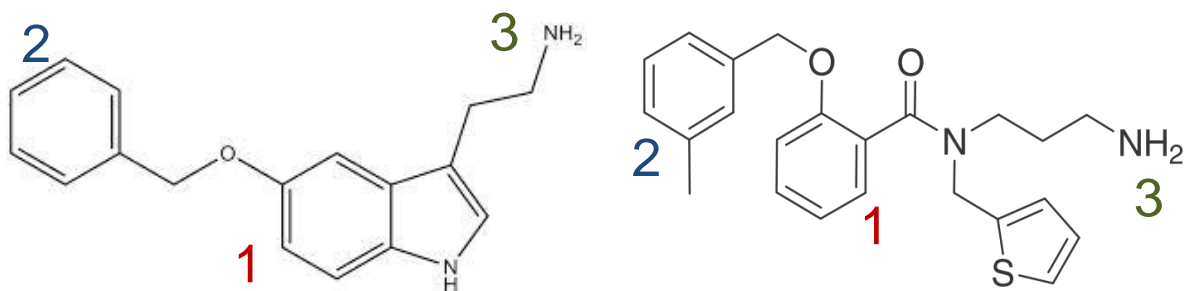


Figure 5.1. Molecular structure of 5-BT (left) and AMTB (right). 5-BT and AMTB share certain characteristics, such as an (hetero)aromatic core (1), a benzyl ether (2) and an amine side chain (3).

Realizing that these groups were found to be indispensable for a potent inhibitory effect of 5-BT, they speculated that this might indicate a similar underlying mechanism of binding and inhibition between the two antagonists. As our study showed that 5-BT primarily exerts its effect through the menthol binding site, it is tempting to further speculate about an interaction of one of these groups with the menthol binding site. Again, molecular docking studies could prove to be helpful in this respect, together with studies of the effect of AMTB on cold-activated HEK293 cells expressing the TRPM8 menthol binding site mutant. If proven successful, these studies might help in the search and synthesis of new TRPM8-antagonists.

In fact, in a recently published study, a series of 2-(benzyloxy)benzamides have been described as potent new antagonists of TRPM8 (Brown *et al.*, 2013). These compounds share structural similarities with 5-BT and AMTB, which highlights the promise of this type of molecular structures as modulators of TRPM8. As 5-BT is a serotonin receptor agonist, it is not surprising it also shares structural similarities with serotonin. Therefore, it is tempting to speculate about potential antagonistic effects of serotonin on the TRPM8 channel. However, in the paper published by DeFalco and colleagues, serotonin was found to have no blocking effect on TRPM8 (DeFalco *et al.*, 2010).

Characterizing drugs that exert antagonism on TRPM8 channels is valuable from different perspectives. First, by studying the action of TRPM8 antagonists we gain further insight into the biophysical properties and gating mechanisms of the channel itself. In addition, and maybe even more importantly, these compounds are also interesting as potential pharmacological agents for treating pathologies involving TRPM8 channels (Fernández-Peña and Viana, 2013; Almaraz *et al.*, 2014).

In order to advance our understanding of the *in vivo* effect of 5-BT on cold-evoked pain and other TRPM8-related pathologies, further behavioral studies in animals are necessary. Intraplantar and/or intraperitoneal injections of 5-BT in mice, followed up by an assessment of their cold response through the cold plantar assay, is an example of such a study. In this particular assay, the paw of the animal is exposed to cold through a glass plate and one measures the latency for paw withdrawal, which is a measure of the cold response threshold. The advantage of this assay over others is that it is found to give more consistent results, allows for a robust estimate of the response threshold and is not stressful to the animals (Brenner *et al.*, 2012).

As is often the case, many compounds lack specificity, and block more than one receptor. Concerning TRPM8, only few antagonists identified so far are specific. For example, BCTC is a potent TRPM8 antagonist (Behrendt *et al.*, 2004; Madrid *et al.*, 2006), but is also a TRPV1 antagonist (Valenzano *et al.*, 2003) and a TRPA1 agonist (Madrid *et al.*, 2006). Similarly, the TRPM8 antagonists Thio-BCTC and capsazepine are also antagonists of TRPV1 (Behrendt *et al.*, 2004; Malkia *et al.*, 2009), while clotrimazole is a TRPV1 and TRPA1 agonist (Meseguer *et al.*, 2008) besides it having inhibitory effects on TRPM8 (Malkia *et al.*, 2009). SKF96365 is a pore blocker of Ca²⁺ channels (Merritt *et al.*, 1990). Thus far, AMTB and PBMC are the only two published TRPM8 antagonists that, as of yet, have not been found to cross-react with other ion channels (Lashinger *et al.*, 2008; Knowlton *et al.*, 2011).

In this regard, a potential pitfall for the usage of 5-BT as a beneficial pharmacological compound *in vivo* could stem from the fact that 5-BT activates the 5-HT_{1D}, 5-HT₂ and 5-HT₆ serotonin receptors (Lyon *et al.*, 1988; Buzzi *et al.*, 1991; Peroutka *et al.*, 1991; Cohen *et al.*, 1992; Boess *et al.*, 1997).

5.2. Activation of TRPM8 by CLF

The main conclusion of the work presented on the effects of CLF on TRPM8 is that CLF robustly activates heterologously expressed TRPM8 channels in a dose-dependent and reversible manner. In whole-cell patch clamp recordings, CLF elicits a transient TRPM8-like outwardly rectifying current with a near-zero reversal potential, which is blocked by BCTC. Natively expressed TRPM8 is also activated by CLF, as indicated by the inhibitory effect of BCTC on the CLF induced calcium influx in TRPM8-expressing somatosensory neurons and the threshold-lowering effect of

lower concentrations of CLF. Cell-attached and whole-cell current clamp recordings corroborated these findings, CLF being able to elicit action potential firing in TRPM8-positive neurons despite the negative effect of CLF on general neuronal excitability through modulation of sodium and potassium channels. As reported for other agonists of TRPM8, CLF shifts the $V_{1/2}$ of TRPM8 towards more negative potentials, facilitating channel opening at physiological potentials. CLF activation of TRPM8 is not dependent on the menthol or icilin binding site, as heterologously expressed TRPM8 with mutations at the corresponding residues are activated normally. Anionic and cationic amphipaths block the CLF induced calcium influx in a recombinant cell line expressing TRPM8 and TRPM8-positive somatosensory neurons alike, suggesting a role for the lipid bilayer in TRPM8 activation by CLF. The block of CLF induced TRPM8-activity by the specific mechanosensitive ion channel blocker GsMTx-4 corroborates these findings. Furthermore, CLF transiently activated single TRPM8 channels in cell-attached and inside-out membrane patches by increasing their open probability. Compared to control and menthol, CLF increased single-channel conductance of TRPM8.

The TRPM8-channel blocker BCTC prevented a rise of intracellular calcium levels upon application of CLF in heterologous and native expression systems, indicating that the rise of intracellular calcium levels were the result of a calcium-influx through TRPM8. Lower concentrations resulted in a lower thermal threshold of activation of TRPM8-positive neurons, but did not culminate in increased intracellular calcium concentrations compared to the first cold pulse. This might be the result of inhibitory effects of CLF on other ion channels expressed in these neurons. CLF activated somatosensory neurons that were not TRPM8-positive, indicating additional effects of CLF in these neurons. Heterologously expressed TRPA1 was shown to be activated by CLF as well, as the TRPA1-channel blocker HC-030031 inhibited the CLF-induced intracellular calcium increase. Even in TRPA1 KO animals, TRPM8-negative somatosensory neurons were activated. BCTC only blocked intracellular calcium increases in TRPM8-positive neurons, indicating that TRPV1, another target inhibited by BCTC, is not responsible for this effect of CLF. The origin of the intracellular calcium increase in these somatosensory remains unknown.

CLF elicited whole-cell currents carried through TRPM8 that rapidly, but reversibly, desensitized. The speed of desensitization was concentration dependent. Desensitization upon continuous stimulation is a typical feature of many

mechanosensitive channels and its rate is also dependent upon stimulus strength (Hamill and Martinac, 2001; Honore *et al.*, 2006; Belyy *et al.*, 2010). Desensitization was independent of Ca²⁺-induced degradation of PIP₂, as the recordings were performed in a bath solution containing no calcium and additionally containing EGTA, a calcium chelator. Single-channel recordings in the cell-attached mode revealed that the desensitization, as observed in whole cell currents, is the result of a sudden decrease in the open probability of the channel and is not the result of a gradual decline in single-channel conductance.

CLF has been shown to be a potent activator of PKC (Roghani *et al.*, 1987; Lester and Baumann, 1991). Thus, desensitization could be an effect of PKC dependent phosphorylation of TRPM8 (Abe *et al.*, 2006). However, the CLF induced decline of TRPM8 open probability remained in excised inside-out patches, ruling out a role for intracellular factors in TRPM8 desensitization. Furthermore, the cytoskeleton is not involved in TRPM8 desensitization, as it is disrupted in excised inside-out membrane patches.

CLF affected the single-channel conductance of TRPM8 and significantly increased it by roughly 25% in both cell-attached as inside-out recordings. Single-channel conductance is a direct measure of the ion-flux rate through an individual open channel. Alterations of the ion-flux rate in unchanging ionic conditions are indicative of changes in pore size, changes in the selectivity filter, or both (Hille, 2001). Increased pore sizes allow for the permeation of more ions, while alterations of the selectivity filter changes the relative ion permeability. Changes in pore size and ion-selectivity of TRP channels by agonist application have previously been reported for TRPA1 (Chen *et al.*, 2009; Banke *et al.*, 2010; Karashima *et al.*, 2010) , TRPV1 (Chung *et al.*, 2008; Banke *et al.*, 2010) and TRPV5 (Yeh *et al.*, 2005). The results reported for TRPM8 are mixed. One study found no uptake of a large cationic dye, used to indicate pore dilation, after exposure to the agonist menthol (Chen *et al.*, 2009), whereas another study did report pore dilation upon stimulation with icilin (Banke *et al.*, 2010). The authors of the latter report ascribed this discrepancy to differences in reagents and/or protocols (Banke *et al.*, 2010). However, a prolonged application of icilin is necessary for pore dilation, as uptake of the cationic dye is not instantaneous and is delayed in the order of minutes. Application of CLF increases single-channel conductance of TRPM8 in a matter of seconds. As such, whatever the

underlying mechanism of icilin induced putative pore dilation is, CLF most probably increases TRPM8-conductance through another type of mechanism.

Setting aside the, still disputed, putative pore dilation of TRPM8, what is the evidence for conductance changes in ion channels resulting from CLF or different volatile anesthetics? Isoflurane has been described to activate a mutant Shaker K⁺ channel, which resulted from an increase in open-probability, paired with an increase in single-channel conductance of around 17%. The conductance increase was ascribed to a stabilization of the open-state of the channel (Li and Correa, 2001). However, single-channel activity of TRPM8 caused by CLF did not reveal any stabilization of the open-state, with the channel still exhibiting its typical flickering behavior. Furthermore, a stabilization of the open-state does not necessarily mean that the measured open conductance increases. Lysophospholipids (LPL's) have been shown to activate TRPM8 in inside-out patches, mainly through stabilizing the open state of the channel. However, no increase of TRPM8 open conductance was noted (Vanden Abeele *et al.*, 2006). Other studies found that anesthetics, such as isoflurane and CLF, activate KvAP, a well-described bacterial voltage-gated potassium channel sharing a similarity with other voltage-gated potassium channels (Tombola *et al.*, 2006). The activation of KvAP with volatile anesthetics is likely the result of bilayer restructuring and was characterized by changes in channel conductance (Finol-Urdaneta *et al.*, 2010).

The mechanism by which anesthetics exert their influence on the nervous system has been controversial for a long time. It was first noted that the potency of an anesthetic correlates with its oil/water partition coefficient (Meyer, 1899; Overton, 1901). This is the famous Meyer-Overton rule and was thought to imply that anesthetics exert their effect through altering the global physical properties of the cell membrane. In much later studies, it was noted that anesthetics inhibit the luciferase enzyme by binding to it, and that this inhibition also correlated to the anesthetics' potency (Franks and Lieb, 1984). Luciferase was the first protein found to directly interact with anesthetics, and later it was discovered that anesthetics interact with other proteins, such as ion channels, as well. As the global changes in physical properties of the membrane were only observed at anesthetic concentrations much higher than those clinically required to induce anesthesia, the consensus was that anesthesia came forth from its direct effect on ion channels [reviewed by Franks (Franks, 2006)]. However, understanding of lipid bilayer mechanics in the context of

anesthetics have progressed and uncovered a potential anesthetic mechanism that is dependent upon local changes of the lateral pressure profile of membranes (Cantor, 1997). The lateral pressure profile describes the lateral tension in the membrane throughout its depth. Although under normal conditions the net tension in a biological membrane is zero, the local pressure within the membrane changes with depth. The basis of the non-uniform distribution of tension throughout the membrane is the large surface tension between the lipids' polar head groups and the non-polar tails offset by attractive interfacial tension (Cantor, 1997, 1999) (Figure 5.2).

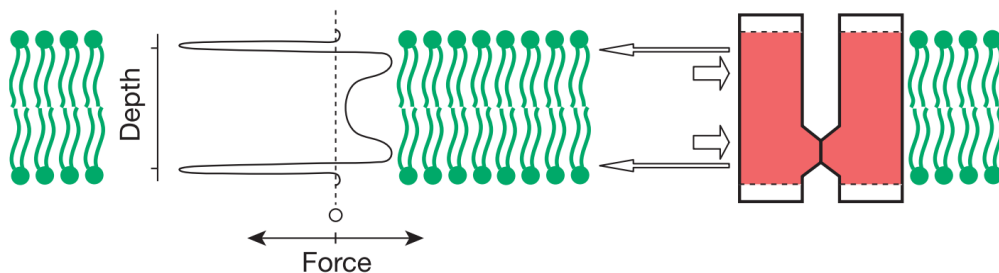


Figure 5.2. The intrinsic force profile plotted as its direction and magnitude along the depth of the bilayer (left) , and a cartoon of a channel protein in section (right), showing how the sharp tension (narrow arrows) near the lipid necks balanced by more diffused pressure nearby (broad arrows) is exerted on the channel–lipid interface (red) [From (Kung, 2005)].

Any ion channel embedded in a lipid bilayer is exposed to these strong localized positive and negative pressures, and, when in equilibrium, the conformational energy of the channel will match the energy profile of the bilayer. Changes in the lateral pressure profile will result in changes in the conformational energy of the channel and thus can modulate ion channel activity. This is thought to be the underlying unifying mechanical principle of ion channels gated by changes in membrane tension (Kung, 2005; Nilius and Honore, 2012). Anesthetics at a concentrations sufficient to induce anesthesia could already alter the pressure profile of the membrane (Cantor, 1997).

The stress distributions within the membrane are difficult to measure directly, but can be calculated by molecular dynamics (MD) studies of models of lipid membranes. MD simulations have recently revealed that CLF preferentially inserts into the inner lipid/water interface section of a membrane leaflet, where the local pressure is positive due to the strong repulsion between hydrocarbon segments close to the headgroup (Figure 5.3). The preferential inclusion of CLF causes an

increase in the local pressure at this location (Reigada, 2013), and thus could affect ion-channel activity.

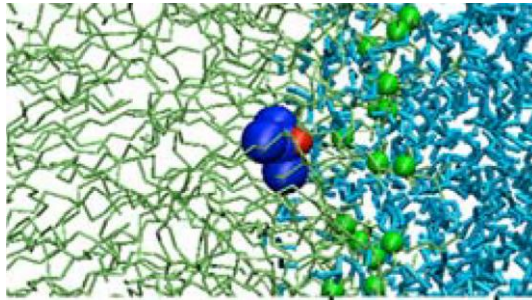


Figure 5.3. Distribution of CLF in a bilayer. The preferred orientation of a CLF molecule in the inner lipid/water interface is shown. Green and cyan sticks correspond to phospholipids and water molecules, respectively. Green beads represent phosphate groups, whereas CLF has been augmented for clarity: blue beads correspond to Cl atoms and the red bead stands for the H atom [Adapted from (Reigada, 2013)].

This might be the underlying reason of activation of TRPM8 by CLF. Furthermore, CLF has a fluidizing effect upon the membrane through the disordering of the lateral lipid organization. This effect of CLF on membranes has been determined experimentally (Mishima *et al.*, 2003; Turkyilmaz *et al.*, 2009; Turkyilmaz *et al.*, 2010; Turkyilmaz *et al.*, 2011) and has been corroborated through MD simulations (Reigada, 2011, 2013).

Of course, the fact that CLF affects membrane properties does not necessarily mean that TRPM8 is activated through this mechanism. The changes in membrane properties might not be large enough to cause any change in activity in TRPM8, or the distributed tensions are changed in the wrong direction and/or location. However, certain results do indicate that the membrane might be involved in TRPM8 activity. GsMTx-4, the specific inhibitor of mechanosensitive channels, did inhibit most of the CLF-induced TRPM8 activity. Interestingly, a minimal effect was observed in cold- or icilin induced TRPM8 activity, but a large inhibitory effect on TRPM8 activation by menthol. Menthol is a monoterpene and has been described to have a fluidizing effect on the membrane (Laub *et al.*, 2012). This is an indication that GsMTx-4 does inhibit certain forms of TRPM8 activity, which is modulated through the membrane. Residue 745 is undeniable involved in the activation of TRPM8 through menthol, but our results indicate that there might be a membrane-component involved as well. For similar reasons, it is conceivable that CLF activates TRPM8 through a direct interaction with the channel protein, even though my work shows that the residues critical for menthol- and icilin-activation of TRPM8 are not involved. Furthermore, I

have not tried the enantiomer of GsMTx-4 (enGsMTx-4), and as such inhibition through a traditional lock-and-key model of ligand-protein interaction cannot be excluded, although enGsMTx-4 was shown to be equally effective as its natural counterpart in blocking the mechanically activated Gramidicin A (gA) ion channel (Suchyna *et al.*, 2004).

Is there any evidence in the literature for TRPM8 as a mechanosensitive ion channel? In a paper by Benedikt and colleagues, in which they investigated the inhibitory effect of ethanol on TRPM8, they noticed that fluctuations in the viscosity of the ethanol/water mixture influenced its inhibitory effect, noting "clear signs of mechanosensitivity of the channel" (Benedikt *et al.*, 2007). Furthermore, ethanol is a solvent, and as such modulates lipid bilayer properties (Ingolfsson and Andersen, 2011). Intriguingly, the effectiveness of ethanol for inhibiting TRPM8 activity was dependent upon the stimulus applied, requiring higher concentrations to block cold-activated TRPM8 than menthol-activated TRPM8. Ethanol only slightly inhibited icilin-induced TRPM8-activity (Benedikt *et al.*, 2007). These results are not unlike my results obtained with GsMTx-4, and, although data is lacking on the inhibitory effect of higher concentrations of GsMTx-4 on TRPM8-activity, could indicate a similar underlying mechanism of inhibition.

Furthermore, lysophospholipids (LPL's), the end products of iPLA2 stimulation, have been shown to activate TRPM8 (Vanden Abeele *et al.*, 2006). The mechanism through which these LPL's activate TRPM8 is not fully understood, but the authors speculate that they convey their effect on TRPM8 through changing the tension in the membrane (Vanden Abeele *et al.*, 2006), as nonbilayer lipids, such as LPL's, have been shown to change the lateral pressure profile of the membrane (Traikia *et al.*, 2002). However, LPL's effect on the membrane lateral pressure profile is different from that of CLF. Whereas CLF inserts itself equally in both membrane leaflets, so the pressure profile in one leaflet mirrors that of the other, LPL's prefer the outer leaflet and changes the pressure profile asymmetrically (Traikia *et al.*, 2002; Reigada, 2013) (Figure 5.4).

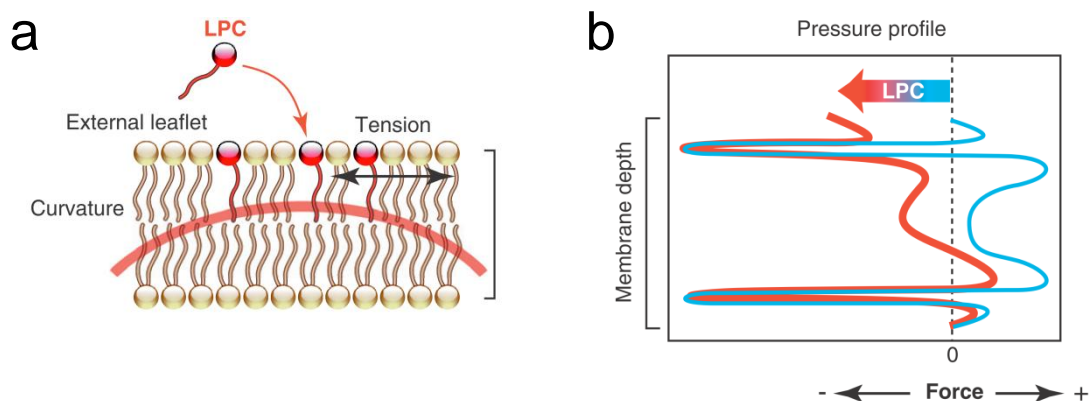


Figure 5.4. Effect of LPL's on lateral pressure profile. **a)** LPL's insert asymmetrically into the membrane, preferring the outer over the inner leaflet. This in contrast to CLF, which displays no preference. **b)** The effect is an asymmetric distribution of lateral pressures throughout the depth of the membrane, whereas CLF would cause a symmetric change in the distribution of lateral pressures [Adapted from (Nilius and Honore, 2012)].

Further evidence pointing towards a possible mechanosensitive role for TRPM8 comes from the observation that hyperosmotic solutions activate TRPM8 (Stuart Bevan, personal communication).

The concentrations of CLF used in this study ranged from a clinical relevant concentration of 1 mM, which is the EC_{50} for general anesthesia in mammals (Franks and Lieb, 1994), to 15 mM. Contribution of TRPM8 towards CLF induced anesthesia is unlikely, as the anesthetic effect of CLF is based upon a reversible loss of consciousness (Franks and Lieb, 1994). Even if TRPM8-activation might somehow be involved in its anesthetic effects, the clinical relevance is low. One reason is the low effectiveness of CLF at 1 mM, the other reason being that the use of CLF as a volatile anesthetic has been discontinued in the medical practice for many years due to it occasionally resulting in lethal cardiac arrhythmias (Himmel, 2008). As such, the relevance of this work lies primarily in the biophysical mechanism underlying TRPM8-activation by CLF.

However, CLF is not the only volatile anesthetic that activates TRPM8. A recent paper not only confirmed our finding of CLF as a TRPM8 antagonist, but additionally found halothane, isoflurane, desflurane and sevoflurane to be TRPM8-activators as well (Vanden Abeele *et al.*, 2013). These are clinically relevant VA's, as they are in common use as inhalational anesthetics in medical practice (Barash *et al.*, 2001). As they describe in their paper, the administration of VA's is accompanied by common side-effects, such as a hypersensitivity to cold and a lowering of the shivering threshold (MacIver and Tanelian, 1990; Kurz *et al.*, 1997). The discovery of

VA's as TRPM8 agonists establishes a clear link between this cold-sensation and VA administration (Vanden Abeele *et al.*, 2013). Another well described side-effect is VA-induced perioperative hypothermia (Kurz, 2008; Sessler, 2008), and is confirmed by the work of Vanden Abeele and colleagues, additionally demonstrating the absence of this effect in TRPM8 KO animals. This is an apparent paradoxical response, as TRPM8 agonists normally enhance thermogenesis (Ding *et al.*, 2008; Masamoto *et al.*, 2009). The authors argue that considering the rapidly desensitizing effect of VA's on TRPM8-activity, in effect, prolonged exposure to VA's might act to block TRPM8 (Vanden Abeele *et al.*, 2013). Antagonists of TRPM8 have been found to induce a decrease in body temperature (Knowlton *et al.*, 2011; Almeida *et al.*, 2012).

Given the role TRPM8 plays in cold pain induced by sickness or by pharmacological compounds used in the treatment of cancer like oxaliplatin, and the role it plays in menthol- and cold-induced anesthesia, the study of pharmacological modulation of TRPM8 is an important issue. Their potential use as therapeutic agents are of great interest, but also their role as a tool to further increase the knowledge of the functioning of TRPM8. Furthermore, a detailed study of the mechanism of action can provide us with more profound knowledge of their biophysical characteristics.

6. Conclusions

En este trabajo he llevado a cabo la caracterización farmacológica de dos moduladores del canal iónico termosensible TRPM8, dando lugar a las siguientes conclusiones:

5-Benzoyloxytriptamina (5-BT)

1. El agonista del receptor serotoninérgico 5-benzyloxytriptamina antagoniza las respuestas del TRPM8 evocadas por el frío, disminuyendo el flujo de calcio a través del receptor TRPM8 expresado tanto de forma heteróloga como de forma nativa. Además, el 5-BT reduce las corrientes evocadas por el frío y el mentol, mediadas por TRPM8 en un sistema de expresión heterólogo. Este efecto se debe a un desplazamiento en la dependencia del voltaje de activación del canal TRPM8 hacia potenciales de membrana más positivos, disminuyendo la probabilidad de apertura de TRPM8 a potenciales de membrana fisiológicos.
2. El sitio de unión para el mentol, en el residuo tirosina 745 del canal TRPM8, está implicado en el efecto antagonista del 5-BT, como lo indica la inhibición diferencial en los mutantes de TRPM8 insensibles al mentol y a la icilina, tanto en experimentos de imagen de calcio como en registros de “patch-clamp”..

Cloroformo (CLF)

1. El CLF es un nuevo agonista del canal TRPM8, produciendo incrementos dosis-dependiente en la concentración del calcio intracelular, debido al flujo de calcio a través del TRPM8 recombinante y del TRPM8 nativo en neuronas somatosensoriales. Además, el CLF activa corrientes con características biofísicas y farmacológicas idénticas a la corriente TRPM8 únicamente en células HEK293 que expresan TRPM8. Este efecto se produce a través de un cambio en la dependencia del voltaje de la activación de TRPM8 hacia potenciales de membrana más negativos, lo cual aumenta la probabilidad de apertura de TRPM8 a potenciales de membrana fisiológicos.
2. El CLF provoca corrientes de acción en neuronas de ganglio raquídeo cultivadas que expresan TRPM8. Además, da lugar a la despolarización y al disparo del potencial de acción en este tipo de neuronas.

3. Los sitios de unión al mentol o a la icilina no están implicados en la activación de TRPM8 por CLF, puesto que la activación de los mutantes de TRPM8 insensibles al mentol y a la icilina es tan efectiva como la observada en el canal silvestre.
4. La bicapa lipídica parece estar implicada en la acción del CLF sobre TRPM8. Los compuestos anfipáticos clorpromazina y trinitrofenol bloquean la activación de TRPM8 por el CLF tanto en sistemas de expresión recombinante como en sistemas nativos. Además, la toxina GsMTX-4, un bloqueante específico de los canales mecanosensibles, también bloquea la activación de TRPM8 por el CLF.
5. Inicialmente, el CLF aumenta la probabilidad de apertura y conductancia unitaria del canal TRPM8 en registros de canal único obtenidos en parches de membrana, tanto en la modalidad "cell-attached" como en la modalidad "inside-out". Posteriormente, la probabilidad de apertura disminuye abruptamente al valor cero en ambas configuraciones. Este descenso brusco en la probabilidad de apertura explicaría la desensibilización de la corriente total, observada en registros de corriente en célula entera.. El hecho de que este efecto continúe manifestándose en los parches "inside-out" excluye la participación de factores intracelulares en este efecto.

In this work I have successfully characterized two novel modulators of TRPM8, resulting in the following main conclusions:

5-Benzoyloxytryptamine (5-BT)

1. The serotonin-receptor agonist 5-benzoyloxytryptamine successfully antagonizes cold evoked responses of TRPM8, decreasing the calcium influx through the heterologously and natively expressed TRPM8 channel. Also, it decreases the cold- and menthol-evoked TRPM8-mediated currents in a heterologous expression system. This effect is explained by a rightward shift in the voltage dependence of activation of TRPM8 towards more positive membrane potentials, decreasing the open probability of TRPM8 at physiological membrane potentials.
2. The menthol binding site at residue tyrosine 745 is involved in the antagonistic effect of 5-BT, as indicated by the differential inhibition of the heterologously expressed menthol- and icilin-insensitive TRPM8 mutants in both calcium-imaging and patch-clamp experiments, which demonstrate a reduced antagonistic effect in the menthol-insensitive mutant.

Chloroform (CLF)

1. CLF is a novel agonist of TRPM8, producing a dose-dependent increment in intracellular calcium concentrations by a calcium influx through recombinant TRPM8, and increasing intracellular calcium in somatosensory neurons natively expressing TRPM8. Furthermore, application of CLF evokes TRPM8-like currents in HEK293 cells expressing TRPM8, which is caused by a leftward shift in the voltage dependence of activation of TRPM8 towards more negative membrane potentials, increasing the open probability of TRPM8 at physiological membrane potentials.
2. CLF elicits action currents in cultured neurons of the DRG that express TRPM8, leading to depolarization and action potential firing in these same type of neurons.
3. The menthol- or icilin- binding sites are not involved in the activation of TRPM8 by CLF, as the activation of the menthol- and icilin-insensitive TRPM8 mutants is as effective as that of the wild type channel.

4. The lipid bilayer appears to be involved in the action of CLF on TRPM8. The amphiphatic compounds chlorpromazine and trinitrophenol block the activation of TRPM8 by CLF in recombinant as well as native systems expressing TRPM8. Furthermore, the spider-toxin GsMTX-4, a specific blocker of mechanosensitive channels, also blocks the activation of TRPM8 by CLF.
5. CLF initially increases the open-probability and open-conductance of TRPM8 in single channel recordings of cell-attached patches as well as in excised inside-out patches containing TRPM8, after which the open-probability abruptly decreases to zero in both configurations. This abrupt decline in the open-probability explains the current-desensitization as observed in CLF evoked whole-cell currents. The fact that this effect continues to be present in excised inside-out patches rules out the involvement of intracellular factors in this effect.

7. Bibliography

- Abe J, Hosokawa H, Sawada Y, Matsumura K, Kobayashi S (2006) Ca²⁺-dependent PKC activation mediates menthol-induced desensitization of transient receptor potential M8. *Neurosci Lett* 397:140-144.
- Abe J, Hosokawa H, Okazawa M, Kandachi M, Sawada Y, Yamanaka K, Matsumura K, Kobayashi S (2005) TRPM8 protein localization in trigeminal ganglion and taste papillae. *Brain Res Mol Brain Res* 136:91-98.
- Abrahamsen B, Zhao J, Asante CO, Cendan CM, Marsh S, Martinez-Barbera JP, Nassar MA, Dickenson AH, Wood JN (2008) The cell and molecular basis of mechanical, cold, and inflammatory pain. *Science* 321:702-705.
- Akiba S, Sato T (2004) Cellular function of calcium-independent phospholipase A2. *Biol Pharm Bull* 27:1174-1178.
- Akopian AN, Sivilotti L, Wood JN (1996) A tetrodotoxin-resistant voltage-gated sodium channel expressed by sensory neurons. *Nature* 379:257-262.
- Akopian AN, Souslova V, England S, Okuse K, Ogata N, Ure J, Smith A, Kerr BJ, McMahon SB, Boyce S, Hill R, Stanfa LC, Dickenson AH, Wood JN (1999) The tetrodotoxin-resistant sodium channel SNS has a specialized function in pain pathways. *Nat Neurosci* 2:541-548.
- Almaraz L, Manenschijn JA, de la Peña E, Viana F (2014) Trpm8. *Handb Exp Pharmacol* 222:547-579.
- Almeida MC, Hew-Butler T, Soriano RN, Rao S, Wang W, Wang J, Tamayo N, Oliveira DL, Nucci TB, Aryal P, Garami A, Bautista D, Gavva NR, Romanovsky AA (2012) Pharmacological blockade of the cold receptor TRPM8 attenuates autonomic and behavioral cold defenses and decreases deep body temperature. *J Neurosci* 32:2086-2099.
- Andersson DA, Chase HW, Bevan S (2004) TRPM8 activation by menthol, icilin, and cold is differentially modulated by intracellular pH. *J Neurosci* 24:5364-5369.
- Andersson DA, Nash M, Bevan S (2007) Modulation of the cold-activated channel TRPM8 by lysophospholipids and polyunsaturated fatty acids. *J Neurosci* 27:3347-3355.
- Babes A, Zorzon D, Reid G (2006) A novel type of cold-sensitive neuron in rat dorsal root ganglia with rapid adaptation to cooling stimuli. *Eur J Neurosci* 24:691-698.
- Bahnasi YM, Wright HM, Milligan CJ, Dedman AM, Zeng F, Hopkins PM, Bateson AN, Beech DJ (2008) Modulation of TRPC5 cation channels by halothane, chloroform and propofol. *Br J Pharmacol* 153:1505-1512.
- Bai VU, Murthy S, Chinnakannu K, Muhletaler F, Tejwani S, Barrack ER, Kim SH, Menon M, Veer Reddy GP (2010) Androgen regulated TRPM8 expression: a potential mRNA marker for metastatic prostate cancer detection in body fluids. *Int J Oncol* 36:443-450.
- Bandell M, Dubin AE, Petrus MJ, Orth A, Mathur J, Hwang SW, Patapoutian A (2006) High-throughput random mutagenesis screen reveals TRPM8 residues specifically required for activation by menthol. *Nat Neurosci* 9:493-500.
- Banke TG, Chaplan SR, Wickenden AD (2010) Dynamic changes in the TRPA1 selectivity filter lead to progressive but reversible pore dilation. *Am J Physiol Cell Physiol* 298:C1457-1468.

- Barash PG, Cullen BF, Stoelting RK (2001) *Clinical anesthesia*. Philadelphia: Lippincott Williams & Wilkins.
- Bard M, Albrecht MR, Gupta N, Guynn CJ, Stillwell W (1988) Geraniol interferes with membrane functions in strains of *Candida* and *Saccharomyces*. *Lipids* 23:534-538.
- Basbaum AI (2008) *The senses : a comprehensive reference*, 1st Edition. Amsterdam ; Boston: Elsevier.
- Basbaum AI, Bautista DM, Scherrer G, Julius D (2009) Cellular and molecular mechanisms of pain. *Cell* 139:267-284.
- Bautista DM, Siemens J, Glazer JM, Tsuruda PR, Basbaum AI, Stucky CL, Jordt SE, Julius D (2007) The menthol receptor TRPM8 is the principal detector of environmental cold. *Nature* 448:204-208.
- Bavencoffe A, Gkika D, Kondratskyi A, Beck B, Borowiec AS, Bidaux G, Busserolles J, Eschalier A, Shuba Y, Skryma R, Prevarskaya N (2010) The transient receptor potential channel TRPM8 is inhibited via the alpha 2A adrenoceptor signaling pathway. *J Biol Chem* 285:9410-9419.
- Beck B, Bidaux G, Bavencoffe A, Lemonnier L, Thebault S, Shuba Y, Barrit G, Skryma R, Prevarskaya N (2007) Prospects for prostate cancer imaging and therapy using high-affinity TRPM8 activators. *Cell Calcium* 41:285-294.
- Beech DJ (2012) Integration of transient receptor potential canonical channels with lipids. *Acta Physiol (Oxf)* 204:227-237.
- Behrendt HJ, Germann T, Gillen C, Hatt H, Jostock R (2004) Characterization of the mouse cold-menthol receptor TRPM8 and vanilloid receptor type-1 VR1 using a fluorometric imaging plate reader (FLIPR) assay. *Br J Pharmacol* 141:737-745.
- Belmonte C, Viana F (2008) Molecular and cellular limits to somatosensory specificity. *Mol Pain* 4:14.
- Belmonte C, Brock JA, Viana F (2009) Converting cold into pain. *Exp Brain Res* 196:13-30.
- Belyy V, Kamaraju K, Akitake B, Anishkin A, Sukharev S (2010) Adaptive behavior of bacterial mechanosensitive channels is coupled to membrane mechanics. *J Gen Physiol* 135:641-652.
- Benedikt J, Teisinger J, Vyklicky L, Vlachova V (2007) Ethanol inhibits cold-menthol receptor TRPM8 by modulating its interaction with membrane phosphatidylinositol 4,5-bisphosphate. *J Neurochem* 100:211-224.
- Berridge MJ, Lipp P, Bootman MD (2000) The versatility and universality of calcium signalling. *Nat Rev Mol Cell Biol* 1:11-21.
- Bindslev N (2008) Drug-acceptor interactions.
- Birder LA, Nakamura Y, Kiss S, Nealen ML, Barrick S, Kanai AJ, Wang E, Ruiz G, De Groat WC, Apodaca G, Watkins S, Caterina MJ (2002) Altered urinary bladder function in mice lacking the vanilloid receptor TRPV1. *Nat Neurosci* 5:856-860.
- Bodding M, Wissenbach U, Flockerzi V (2007) Characterisation of TRPM8 as a pharmacophore receptor. *Cell Calcium* 42:618-628.

- Boess FG, Monsma FJ, Jr., Carolo C, Meyer V, Rudler A, Zwingelstein C, Sleight AJ (1997) Functional and radioligand binding characterization of rat 5-HT₆ receptors stably expressed in HEK293 cells. *Neuropharmacology* 36:713-720.
- Bowsher D, Haggett C (2005) Paradoxical burning sensation produced by cold stimulation in patients with neuropathic pain. *Pain* 117:230.
- Brauchi S, Orio P, Latorre R (2004) Clues to understanding cold sensation: thermodynamics and electrophysiological analysis of the cold receptor TRPM8. *Proc Natl Acad Sci U S A* 101:15494-15499.
- Brauchi S, Orta G, Salazar M, Rosenmann E, Latorre R (2006) A hot-sensing cold receptor: C-terminal domain determines thermosensation in transient receptor potential channels. *J Neurosci* 26:4835-4840.
- Brauchi S, Orta G, Mascayano C, Salazar M, Raddatz N, Urbina H, Rosenmann E, Gonzalez-Nilo F, Latorre R (2007) Dissection of the components for PIP₂ activation and thermosensation in TRP channels. *Proc Natl Acad Sci U S A* 104:10246-10251.
- Brenner DS, Golden JP, Gereau RWt (2012) A novel behavioral assay for measuring cold sensation in mice. *PLoS One* 7:e39765.
- Brown A, Ellis D, Favor DA, Kirkup T, Klute W, MacKenny M, McMurray G, Stennett A (2013) Serendipity in drug-discovery: a new series of 2-(benzyloxy)benzamides as TRPM8 antagonists. *Bioorg Med Chem Lett* 23:6118-6122.
- Buzzi MG, Moskowitz MA, Peroutka SJ, Byun B (1991) Further characterization of the putative 5-HT receptor which mediates blockade of neurogenic plasma extravasation in rat dura mater. *Br J Pharmacol* 103:1421-1428.
- Callejo G, Giblin JP, Gasull X (2013) Modulation of TRESK background K⁺ channel by membrane stretch. *PLoS One* 8:e64471.
- Cantor RS (1997) The lateral pressure profile in membranes: a physical mechanism of general anesthesia. *Biochemistry* 36:2339-2344.
- Cantor RS (1999) The influence of membrane lateral pressures on simple geometric models of protein conformational equilibria. *Chem Phys Lipids* 101:45-56.
- Cao E, Liao M, Cheng Y, Julius D (2013) TRPV1 structures in distinct conformations reveal activation mechanisms. *Nature* 504:113-118.
- Carr RW, Brock JA (2002) Electrophysiology of corneal cold receptor nerve terminals. *Adv Exp Med Biol* 508:19-23.
- Caterina MJ, Rosen TA, Tominaga M, Brake AJ, Julius D (1999) A capsaicin-receptor homologue with a high threshold for noxious heat. *Nature* 398:436-441.
- Caterina MJ, Schumacher MA, Tominaga M, Rosen TA, Levine JD, Julius D (1997) The capsaicin receptor: a heat-activated ion channel in the pain pathway. *Nature* 389:816-824.
- Chandrashekar J, Hoon MA, Ryba NJ, Zuker CS (2006) The receptors and cells for mammalian taste. *Nature* 444:288-294.
- Chen J, Kim D, Bianchi BR, Cavanaugh EJ, Faltynek CR, Kym PR, Reilly RM (2009) Pore dilation occurs in TRPA1 but not in TRPM8 channels. *Mol Pain* 5:3.

- Chen J et al. (2011) Selective blockade of TRPA1 channel attenuates pathological pain without altering noxious cold sensation or body temperature regulation. *Pain* 152:1165-1172.
- Chen JJ, Vasko MR, Wu X, Staeva TP, Baez M, Zgombick JM, Nelson DL (1998) Multiple subtypes of serotonin receptors are expressed in rat sensory neurons in culture. *J Pharmacol Exp Ther* 287:1119-1127.
- Chodon D, Guilbert A, Dhennin-Duthille I, Gautier M, Telliez MS, Sevestre H, Ouadid-Ahidouch H (2010) Estrogen regulation of TRPM8 expression in breast cancer cells. *BMC Cancer* 10:212.
- Chuang HH, Neuhausser WM, Julius D (2004) The super-cooling agent icilin reveals a mechanism of coincidence detection by a temperature-sensitive TRP channel. *Neuron* 43:859-869.
- Chung MK, Guler AD, Caterina MJ (2008) TRPV1 shows dynamic ionic selectivity during agonist stimulation. *Nat Neurosci* 11:555-564.
- Clapham DE (2003) TRP channels as cellular sensors. *Nature* 426:517-524.
- Clapham DE, Julius D, Montell C, Schultz G (2005) International Union of Pharmacology. XLIX. Nomenclature and structure-function relationships of transient receptor potential channels. *Pharmacol Rev* 57:427-450.
- Cohen ML, Schenck K, Nelson D, Robertson DW (1992) Sumatriptan and 5-benzyloxytryptamine: contractility of two 5-HT_{1D} receptor ligands in canine saphenous veins. *Eur J Pharmacol* 211:43-46.
- Colburn RW, Lubin ML, Stone DJ, Jr., Wang Y, Lawrence D, D'Andrea MR, Brandt MR, Liu Y, Flores CM, Qin N (2007) Attenuated cold sensitivity in TRPM8 null mice. *Neuron* 54:379-386.
- Colquhoun D (1998) Binding, gating, affinity and efficacy: the interpretation of structure-activity relationships for agonists and of the effects of mutating receptors. *Br J Pharmacol* 125:924-947.
- Colsohl B, Vennekens R, Nilius B (2011) Transient receptor potential cation channels in pancreatic beta cells. *Rev Physiol Biochem Pharmacol* 161:87-110.
- Cosens DJ, Manning A (1969) Abnormal electroretinogram from a *Drosophila* mutant. *Nature* 224:285-287.
- da Costa DS, Meotti FC, Andrade EL, Leal PC, Motta EM, Calixto JB (2010) The involvement of the transient receptor potential A1 (TRPA1) in the maintenance of mechanical and cold hyperalgesia in persistent inflammation. *Pain* 148:431-437.
- Damann N, Voets T, Nilius B (2008) TRPs in our senses. *Curr Biol* 18:R880-889.
- Daniels RL, Takashima Y, McKemy DD (2009) Activity of the neuronal cold sensor TRPM8 is regulated by phospholipase C via the phospholipid phosphoinositol 4,5-bisphosphate. *J Biol Chem* 284:1570-1582.
- Davis KD (1998) Cold-induced pain and prickle in the glabrous and hairy skin. *Pain* 75:47-57.
- Davis KD, Pope GE (2002) Noxious cold evokes multiple sensations with distinct time courses. *Pain* 98:179-185.

- De Blas GA, Darszon A, Ocampo AY, Serrano CJ, Castellano LE, Hernandez-Gonzalez EO, Chirinos M, Larrea F, Beltran C, Trevino CL (2009) TRPM8, a versatile channel in human sperm. *PLoS One* 4:e6095.
- de la Peña E, Malkia A, Cabedo H, Belmonte C, Viana F (2005) The contribution of TRPM8 channels to cold sensing in mammalian neurones. *J Physiol* 567:415-426.
- de la Peña E, Malkia A, Vara H, Caires R, Ballesta JJ, Belmonte C, Viana F (2012) The influence of cold temperature on cellular excitability of hippocampal networks. *PLoS One* 7:e52475.
- De Petrocellis L, Starowicz K, Moriello AS, Vivese M, Orlando P, Di Marzo V (2007) Regulation of transient receptor potential channels of melastatin type 8 (TRPM8): effect of cAMP, cannabinoid CB(1) receptors and endovanilloids. *Exp Cell Res* 313:1911-1920.
- DeFalco J, Steiger D, Dourado M, Emerling D, Duncton MA (2010) 5-benzyloxytryptamine as an antagonist of TRPM8. *Bioorg Med Chem Lett* 20:7076-7079.
- del Camino D, Murphy S, Heiry M, Barrett LB, Earley TJ, Cook CA, Petrus MJ, Zhao M, D'Amours M, Deering N, Brenner GJ, Costigan M, Hayward NJ, Chong JA, Fanger CM, Woolf CJ, Patapoutian A, Moran MM (2010) TRPA1 contributes to cold hypersensitivity. *J Neurosci* 30:15165-15174.
- Delmas P, Brown DA (2005) Pathways modulating neural KCNQ/M (Kv7) potassium channels. *Nat Rev Neurosci* 6:850-862.
- Deuticke B (1968) Transformation and restoration of biconcave shape of human erythrocytes induced by amphiphilic agents and changes of ionic environment. *Biochim Biophys Acta* 163:494-500.
- Dhaka A, Earley TJ, Watson J, Patapoutian A (2008) Visualizing cold spots: TRPM8-expressing sensory neurons and their projections. *J Neurosci* 28:566-575.
- Dhaka A, Murray AN, Mathur J, Earley TJ, Petrus MJ, Patapoutian A (2007) TRPM8 is required for cold sensation in mice. *Neuron* 54:371-378.
- Dietrich A, Mederos YSM, Gollasch M, Gross V, Storch U, Dubrovskaja G, Obst M, Yildirim E, Salanova B, Kalwa H, Essin K, Pinkenburg O, Luft FC, Gudermann T, Birnbaumer L (2005) Increased vascular smooth muscle contractility in TRPC6-/- mice. *Mol Cell Biol* 25:6980-6989.
- Ding Z, Gomez T, Werkheiser JL, Cowan A, Rawls SM (2008) Icilin induces a hyperthermia in rats that is dependent on nitric oxide production and NMDA receptor activation. *Eur J Pharmacol* 578:201-208.
- Dragoni I, Guida E, McIntyre P (2006) The cold and menthol receptor TRPM8 contains a functionally important double cysteine motif. *J Biol Chem* 281:37353-37360.
- Duncan LM, Deeds J, Hunter J, Shao J, Holmgren LM, Woolf EA, Tepper RI, Shyjan AW (1998) Down-regulation of the novel gene melastatin correlates with potential for melanoma metastasis. *Cancer Res* 58:1515-1520.
- Earley S (2012) TRPA1 channels in the vasculature. *Br J Pharmacol* 167:13-22.
- Eccles R (1994) Menthol and related cooling compounds. *J Pharm Pharmacol* 46:618-630.

- Elitt CM, McIlwrath SL, Lawson JJ, Malin SA, Molliver DC, Cornuet PK, Koerber HR, Davis BM, Albers KM (2006) Artemin overexpression in skin enhances expression of TRPV1 and TRPA1 in cutaneous sensory neurons and leads to behavioral sensitivity to heat and cold. *J Neurosci* 26:8578-8587.
- Engelke M, Jessel R, Wiechmann A, Diehl HA (1997) Effect of inhalation anaesthetics on the phase behaviour, permeability and order of phosphatidylcholine bilayers. *Biophys Chem* 67:127-138.
- Erler I, Al-Ansary DM, Wissenbach U, Wagner TF, Flockerzi V, Niemeyer BA (2006) Trafficking and assembly of the cold-sensitive TRPM8 channel. *J Biol Chem* 281:38396-38404.
- Fajardo O, Meseguer V, Belmonte C, Viana F (2008) TRPA1 channels mediate cold temperature sensing in mammalian vagal sensory neurons: pharmacological and genetic evidence. *J Neurosci* 28:7863-7875.
- Fenwick EM, Marty A, Neher E (1982) A patch-clamp study of bovine chromaffin cells and of their sensitivity to acetylcholine. *J Physiol* 331:577-597.
- Fernández-Peña C, Viana F (2013) Targeting TRPM8 for Pain Relief. *The Open Pain Journal* 6:154-164.
- Fernandez JA, Skryma R, Bidaux G, Magleby KL, Scholfield CN, McGeown JG, Prevarskaya N, Zholos AV (2011) Voltage- and cold-dependent gating of single TRPM8 ion channels. *J Gen Physiol* 137:173-195.
- Finol-Urdaneta RK, McArthur JR, Juranka PF, French RJ, Morris CE (2010) Modulation of KvAP unitary conductance and gating by 1-alkanols and other surface active agents. *Biophys J* 98:762-772.
- Fischer MJ, Balasuriya D, Jeggle P, Goetze TA, McNaughton PA, Reeh PW, Edwardson JM (2014) Direct evidence for functional TRPV1/TRPA1 heteromers. *Pflugers Arch*.
- Fleig A, Penner R (2004) The TRPM ion channel subfamily: molecular, biophysical and functional features. *Trends Pharmacol Sci* 25:633-639.
- Franks NP (2006) Molecular targets underlying general anaesthesia. *Br J Pharmacol* 147 Suppl 1:S72-81.
- Franks NP, Lieb WR (1984) Do general anaesthetics act by competitive binding to specific receptors? *Nature* 310:599-601.
- Franks NP, Lieb WR (1994) Molecular and cellular mechanisms of general anaesthesia. *Nature* 367:607-614.
- Freichel M, Suh SH, Pfeifer A, Schweig U, Trost C, Weissgerber P, Biel M, Philipp S, Freise D, Droogmans G, Hofmann F, Flockerzi V, Nilius B (2001) Lack of an endothelial store-operated Ca²⁺ current impairs agonist-dependent vasorelaxation in TRP4^{-/-} mice. *Nat Cell Biol* 3:121-127.
- Fujita F, Uchida K, Takaishi M, Sokabe T, Tominaga M (2013) Ambient Temperature Affects the Temperature Threshold for TRPM8 Activation through Interaction of Phosphatidylinositol 4,5-Bisphosphate. *J Neurosci* 33:6154-6159.
- Gauchan P, Andoh T, Kato A, Kuraishi Y (2009) Involvement of increased expression of transient receptor potential melastatin 8 in oxaliplatin-induced cold allodynia in mice. *Neurosci Lett* 458:93-95.

- Gaudioso C, Hao J, Martin-Eauclaire MF, Gabriac M, Delmas P (2012) Menthol pain relief through cumulative inactivation of voltage-gated sodium channels. *Pain* 153:473-484.
- Gavva NR, Davis C, Lehto SG, Rao S, Wang W, Zhu DX (2012) Transient receptor potential melastatin 8 (TRPM8) channels are involved in body temperature regulation. *Mol Pain* 8:36.
- Gees M, Owsianik G, Nilius B, Voets T (2012) TRP Channels. *Compr Physiol* 2:563-608.
- Gentry C, Stoakley N, Andersson DA, Bevan S (2010) The roles of iPLA2, TRPM8 and TRPA1 in chemically induced cold hypersensitivity. *Mol Pain* 6:4.
- Gomis A, Soriano S, Belmonte C, Viana F (2008) Hypoosmotic- and pressure-induced membrane stretch activate TRPC5 channels. *J Physiol* 586:5633-5649.
- Grynkiewicz G, Poenie M, Tsien RY (1985) A new generation of Ca²⁺ indicators with greatly improved fluorescence properties. *J Biol Chem* 260:3440-3450.
- Hamill OP, Martinac B (2001) Molecular basis of mechanotransduction in living cells. *Physiol Rev* 81:685-740.
- Hamill OP, Marty A, Neher E, Sakmann B, Sigworth FJ (1981) Improved patch-clamp techniques for high-resolution current recording from cells and cell-free membrane patches. *Pflugers Arch* 391:85-100.
- Hardie RC, Minke B (1992) The *trp* gene is essential for a light-activated Ca²⁺ channel in *Drosophila* photoreceptors. *Neuron* 8:643-651.
- Harrington AM, Hughes PA, Martin CM, Yang J, Castro J, Isaacs NJ, Blackshaw LA, Brierley SM (2011) A novel role for TRPM8 in visceral afferent function. *Pain* 152:1459-1468.
- Hayashi T, Kondo T, Ishimatsu M, Yamada S, Nakamura K, Matsuoka K, Akasu T (2009) Expression of the TRPM8-immunoreactivity in dorsal root ganglion neurons innervating the rat urinary bladder. *Neurosci Res* 65:245-251.
- Haydon DA, Urban BW (1983) The effects of some inhalation anaesthetics on the sodium current of the squid giant axon. *J Physiol* 341:429-439.
- Hensel H, Zotterman Y (1951) The effect of menthol on the thermoreceptors. *Acta Physiol Scand* 24:27-34.
- Henshall SM, Afar DE, Hiller J, Horvath LG, Quinn DI, Rasiah KK, Gish K, Willhite D, Kench JG, Gardiner-Garden M, Stricker PD, Scher HI, Grygiel JJ, Agus DB, Mack DH, Sutherland RL (2003) Survival analysis of genome-wide gene expression profiles of prostate cancers identifies new prognostic targets of disease relapse. *Cancer Res* 63:4196-4203.
- Hille B (2001) *Ion channels of excitable membranes*, 3rd Edition. Sunderland, Mass.: Sinauer.
- Himmel HM (2008) Mechanisms involved in cardiac sensitization by volatile anesthetics: general applicability to halogenated hydrocarbons? *Crit Rev Toxicol* 38:773-803.

- Hjerling-Leffler J, Alqatari M, Ernfors P, Koltzenburg M (2007) Emergence of functional sensory subtypes as defined by transient receptor potential channel expression. *J Neurosci* 27:2435-2443.
- Hoenderop JG, van Leeuwen JP, van der Eerden BC, Kersten FF, van der Kemp AW, Merillat AM, Waarsing JH, Rossier BC, Vallon V, Hummler E, Bindels RJ (2003) Renal Ca²⁺ wasting, hyperabsorption, and reduced bone thickness in mice lacking TRPV5. *J Clin Invest* 112:1906-1914.
- Honore E, Patel AJ, Chemin J, Suchyna T, Sachs F (2006) Desensitization of mechano-gated K₂P channels. *Proc Natl Acad Sci U S A* 103:6859-6864.
- Ingolfsson HI, Andersen OS (2011) Alcohol's effects on lipid bilayer properties. *Biophys J* 101:847-855.
- Janssens A, Voets T (2011) Ligand stoichiometry of the cold- and menthol-activated channel TRPM8. *J Physiol* 589:4827-4835.
- Johar P, Grover V, Topp R, Behm DG (2012) A comparison of topical menthol to ice on pain, evoked tetanic and voluntary force during delayed onset muscle soreness. *Int J Sports Phys Ther* 7:314-322.
- Johnson CD, Melanaphy D, Purse A, Stokesberry SA, Dickson P, Zholos AV (2009) Transient receptor potential melastatin 8 channel involvement in the regulation of vascular tone. *Am J Physiol Heart Circ Physiol* 296:H1868-1877.
- Julius D, Basbaum AI (2001) Molecular mechanisms of nociception. *Nature* 413:203-210.
- Jutila A, Soderlund T, Pakkanen AL, Huttunen M, Kinnunen PK (2001) Comparison of the effects of clozapine, chlorpromazine, and haloperidol on membrane lateral heterogeneity. *Chem Phys Lipids* 112:151-163.
- Kang D, Choe C, Kim D (2005) Thermosensitivity of the two-pore domain K⁺ channels TREK-2 and TRAAK. *J Physiol* 564:103-116.
- Karashima Y, Prenen J, Talavera K, Janssens A, Voets T, Nilius B (2010) Agonist-induced changes in Ca²⁺ permeation through the nociceptor cation channel TRPA1. *Biophys J* 98:773-783.
- Katsura H, Obata K, Mizushima T, Yamanaka H, Kobayashi K, Dai Y, Fukuoka T, Tokunaga A, Sakagami M, Noguchi K (2006) Antisense knock down of TRPA1, but not TRPM8, alleviates cold hyperalgesia after spinal nerve ligation in rats. *Exp Neurol* 200:112-123.
- Kim AY, Tang Z, Liu Q, Patel KN, Maag D, Geng Y, Dong X (2008) Pirt, a phosphoinositide-binding protein, functions as a regulatory subunit of TRPV1. *Cell* 133:475-485.
- Kim SJ, Kim YS, Yuan JP, Petralia RS, Worley PF, Linden DJ (2003) Activation of the TRPC1 cation channel by metabotropic glutamate receptor mGluR1. *Nature* 426:285-291.
- Knowlton WM, Daniels RL, Palkar R, McCoy DD, McKemy DD (2011) Pharmacological Blockade of TRPM8 Ion Channels Alters Cold and Cold Pain Responses in Mice. *PLoS One* 6:e25894.

- Knowlton WM, Palkar R, Lippoldt EK, McCoy DD, Baluch F, Chen J, McKemy DD (2013) A Sensory-Labeled Line for Cold: TRPM8-Expressing Sensory Neurons Define the Cellular Basis for Cold, Cold Pain, and Cooling-Mediated Analgesia. *The Journal of Neuroscience* 33:2837-2848.
- Kress M, Reeh PW (1996) More sensory competence for nociceptive neurons in culture. *Proc Natl Acad Sci U S A* 93:14995-14997.
- Kuhn FJ, Winking M, Kuhn C, Hoffmann DC, Luckhoff A (2013) Surface expression and channel function of TRPM8 are cooperatively controlled by transmembrane segments S3 and S4. *Pflugers Arch* 465:1599-1610.
- Kung C (2005) A possible unifying principle for mechanosensation. *Nature* 436:647-654.
- Kurz A (2008) Thermal care in the perioperative period. *Best Pract Res Clin Anaesthesiol* 22:39-62.
- Kurz A, Xiong J, Sessler DI, Plattner O, Christensen R, Dechert M, Ikeda T (1997) Isoflurane produces marked and nonlinear decreases in the vasoconstriction and shivering thresholds. *Ann N Y Acad Sci* 813:778-785.
- Kwan KY, Corey DP (2009) Burning cold: involvement of TRPA1 in noxious cold sensation. *J Gen Physiol* 133:251-256.
- Lashinger ES, Steingra MS, Hieble JP, Leon LA, Gardner SD, Nagilla R, Davenport EA, Hoffman BE, Laping NJ, Su X (2008) AMTB, a TRPM8 channel blocker: evidence in rats for activity in overactive bladder and painful bladder syndrome. *Am J Physiol Renal Physiol* 295:F803-810.
- Laub KR, Witschas K, Blicher A, Madsen SB, Luckhoff A, Heimburg T (2012) Comparing ion conductance recordings of synthetic lipid bilayers with cell membranes containing TRP channels. *Biochim Biophys Acta* 1818:1123-1134.
- Lehky TJ, Leonard GD, Wilson RH, Grem JL, Floeter MK (2004) Oxaliplatin-induced neurotoxicity: acute hyperexcitability and chronic neuropathy. *Muscle Nerve* 29:387-392.
- Lesage F, Terrenoire C, Romey G, Lazdunski M (2000) Human TREK2, a 2P domain mechano-sensitive K⁺ channel with multiple regulations by polyunsaturated fatty acids, lysophospholipids, and Gs, Gi, and Gq protein-coupled receptors. *J Biol Chem* 275:28398-28405.
- Lester DS, Baumann D (1991) Action of organic solvents on protein kinase C. *Eur J Pharmacol* 206:301-308.
- Li J, Correa AM (2001) Single-channel basis for conductance increase induced by isoflurane in Shaker H4 IR K(+) channels. *Am J Physiol Cell Physiol* 280:C1130-1139.
- Li Q, Wang X, Yang Z, Wang B, Li S (2009) Menthol induces cell death via the TRPM8 channel in the human bladder cancer cell line T24. *Oncology* 77:335-341.
- Li Y, Jia YC, Cui K, Li N, Zheng ZY, Wang YZ, Yuan XB (2005) Essential role of TRPC channels in the guidance of nerve growth cones by brain-derived neurotrophic factor. *Nature* 434:894-898.

- Lieb WR, Kovalycsik M, Mendelsohn R (1982) Do clinical levels of general anaesthetics affect lipid bilayers? Evidence from Raman scattering. *Biochim Biophys Acta* 688:388-398.
- Liman ER (2006) Thermal gating of TRP ion channels: food for thought? *Sci STKE* 2006:pe12.
- Lin W, Margolskee R, Donnert G, Hell SW, Restrepo D (2007) Olfactory neurons expressing transient receptor potential channel M5 (TRPM5) are involved in sensing semiochemicals. *Proc Natl Acad Sci U S A* 104:2471-2476.
- Linte RM, Ciobanu C, Reid G, Babes A (2007) Desensitization of cold- and menthol-sensitive rat dorsal root ganglion neurones by inflammatory mediators. *Exp Brain Res* 178:89-98.
- Lippoldt EK, Elmes RR, McCoy DD, Knowlton WM, McKemy DD (2013) Artemin, a Glial Cell Line-Derived Neurotrophic Factor Family Member, Induces TRPM8-Dependent Cold Pain. *J Neurosci* 33:12543-12552.
- Liu B, Qin F (2005) Functional control of cold- and menthol-sensitive TRPM8 ion channels by phosphatidylinositol 4,5-bisphosphate. *J Neurosci* 25:1674-1681.
- Liu B, Fan L, Balakrishna S, Sui A, Morris JB, Jordt SE (2013) TRPM8 is the Principal Mediator of Menthol-induced Analgesia of Acute and Inflammatory Pain. *Pain*.
- Liu X, Cheng KT, Bandyopadhyay BC, Pani B, Dietrich A, Paria BC, Swaim WD, Beech D, Yildirim E, Singh BB, Birnbaumer L, Ambudkar IS (2007) Attenuation of store-operated Ca²⁺ current impairs salivary gland fluid secretion in TRPC1(-/-) mice. *Proc Natl Acad Sci U S A* 104:17542-17547.
- Louhivuori LM, Bart G, Larsson KP, Louhivuori V, Nasman J, Nordstrom T, Koivisto AP, Akerman KE (2009) Differentiation dependent expression of TRPA1 and TRPM8 channels in IMR-32 human neuroblastoma cells. *J Cell Physiol* 221:67-74.
- Lundbaek JA, Collingwood SA, Ingolfsson HI, Kapoor R, Andersen OS (2010) Lipid bilayer regulation of membrane protein function: gramicidin channels as molecular force probes. *J R Soc Interface* 7:373-395.
- Lyon RA, Titeler M, Seggel MR, Glennon RA (1988) Indolealkylamine analogs share 5-HT₂ binding characteristics with phenylalkylamine hallucinogens. *Eur J Pharmacol* 145:291-297.
- Ma S, Yu H, Zhao Z, Luo Z, Chen J, Ni Y, Jin R, Ma L, Wang P, Zhu Z, Li L, Zhong J, Liu D, Nilius B (2012) Activation of the cold-sensing TRPM8 channel triggers UCP1-dependent thermogenesis and prevents obesity. *J Mol Cell Biol* 4:88-96.
- MacIver MB, Tanelian DL (1990) Volatile anesthetics excite mammalian nociceptor afferents recorded in vitro. *Anesthesiology* 72:1022-1030.
- Madrid R, de la Peña E, Donovan-Rodriguez T, Belmonte C, Viana F (2009) Variable threshold of trigeminal cold-thermosensitive neurons is determined by a balance between TRPM8 and Kv1 potassium channels. *J Neurosci* 29:3120-3131.
- Madrid R, Donovan-Rodriguez T, Meseguer V, Acosta MC, Belmonte C, Viana F (2006) Contribution of TRPM8 channels to cold transduction in primary sensory neurons and peripheral nerve terminals. *J Neurosci* 26:12512-12525.

- Mahieu F, Janssens A, Gees M, Talavera K, Nilius B, Voets T (2010) Modulation of the cold-activated cation channel TRPM8 by surface charge screening. *J Physiol* 588:315-324.
- Maingret F, Lauritzen I, Patel AJ, Heurteaux C, Reyes R, Lesage F, Lazdunski M, Honore E (2000) TREK-1 is a heat-activated background K(+) channel. *EMBO J* 19:2483-2491.
- Malin SA, Molliver DC, Koerber HR, Cornuet P, Frye R, Albers KM, Davis BM (2006) Glial cell line-derived neurotrophic factor family members sensitize nociceptors in vitro and produce thermal hyperalgesia in vivo. *J Neurosci* 26:8588-8599.
- Malkia A, Morenilla-Palao C, Viana F (2011) The emerging pharmacology of TRPM8 channels: hidden therapeutic potential underneath a cold surface. *Curr Pharm Biotechnol* 12:54-67.
- Malkia A, Pertusa M, Fernandez-Ballester G, Ferrer-Montiel A, Viana F (2009) Differential role of the menthol-binding residue Y745 in the antagonism of thermally gated TRPM8 channels. *Mol Pain* 5:62.
- Malkia A, Madrid R, Meseguer V, de la Peña E, Valero M, Belmonte C, Viana F (2007) Bidirectional shifts of TRPM8 channel gating by temperature and chemical agents modulate the cold sensitivity of mammalian thermoreceptors. *J Physiol* 581:155-174.
- Marco R, Marnie G, Veronica M, Andrea P, Lucia P, Alessandra C, Juri V, Diego DS, Valentina S, Rosario R, Franco B, Raffaele DC, Roberto V (2013) Human white adipocytes express the cold receptor trpm8 which activation induces ucp1 expression, mitochondrial activation and heat production. *Mol Cell Endocrinol*.
- Maroto R, Raso A, Wood TG, Kurosky A, Martinac B, Hamill OP (2005) TRPC1 forms the stretch-activated cation channel in vertebrate cells. *Nat Cell Biol* 7:179-185.
- Martinac B, Adler J, Kung C (1990) Mechanosensitive ion channels of *E. coli* activated by amphipaths. *Nature* 348:261-263.
- Masamoto Y, Kawabata F, Fushiki T (2009) Intragastric administration of TRPV1, TRPV3, TRPM8, and TRPA1 agonists modulates autonomic thermoregulation in different manners in mice. *Biosci Biotechnol Biochem* 73:1021-1027.
- Matta JA, Ahern GP (2007) Voltage is a partial activator of rat thermosensitive TRP channels. *J Physiol* 585:469-482.
- Matta JA, Cornett PM, Miyares RL, Abe K, Sahibzada N, Ahern GP (2008) General anesthetics activate a nociceptive ion channel to enhance pain and inflammation. *Proc Natl Acad Sci U S A* 105:8784-8789.
- McKemy DD, Neuhausser WM, Julius D (2002) Identification of a cold receptor reveals a general role for TRP channels in thermosensation. *Nature* 416:52-58.
- McNamara CR, Mandel-Brehm J, Bautista DM, Siemens J, Deranian KL, Zhao M, Hayward NJ, Chong JA, Julius D, Moran MM, Fanger CM (2007) TRPA1 mediates formalin-induced pain. *Proc Natl Acad Sci U S A* 104:13525-13530.
- Mergler S, Plath T, Groetzing C, Kaiser S, Neuhaus P, Bechstein WO, Wiedenmann B (2004) Human neuroendocrine tumor cells express cold sensitive TRPM8 channels. *Gastroenterology* 126:A245.

- Mergler S, Derckx R, Reinach PS, Garreis F, Bohm A, Schmelzer L, Skosyrski S, Ramesh N, Abdelmessih S, Polat OK, Khajavi N, Riechardt AI (2014) Calcium regulation by temperature-sensitive transient receptor potential channels in human uveal melanoma cells. *Cell Signal* 26:56-69.
- Merritt JE, Armstrong WP, Benham CD, Hallam TJ, Jacob R, Jaxa-Chamiec A, Leigh BK, McCarthy SA, Moores KE, Rink TJ (1990) SK&F 96365, a novel inhibitor of receptor-mediated calcium entry. *Biochem J* 271:515-522.
- Meseguer V, Karashima Y, Talavera K, D'Hoedt D, Donovan-Rodriguez T, Viana F, Nilius B, Voets T (2008) Transient receptor potential channels in sensory neurons are targets of the antimycotic agent clotrimazole. *J Neurosci* 28:576-586.
- Meseguer V, Alpizar YA, Luis E, Tajada S, Denlinger B, Fajardo O, Manenschijn JA, Fernandez-Pena C, Talavera A, Kichko T, Navia B, Sanchez A, Senaris R, Reeh P, Perez-Garcia MT, Lopez-Lopez JR, Voets T, Belmonte C, Talavera K, Viana F (2014) TRPA1 channels mediate acute neurogenic inflammation and pain produced by bacterial endotoxins. *Nat Commun* 5:3125.
- Meyer H (1899) Zur Theorie der Alkoholnarkose. *Archiv für experimentelle Pathologie und Pharmakologie* 42:109-118.
- Mishima K, Watanabe H, Kaneko S, Ogihara T (2003) Membrane disordering induced by chloroform and carbon tetrachloride. *Colloids and Surfaces B: Biointerfaces* 28:307-312.
- Momin A, Cadiou H, Mason A, McNaughton PA (2008) Role of the hyperpolarization-activated current I_h in somatosensory neurons. *J Physiol* 586:5911-5929.
- Monteith GR, McAndrew D, Faddy HM, Roberts-Thomson SJ (2007) Calcium and cancer: targeting Ca^{2+} transport. *Nat Rev Cancer* 7:519-530.
- Montell C (2005) The TRP superfamily of cation channels. *Sci STKE* 2005:re3.
- Montell C, Rubin GM (1989) Molecular characterization of the *Drosophila* trp locus: a putative integral membrane protein required for phototransduction. *Neuron* 2:1313-1323.
- Montell C, Birnbaumer L, Flockerzi V, Bindels RJ, Bruford EA, Caterina MJ, Clapham DE, Harteneck C, Heller S, Julius D, Kojima I, Mori Y, Penner R, Prawitt D, Scharenberg AM, Schultz G, Shimizu N, Zhu MX (2002) A Unified Nomenclature for the Superfamily of TRP Cation Channels. *Molecular Cell* 9:229-231.
- Moran MM, McAlexander MA, Biro T, Szallasi A (2011) Transient receptor potential channels as therapeutic targets. *Nat Rev Drug Discov* 10:601-620.
- Morenilla-Palao C, Pertusa M, Meseguer V, Cabedo H, Viana F (2009) Lipid raft segregation modulates TRPM8 channel activity. *J Biol Chem* 284:9215-9224.
- Morin C, Bushnell MC (1998) Temporal and qualitative properties of cold pain and heat pain: a psychophysical study. *Pain* 74:67-73.
- Munsch T, Freichel M, Flockerzi V, Pape HC (2003) Contribution of transient receptor potential channels to the control of GABA release from dendrites. *Proc Natl Acad Sci U S A* 100:16065-16070.

- Nassini R, Gees M, Harrison S, De Siena G, Materazzi S, Moretto N, Failli P, Preti D, Marchetti N, Cavazzini A, Mancini F, Pedretti P, Nilius B, Patacchini R, Geppetti P (2011) Oxaliplatin elicits mechanical and cold allodynia in rodents via TRPA1 receptor stimulation. *Pain* 152:1621-1631.
- Neher E, Sakmann B (1976) Single-channel currents recorded from membrane of denervated frog muscle fibres. *Nature* 260:799-802.
- Neher E, Sakmann B, Steinbach JH (1978) The extracellular patch clamp: a method for resolving currents through individual open channels in biological membranes. *Pflugers Arch* 375:219-228.
- Nicholson R, Small J, Dixon AK, Spanswick D, Lee K (2003) Serotonin receptor mRNA expression in rat dorsal root ganglion neurons. *Neurosci Lett* 337:119-122.
- Nilius B (2007) TRP channels in disease. *Biochim Biophys Acta* 1772:805-812.
- Nilius B, Owsianik G (2011) The transient receptor potential family of ion channels. *Genome Biol* 12:218.
- Nilius B, Honore E (2012) Sensing pressure with ion channels. *Trends Neurosci* 35:477-486.
- Nilius B, Owsianik G, Voets T, Peters JA (2007) Transient receptor potential cation channels in disease. *Physiol Rev* 87:165-217.
- Nilius B, Mahieu F, Prenen J, Janssens A, Owsianik G, Vennekens R, Voets T (2006) The Ca²⁺-activated cation channel TRPM4 is regulated by phosphatidylinositol 4,5-bisphosphate. *EMBO J* 25:467-478.
- Noel J, Zimmermann K, Busserolles J, Deval E, Alloui A, Diochot S, Guy N, Borsotto M, Reeh P, Eschalièr A, Lazdunski M (2009) The mechano-activated K⁺ channels TRAAK and TREK-1 control both warm and cold perception. *EMBO J* 28:1308-1318.
- Okazawa M, Terauchi T, Shiraki T, Matsumura K, Kobayashi S (2000) I-Menthol-induced [Ca²⁺]_i increase and impulses in cultured sensory neurons. *Neuroreport* 11:2151-2155.
- Okazawa M, Takao K, Hori A, Shiraki T, Matsumura K, Kobayashi S (2002) Ionic basis of cold receptors acting as thermostats. *J Neurosci* 22:3994-4001.
- Orio P, Parra A, Madrid R, Gonzalez O, Belmonte C, Viana F (2012) Role of I_h in the firing pattern of mammalian cold thermoreceptor endings. *J Neurophysiol* 108:3009-3023.
- Orio P, Madrid R, de la Peña E, Parra A, Meseguer V, Bayliss DA, Belmonte C, Viana F (2009) Characteristics and physiological role of hyperpolarization activated currents in mouse cold thermoreceptors. *J Physiol* 587:1961-1976.
- Oshimoto A, Wakabayashi Y, Garske A, Lopez R, Rolen S, Flowers M, Arevalo N, Restrepo D (2013) Potential role of transient receptor potential channel M5 in sensing putative pheromones in mouse olfactory sensory neurons. *PLoS One* 8:e61990.
- Overton CE (1901) Studien über die Narkose zugleich ein Beitrag zur Allgemeinen Pharmakologie: Fischer.

- Owsianik G, Talavera K, Voets T, Nilius B (2006) Permeation and selectivity of TRP channels. *Annu Rev Physiol* 68:685-717.
- Panda S, Nayak SK, Campo B, Walker JR, Hogenesch JB, Jegla T (2005) Illumination of the melanopsin signaling pathway. *Science* 307:600-604.
- Pape HC (1996) Queer current and pacemaker: the hyperpolarization-activated cation current in neurons. *Annu Rev Physiol* 58:299-327.
- Parra A, Madrid R, Echevarria D, del Olmo S, Morenilla-Palao C, Acosta MC, Gallar J, Dhaka A, Viana F, Belmonte C (2010) Ocular surface wetness is regulated by TRPM8-dependent cold thermoreceptors of the cornea. *Nat Med* 16:1396-1399.
- Patapoutian A, Peier AM, Story GM, Viswanath V (2003) ThermoTRP channels and beyond: mechanisms of temperature sensation. *Nat Rev Neurosci* 4:529-539.
- Patel AJ, Honore E, Lesage F, Fink M, Romey G, Lazdunski M (1999) Inhalational anesthetics activate two-pore-domain background K⁺ channels. *Nat Neurosci* 2:422-426.
- Patel AJ, Honore E, Maingret F, Lesage F, Fink M, Duprat F, Lazdunski M (1998) A mammalian two pore domain mechano-gated S-like K⁺ channel. *EMBO J* 17:4283-4290.
- Peier AM, Moqrich A, Hergarden AC, Reeve AJ, Andersson DA, Story GM, Earley TJ, Dragoni I, McIntyre P, Bevan S, Patapoutian A (2002a) A TRP channel that senses cold stimuli and menthol. *Cell* 108:705-715.
- Peier AM, Reeve AJ, Andersson DA, Moqrich A, Earley TJ, Hergarden AC, Story GM, Colley S, Hogenesch JB, McIntyre P, Bevan S, Patapoutian A (2002b) A heat-sensitive TRP channel expressed in keratinocytes. *Science* 296:2046-2049.
- Perkins KL (2006) Cell-attached voltage-clamp and current-clamp recording and stimulation techniques in brain slices. *J Neurosci Methods* 154:1-18.
- Peroutka SJ, McCarthy BG, Guan XM (1991) 5-benzyloxytryptamine: a relatively selective 5-hydroxytryptamine 1D/1B agent. *Life Sci* 49:409-418.
- Pertusa M, Madrid R, Morenilla-Palao C, Belmonte C, Viana F (2012) N-glycosylation of TRPM8 ion channels modulates temperature sensitivity of cold thermoreceptor neurons. *J Biol Chem* 287:18218-18229.
- Petrus M, Peier AM, Bandell M, Hwang SW, Huynh T, Olney N, Jegla T, Patapoutian A (2007) A role of TRPA1 in mechanical hyperalgesia is revealed by pharmacological inhibition. *Mol Pain* 3:40.
- Phelps CB, Gaudet R (2007) The role of the N terminus and transmembrane domain of TRPM8 in channel localization and tetramerization. *J Biol Chem* 282:36474-36480.
- Pierce PA, Xie GX, Meuser T, Peroutka SJ (1997) 5-Hydroxytryptamine receptor subtype messenger RNAs in human dorsal root ganglia: a polymerase chain reaction study. *Neuroscience* 81:813-819.
- Pogorzala LA, Mishra SK, Hoon MA (2013) The cellular code for Mammalian thermosensation. *J Neurosci* 33:5533-5541.

- Premkumar LS, Raisinghani M, Pingle SC, Long C, Pimentel F (2005) Downregulation of transient receptor potential melastatin 8 by protein kinase C-mediated dephosphorylation. *J Neurosci* 25:11322-11329.
- Proudfoot CJ, Garry EM, Cottrell DF, Rosie R, Anderson H, Robertson DC, Fleetwood-Walker SM, Mitchell R (2006) Analgesia mediated by the TRPM8 cold receptor in chronic neuropathic pain. *Curr Biol* 16:1591-1605.
- Purves D (2008) *Neuroscience*, 4th Edition. Sunderland, Mass.: Sinauer.
- Qiu X, Kumbalasisiri T, Carlson SM, Wong KY, Krishna V, Provencio I, Berson DM (2005) Induction of photosensitivity by heterologous expression of melanopsin. *Nature* 433:745-749.
- Reid G, Flonta ML (2001a) Physiology. Cold current in thermoreceptive neurons. *Nature* 413:480.
- Reid G, Flonta M (2001b) Cold transduction by inhibition of a background potassium conductance in rat primary sensory neurones. *Neurosci Lett* 297:171-174.
- Reid G, Babes A, Pluteanu F (2002) A cold- and menthol-activated current in rat dorsal root ganglion neurones: properties and role in cold transduction. *The Journal of Physiology* 545:595-614.
- Reigada R (2011) Influence of chloroform in liquid-ordered and liquid-disordered phases in lipid membranes. *J Phys Chem B* 115:2527-2535.
- Reigada R (2013) Atomistic study of lipid membranes containing chloroform: looking for a lipid-mediated mechanism of anesthesia. *PLoS One* 8:e52631.
- Roghani M, Da Silva C, Castagna M (1987) Tumor promoter chloroform is a potent protein kinase C activator. *Biochem Biophys Res Commun* 142:738-744.
- Rohacs T, Lopes CM, Michailidis I, Logothetis DE (2005) PI(4,5)P₂ regulates the activation and desensitization of TRPM8 channels through the TRP domain. *Nat Neurosci* 8:626-634.
- Roza C, Belmonte C, Viana F (2006) Cold sensitivity in axotomized fibers of experimental neuromas in mice. *Pain* 120:24-35.
- Sabnis AS, Reilly CA, Veranth JM, Yost GS (2008a) Increased transcription of cytokine genes in human lung epithelial cells through activation of a TRPM8 variant by cold temperatures. *Am J Physiol Lung Cell Mol Physiol* 295:L194-200.
- Sabnis AS, Shadid M, Yost GS, Reilly CA (2008b) Human lung epithelial cells express a functional cold-sensing TRPM8 variant. *Am J Respir Cell Mol Biol* 39:466-474.
- Sakmann B, Neher E (2009) *Single-channel recording*, 2nd Edition. New York, NY: Springer.
- Sarria I, Ling J, Xu GY, Gu JG (2012) Sensory discrimination between innocuous and noxious cold by TRPM8-expressing DRG neurons of rats. *Mol Pain* 8:79.
- Sauls J (1999) Efficacy of cold for pain: fact or fallacy? *Online J Knowl Synth Nurs* 6:8.
- Schaefer M (2005) Homo- and heteromeric assembly of TRP channel subunits. *Pflugers Arch* 451:35-42.

- Schafer K, Braun HA, Isenberg C (1986) Effect of menthol on cold receptor activity. Analysis of receptor processes. *J Gen Physiol* 88:757-776.
- Schmidt RF, Willis WD (2007) *Encyclopedia of Pain*. Springer.
- Scroggs RS, Todorovic SM, Anderson EG, Fox AP (1994) Variation in IH, IIR, and ILEAK between acutely isolated adult rat dorsal root ganglion neurons of different size. *J Neurophysiol* 71:271-279.
- Sessler DI (2008) Temperature monitoring and perioperative thermoregulation. *Anesthesiology* 109:318-338.
- Sheetz MP, Singer SJ (1974) Biological membranes as bilayer couples. A molecular mechanism of drug-erythrocyte interactions. *Proc Natl Acad Sci U S A* 71:4457-4461.
- Sheetz MP, Singer SJ (1976) Equilibrium and kinetic effects of drugs on the shapes of human erythrocytes. *J Cell Biol* 70:247-251.
- Shin JB, Adams D, Paukert M, Siba M, Sidi S, Levin M, Gillespie PG, Grunder S (2005) *Xenopus* TRPN1 (NOMPC) localizes to microtubule-based cilia in epithelial cells, including inner-ear hair cells. *Proc Natl Acad Sci U S A* 102:12572-12577.
- Sidell N, Verity MA, Nord EP (1990) Menthol blocks dihydropyridine-insensitive Ca²⁺ channels and induces neurite outgrowth in human neuroblastoma cells. *J Cell Physiol* 142:410-419.
- Sidi S, Friedrich RW, Nicolson T (2003) NompC TRP channel required for vertebrate sensory hair cell mechanotransduction. *Science* 301:96-99.
- Sikkema J, de Bont JA, Poolman B (1994) Interactions of cyclic hydrocarbons with biological membranes. *J Biol Chem* 269:8022-8028.
- Singh BB, Liu X, Tang J, Zhu MX, Ambudkar IS (2002) Calmodulin regulates Ca²⁺-dependent feedback inhibition of store-operated Ca²⁺ influx by interaction with a site in the C terminus of TrpC1. *Mol Cell* 9:739-750.
- Spassova MA, Hewavitharana T, Xu W, Soboloff J, Gill DL (2006) A common mechanism underlies stretch activation and receptor activation of TRPC6 channels. *Proc Natl Acad Sci U S A* 103:16586-16591.
- Stein RJ, Santos S, Nagatomi J, Hayashi Y, Minnery BS, Xavier M, Patel AS, Nelson JB, Futrell WJ, Yoshimura N, Chancellor MB, De Miguel F (2004) Cool (TRPM8) and hot (TRPV1) receptors in the bladder and male genital tract. *J Urol* 172:1175-1178.
- Stewart AP, Egressy K, Lim A, Edwardson JM (2010) AFM imaging reveals the tetrameric structure of the TRPM8 channel. *Biochem Biophys Res Commun* 394:383-386.
- Story GM, Peier AM, Reeve AJ, Eid SR, Mosbacher J, Hricik TR, Earley TJ, Hergarden AC, Andersson DA, Hwang SW, McIntyre P, Jegla T, Bevan S, Patapoutian A (2003) ANKTM1, a TRP-like channel expressed in nociceptive neurons, is activated by cold temperatures. *Cell* 112:819-829.
- Strotmann R, Harteneck C, Nunnenmacher K, Schultz G, Plant TD (2000) OTRPC4, a nonselective cation channel that confers sensitivity to extracellular osmolarity. *Nat Cell Biol* 2:695-702.

- Su L, Wang C, Yu YH, Ren YY, Xie KL, Wang GL (2011) Role of TRPM8 in dorsal root ganglion in nerve injury-induced chronic pain. *BMC Neurosci* 12:120.
- Suchyna TM, Tape SE, Koeppe RE, 2nd, Andersen OS, Sachs F, Gottlieb PA (2004) Bilayer-dependent inhibition of mechanosensitive channels by neuroactive peptide enantiomers. *Nature* 430:235-240.
- Sun M, Goldin E, Stahl S, Falardeau JL, Kennedy JC, Acierno JS, Jr., Bove C, Kaneshi CR, Nagle J, Bromley MC, Colman M, Schiffmann R, Slaugenhaupt SA (2000) Mucopolidosis type IV is caused by mutations in a gene encoding a novel transient receptor potential channel. *Hum Mol Genet* 9:2471-2478.
- Swandulla D, Carbone E, Schafer K, Lux HD (1987) Effect of menthol on two types of Ca currents in cultured sensory neurons of vertebrates. *Pflugers Arch* 409:52-59.
- Takashima Y, Daniels RL, Knowlton W, Teng J, Liman ER, McKemy DD (2007) Diversity in the neural circuitry of cold sensing revealed by genetic axonal labeling of transient receptor potential melastatin 8 neurons. *J Neurosci* 27:14147-14157.
- Talavera K, Nilius B, Voets T (2008) Neuronal TRP channels: thermometers, pathfinders and life-savers. *Trends Neurosci* 31:287-295.
- Talavera K, Yasumatsu K, Voets T, Droogmans G, Shigemura N, Ninomiya Y, Margolskee RF, Nilius B (2005) Heat activation of TRPM5 underlies thermal sensitivity of sweet taste. *Nature* 438:1022-1025.
- Tang Z, Kim A, Masuch T, Park K, Weng H, Wetzel C, Dong X (2013) Pirt functions as an endogenous regulator of TRPM8. *Nat Commun* 4.
- Thut P (2003) Cold transduction in rat trigeminal ganglia neurons in vitro. *Neuroscience* 119:1071-1083.
- Togashi K, Hara Y, Tominaga T, Higashi T, Konishi Y, Mori Y, Tominaga M (2006) TRPM2 activation by cyclic ADP-ribose at body temperature is involved in insulin secretion. *EMBO J* 25:1804-1815.
- Tombola F, Pathak MM, Isacoff EY (2006) How does voltage open an ion channel? *Annu Rev Cell Dev Biol* 22:23-52.
- Traherne JB (1962) Evaluation of the cold spray technique in the treatment of muscle pain in general practice. *Practitioner* 189:210-212.
- Traikia M, Warschawski DE, Lambert O, Rigaud JL, Devaux PF (2002) Asymmetrical membranes and surface tension. *Biophys J* 83:1443-1454.
- Tsavalier L, Shapero MH, Morkowski S, Laus R (2001) Trp-p8, a novel prostate-specific gene, is up-regulated in prostate cancer and other malignancies and shares high homology with transient receptor potential calcium channel proteins. *Cancer Res* 61:3760-3769.
- Tsuruda PR, Julius D, Minor DL, Jr. (2006) Coiled coils direct assembly of a cold-activated TRP channel. *Neuron* 51:201-212.
- Turkyilmaz S, Almeida PF, Regen SL (2011) Effects of isoflurane, halothane, and chloroform on the interactions and lateral organization of lipids in the liquid-ordered phase. *Langmuir* 27:14380-14385.
- Turkyilmaz S, Chen WH, Mitomo H, Regen SL (2009) Loosening and reorganization of fluid phospholipid bilayers by chloroform. *J Am Chem Soc* 131:5068-5069.

- Turkyilmaz S, Mitomo H, Chen WH, Regen SL (2010) Phospholipid complexation of general anesthetics in fluid bilayers. *Langmuir* 26:5309-5311.
- Valente P, Garcia-Sanz N, Gomis A, Fernandez-Carvajal A, Fernandez-Ballester G, Viana F, Belmonte C, Ferrer-Montiel A (2008) Identification of molecular determinants of channel gating in the transient receptor potential box of vanilloid receptor I. *FASEB J* 22:3298-3309.
- Valenzano KJ, Grant ER, Wu G, Hachicha M, Schmid L, Tafesse L, Sun Q, Rotshteyn Y, Francis J, Limberis J, Malik S, Whittemore ER, Hodges D (2003) N-(4-tertiarybutylphenyl)-4-(3-chloropyridin-2-yl)tetrahydropyrazine -1(2H)-carboxamide (BCTC), a novel, orally effective vanilloid receptor 1 antagonist with analgesic properties: I. in vitro characterization and pharmacokinetic properties. *J Pharmacol Exp Ther* 306:377-386.
- Valero M, Morenilla-Palao C, Belmonte C, Viana F (2011) Pharmacological and functional properties of TRPM8 channels in prostate tumor cells. *Pflugers Arch* 461:99-114.
- Valero ML, Mello de Queiroz F, Stühmer W, Viana F, Pardo LA (2012) TRPM8 Ion Channels Differentially Modulate Proliferation and Cell Cycle Distribution of Normal and Cancer Prostate Cells. *PLoS One* 7:e51825.
- Vanden Abeele F, Kondratskyi A, Dubois C, Shapovalov G, Gkika D, Busserolles J, Shuba Y, Skryma R, Prevarskaya N (2013) Complex modulation of the cold receptor TRPM8 by volatile anaesthetics and its role in complications of general anaesthesia. *J Cell Sci* 126:4479-4489.
- Vanden Abeele F, Zholos A, Bidaux G, Shuba Y, Thebault S, Beck B, Flourakis M, Panchin Y, Skryma R, Prevarskaya N (2006) Ca²⁺-independent phospholipase A₂-dependent gating of TRPM8 by lysophospholipids. *J Biol Chem* 281:40174-40182.
- Venkatachalam K, Montell C (2007) TRP channels. *Annu Rev Biochem* 76:387-417.
- Vetter I, Hein A, Sattler S, Hessler S, Touska F, Bressan E, Parra A, Hager U, Leffler A, Boukalova S, Nissen M, Lewis RJ, Belmonte C, Alzheimer C, Huth T, Vlachova V, Reeh PW, Zimmermann K (2013) Amplified cold transduction in native nociceptors by M-channel inhibition. *J Neurosci* 33:16627-16641.
- Viana F (2011) Chemosensory properties of the trigeminal system. *ACS Chem Neurosci* 2:38-50.
- Viana F, de la Peña E, Belmonte C (2002) Specificity of cold thermotransduction is determined by differential ionic channel expression. *Nat Neurosci* 5:254-260.
- Voets T (2012) Quantifying and Modeling the Temperature-Dependent Gating of TRP Channels. *Rev Physiol Biochem Pharmacol*.
- Voets T, Owsianik G, Janssens A, Talavera K, Nilius B (2007) TRPM8 voltage sensor mutants reveal a mechanism for integrating thermal and chemical stimuli. *Nat Chem Biol* 3:174-182.
- Voets T, Droogmans G, Wissenbach U, Janssens A, Flockerzi V, Nilius B (2004) The principle of temperature-dependent gating in cold- and heat-sensitive TRP channels. *Nature* 430:748-754.

- Vriens J, Owsianik G, Hofmann T, Philipp SE, Stab J, Chen X, Benoit M, Xue F, Janssens A, Kerselaers S, Oberwinkler J, Vennekens R, Gudermann T, Nilius B, Voets T (2011) TRPM3 is a nociceptor channel involved in the detection of noxious heat. *Neuron* 70:482-494.
- Watanabe H, Vriens J, Suh SH, Benham CD, Droogmans G, Nilius B (2002) Heat-evoked activation of TRPV4 channels in a HEK293 cell expression system and in native mouse aorta endothelial cells. *J Biol Chem* 277:47044-47051.
- Watt EE, Betts BA, Kotey FO, Humbert DJ, Griffith TN, Kelly EW, Veneskey KC, Gill N, Rowan KC, Jenkins A, Hall AC (2008) Menthol shares general anesthetic activity and sites of action on the GABA(A) receptor with the intravenous agent, propofol. *Eur J Pharmacol* 590:120-126.
- Wes PD, Chevesich J, Jeromin A, Rosenberg C, Stetten G, Montell C (1995) TRPC1, a human homolog of a *Drosophila* store-operated channel. *Proc Natl Acad Sci U S A* 92:9652-9656.
- Williams DA, Fogarty KE, Tsien RY, Fay FS (1985) Calcium gradients in single smooth muscle cells revealed by the digital imaging microscope using Fura-2. *Nature* 318:558-561.
- Wu G, D'Agati V, Cai Y, Markowitz G, Park JH, Reynolds DM, Maeda Y, Le TC, Hou H, Jr., Kucherlapati R, Edelmann W, Somlo S (1998) Somatic inactivation of Pkd2 results in polycystic kidney disease. *Cell* 93:177-188.
- Xing H, Ling J, Chen M, Gu JG (2006) Chemical and cold sensitivity of two distinct populations of TRPM8-expressing somatosensory neurons. *J Neurophysiol* 95:1221-1230.
- Xing H, Chen M, Ling J, Tan W, Gu JG (2007) TRPM8 mechanism of cold allodynia after chronic nerve injury. *J Neurosci* 27:13680-13690.
- Xing H, Ling JX, Chen M, Johnson RD, Tominaga M, Wang CY, Gu J (2008) TRPM8 mechanism of autonomic nerve response to cold in respiratory airway. *Mol Pain* 4:22.
- Yamamura H, Ugawa S, Ueda T, Morita A, Shimada S (2008) TRPM8 activation suppresses cellular viability in human melanoma. *Am J Physiol Cell Physiol* 295:C296-301.
- Yang F, Cui Y, Wang K, Zheng J (2010) Thermosensitive TRP channel pore turret is part of the temperature activation pathway. *Proc Natl Acad Sci U S A* 107:7083-7088.
- Yang XR, Lin MJ, McIntosh LS, Sham JS (2006) Functional expression of transient receptor potential melastatin- and vanilloid-related channels in pulmonary arterial and aortic smooth muscle. *Am J Physiol Lung Cell Mol Physiol* 290:L1267-1276.
- Yeh BI, Kim YK, Jabbar W, Huang CL (2005) Conformational changes of pore helix coupled to gating of TRPV5 by protons. *EMBO J* 24:3224-3234.
- Zakharian E, Cao C, Rohacs T (2010) Gating of transient receptor potential melastatin 8 (TRPM8) channels activated by cold and chemical agonists in planar lipid bilayers. *J Neurosci* 30:12526-12534.
- Zakharian E, Thyagarajan B, French RJ, Pavlov E, Rohacs T (2009) Inorganic polyphosphate modulates TRPM8 channels. *PLoS One* 4:e5404.

- Zhang L, Barritt GJ (2004) Evidence that TRPM8 is an androgen-dependent Ca²⁺ channel required for the survival of prostate cancer cells. *Cancer Res* 64:8365-8373.
- Zhang L, Barritt GJ (2006) TRPM8 in prostate cancer cells: a potential diagnostic and prognostic marker with a secretory function? *Endocr Relat Cancer* 13:27-38.
- Zhang X, Mak S, Li L, Parra A, Denlinger B, Belmonte C, McNaughton PA (2012) Direct inhibition of the cold-activated TRPM8 ion channel by Galphaq. *Nat Cell Biol* 14:851-858.
- Zhang XB, Jiang P, Gong N, Hu XL, Fei D, Xiong ZQ, Xu L, Xu TL (2008) A-type GABA receptor as a central target of TRPM8 agonist menthol. *PLoS One* 3:e3386.
- Zimmermann K, Leffler A, Babes A, Cendan CM, Carr RW, Kobayashi J, Nau C, Wood JN, Reeh PW (2007) Sensory neuron sodium channel Nav1.8 is essential for pain at low temperatures. *Nature* 447:855-858.
- Zimmermann K, Lennerz JK, Hein A, Link AS, Kaczmarek JS, Delling M, Uysal S, Pfeifer JD, Riccio A, Clapham DE (2011) Transient receptor potential cation channel, subfamily C, member 5 (TRPC5) is a cold-transducer in the peripheral nervous system. *Proc Natl Acad Sci U S A*.